WAVE-CURRENT-INDUCED SCOURING PROCESSES AND PROTECTION BY WIDELY GRADED MATERIAL

Von der Fakultät für Bauingenieurwesen und Geodäsie

der Gottfried Wilhelm Leibniz Universität Hannover

zur Erlangung des Grades

DOKTOR-INGENIEUR

Dr.-Ing.

genehmigte Dissertation

von

Dipl.-Ing. Alexander Schendel

geboren am 6. Februar 1984

in Hildesheim

Hannover, 2018

PREFACE

The robust design of offshore structures requires both reliable predictions of the environmental loading and structure-induced effects stemming from waves and currents in the marine environment itself. This focus of investigation includes the proper description of the interaction between waves and currents with the offshore structure itself and its subsequent effects on the near-field marine environment most often activating erosive forces on the mobile seabed which finally may lead to scour in the vicinity of the offshore structure.

The present doctoral thesis submitted and successfully defended by Dr. Alexander Schendel in June 2018 focusses on this particular topic. It revisits the phenomena of scour and the protection of scour by very wide-graded rock material in the marine environment under wave and current loading around monopiles. The scientific value of the thesis is remarkable both in its structural quality and its scientific originality.

The backbone of the thesis is built upon four peer-reviewed publications in well-recognized journals in coastal and ocean engineering together with additional, yet, unpublished experimental investigations and findings. As such, it profoundly improves the understanding of the underlying processes and progression of scour around monopiles induced by tidal currents in juxtaposition to unidirectional loading of the mobile seabed. It moreover reveals the erosion stability of wide-graded rock material under unidirectional currents and broadens our understanding how and to what extent the seabed is degraded under reversing currents given the same scour protection material. Further improvement of knowledge is made available on the erosion stability of coarse grain materials under unidirectional waves and how scour patterns and extent are altered due to directional spreading of waves.

All these studies are embedded in a sort of umbrella document that encompasses previously disclosed findings and, moreover, extensively discusses experimental set-ups, methodologies and analysis conducted in any of the laboratory investigations and subsequent examination of acquired, yet exhaustive amounts of data. Yet, Dr. Schendel finally provides a practical design toolkit to help enabling the robust design of offshore structure in regard of an adequate and durable scour protection system by means of wide-graded rock material.

The thesis denotes a unique contribution towards enhancing the primary knowledge of the subject. Dr. Alexander Schendel proposes and thoroughly investigates wave-current-induced scouring processes and protection at offshore structures in a compendium-like thesis. He proves in this thesis one-of-a-kind originality by describing

and analysing processes which are highly relevant for the design of offshore infrastructure. At present, neither comprehensive studies of the inherent physical processes nor consensus about the functioning or the overall efficiency of wide-graded rock material as scour protection have been given in literature; evidently leading to a profound lack of knowledge of design guidelines and practical recommendations for construction. Dr. Schendel facilitates closing these knowledge gaps with presenting and discussing his research findings so that the responsible design engineer can start using the depicted design formulae for any practical application from scratch. Hoping that you enjoy studying this thesis and obtain a number of fruitful new insights in order to advance scientific knowledge, to stimulate new research approaches and to progress the exchange in between research institutions.

Prof. Dr. Torsten Schlurmann

DANKSAGUNG

Die vorliegende Arbeit entstand während meiner Zeit als wissenschaftlicher Mitarbeiter am Ludwig-Franzius-Institut für Wasserbau, Ästuar- und Küsteningenieurwesen der Leibniz Universität Hannover. Ich hatte das Privileg in dieser Zeit mehrere Forschungsprojekte betreuen zu dürfen, in denen die unterschiedlichsten Aspekte der Kolkgenese und Möglichkeiten des Kolkschutzes thematisiert wurden. Motiviert durch die Erfahrungen und Erkenntnisse, die ich aus den projektbegleitenden Modellversuchen gewinnen könnte, entstand letztendlich diese Arbeit. Besonderer Dank gilt meinem Doktorvater Herrn Prof. Dr.-Ing. habil. Torsten Schlurmann, der mich auf dem Weg zur Promotion stets gefördert sowie durch hilfreiche Anregungen und aufmerksame Kritik wesentlich zum Gelingen dieser Arbeit beigetragen hat.

Weiterer Dank gebührt Herrn Prof. Dr.-Ing. habil. Nils Goseberg und Prof. Dr. ir. Bas Hofland für die Übernahme des Koreferates und das Anfertigen ihrer schriftlichen Gutachten. Herrn Prof. Dr.-Ing. Martin Achmus für die Übernahme des Kommissionsvorsitzes und Prof. Dr.-Ing. Arndt Hildebrandt für seinen Einsatz und seine Zeit als weiteres Kommissionsmitglied.

Die Hauptergebnisse dieser kumulativen Dissertation wurden in internationalen Fachjournalen veröffentlicht. Dies wäre ohne die Mithilfe der Koautoren Prof. Dr.-Ing. habil. Torsten Schlurmann, Prof. Dr.-Ing. habil. Nils Goseberg und Prof. Dr.-Ing. Arndt Hildebrandt nicht möglich gewesen. Ich bedanke mich daher ausdrücklich bei meinen Koautoren für die hilfreichen Diskussionen der Ergebnisse sowie die inhaltlichen und redaktionellen Ergänzungen der Publikations-Manuskripte.

Danken möchte ich außerdem meinen Kollegen, HiWis und Studenten für wertvolle fachliche und auch fachfremde Diskussionen, Unterstützung in der planerischen und technischen Vorbereitung und Durchführung zahlreicher Modellversuche sowie der exzellenten Zusammenarbeit in den letzten Jahren.

Mein größter Dank geht an meine Familie, die mich während der Zeit meines Studiums und meiner Promotion durch endlose Geduld, uneingeschränktes Verständnis und unerlässliche Aufmunterung immens unterstützt hat.

<div align="right">Alexander Schendel</div>

ABSTRACT

The expansion of offshore wind energy depicts an important contribution to the fulfilment of renewable energy targets. Seeking for higher load factors, offshore wind energy steadily expands towards greater water depths. In addition, considering the already showing effects of climate change on extreme weather events, intensified hydrodynamic loads acting on offshore structures have to be expected in the future. In order to further improve the scour prediction and consequently optimize the design of foundation structures in the marine environment, a wide range of hydraulic conditions should thus be considered, including directional flow aspects.

Furthermore, a flexible and sustainable scour protection system is required that provides resilience against those hydraulic conditions. Due to its cost-efficient production and undemanding installation procedure, a scour protection system made of widely graded broken stone material might depict a suitable alternative to the typical multi-layer setup. However, no systematic research on the behaviour and stability of this material exposed to flow has been carried out so far, and consequently, no design guidelines for a scour protection made of widely graded material exist, leaving its promising potential as scour protection system unused.

This thesis aims at contributing to the further expansion of offshore wind energy by improving the design process of scour protection for offshore foundation structures. This is accomplished by carrying out a series of novel laboratory experiments addressing two major elements of scour protection design. At first, experiments on the scouring process around a monopile structure induced by complex marine flows were conducted. To advance the understanding of effects of flow directionality on the progression of scour, these experiments included tests with realistically represented tidal currents and multi-directional waves. The findings of these experiments emphasize the importance of selecting suitable reference flow velocities to reliable predict the scour development at offshore structures.

Secondly, systematic experiments regarding the fluid-sediment interactions and stability affecting processes of widely graded broken stone material exposed to different flow conditions were carried out. An assessment of the material's protective performance as scour and bed protection system is given and application-oriented design recommendations are provided for the dimensioning of a widely graded granular scour protection. The design recommendations link available and newly gained knowledge on the erosional behaviour of widely graded materials to present design methods for scour protections around offshore structures.

ZUSAMMENFASSUNG

Der fortschreitende Ausbau von Offshore-Windenergie leistet einen wichtigen Betrag zur Erfüllung der Ziele der Erneuerbare Energien Direktive. Auf der Suche nach höheren Auslastungsfaktoren expandiert die Offshore-Windenergie in immer tiefere Gewässer. Als Folge des Klimawandels, dessen Auswirkungen auf extreme Wetterereignisse schon jetzt zu beobachten sind, muss zudem mit einer zunehmenden hydrodynamischen Beanspruchung von Offshore-Strukturen gerechnet werden.

Zur Verbesserung der Kolkvorhersage und damit Optimierung der Bemessung von Offshore-Gründungsstrukturen müssen daher umfassende hydraulische Randbedingungen in Betracht gezogen werden. Hierzu zählt im Besonderen der Einfluss richtungsabhängiger Strömung auf die Kolkgenese. Weiterhin besteht die Notwendigkeit eines anpassungsfähigen und nachhaltigen Kolkschutzsystems, das diesen fordernden Belastungen ausreichend Widerstand entgegenbringen kann. Aufgrund einer kostengünstigen Herstellung sowie eines einfachen Installationsprozesses könnte ein System aus weitgestuftem Bruchsteinmaterial eine geeignete Alternative zu mehrlagigen Kolkschutzaufbauten darstellen. Allerdings wurde das charakteristische Verhalten und die Stabilität des Materials unter Strömungsbelastung bisher nicht systematisch untersucht. Entsprechend fehlt es an Ansätzen zur Bemessung eines Kolkschutzes aus weitgestuftem Steinmaterial, sodass das vielversprechende Potential des Materials bislang ungenutzt ist.

Diese Arbeit trägt zum sicheren Ausbau von Offshore-Windenergie bei, indem die Bemessungsgrundlagen von Kolkschutz an Offshore-Strukturen wesentlich erweitert werden. Hierzu wurden physikalische Modellversuche zu zwei maßgeblichen Schritten innerhalb einer Kolkschutzbemessung durchgeführt. Diese beinhalten zum einen Modellversuche zu Kolkprozessen an einer Monopile-Struktur infolge von komplexen marinen Strömungsbedingungen. Zur Berücksichtigung von richtungsabhängigen Strömungseinflüssen auf die Kolkentwicklung umfassen diese Modellversuche insbesondere Untersuchungen zum Einfluss von Tideströmungen sowie multidirektionalen Seegangs auf die Kolkgenese. Die Ergebnisse dieser Untersuchungen bestätigen die Notwendigkeit geeignete Strömungsgeschwindigkeit für eine verlässliche Kolkvorhersage zu definieren.

Zum anderen wurden Modellversuche zur Fluid-Sediment-Wechselwirkung sowie zur Erosionsstabilität weitgestuften Bruchsteinmaterials unter mariner Strömungsbelastung durchgeführt. Darauf aufbauend konnte die Eignung des Materials als Kolkschutz bewertet und anwendungsorientierte Bemessungsempfehlungen für die Di-

mensionierung eines weitgestuften Kolkschutzes abgeleitet werden. Die Empfehlungen verbinden dabei bereits verfügbare sowie neu gewonnen Erkenntnisse über das charakteristische Erosionsverhalten weitgestufter Sedimente mit aktuellen Bemessungsmethoden für den Kolkschutz von Offshore-Strukturen.

CONTENTS

LIST OF TABLES

A	amplitude of the wave orbital motion at the bed
A_r	cross-sectional area of particle facing the flow
C	Chezy roughness coefficient
C_D	drag coefficient
C_L	lift coefficient
D	pile diameter
$D(f, \Theta)$	directional spreading function
D_f	critical filter thickness
D_*	dimensionless particle diameter
E	dimensionless stability parameter
F_1	frictional force
F_2	pressure force
F_D	drag force
F_G	force of submerged particle weight
F_L	lift force
H	wave height
$H_{1/10}$	average of the 10% highest waves
H_{m0}	spectral wave height
H_s	significant wave height
I	bed slope
I_c	hydraulic gradient
KC	Keulegan-Carpenter number
L	wave length
N	number of waves
Re	current Reynolds number
Re_D	pile Reynolds number
Re_w	wave Reynolds number
Re_*	grain Reynolds number
S	scour depth
S_c	current induced scour depth
$S(f)$	frequency spectrum
$S(f, \Theta)$	directional spectrum

$\overline{\tau_\infty}$ bed shear stress exerted by undisturbed flow

ϕ angle of repose for sediment

INTRODUCTION

As an important contribution to the fulfilment of renewable energy directives, the expansion of offshore wind energy is steadily progressing in Europe. With 754 additional offshore wind turbines added in 2016 (WindEurope, 2017), amounting to a total number of 3,589 turbines (12.6 GW) at the end of the same year, the share of regenerative energy sources on the gross power production is continuously increasing in Europe. By 2020, European offshore wind capacity is projected to grow to a cumulatively installed capacity of 24.6 GW (WindEurope, 2017), doubling the capacity since 2016. Those numbers emphasize the need for a reliable and economically optimised design concept for foundation structures of offshore wind turbines, that is also adoptable to future requirements and challenges.

In contrast to onshore installations, foundation structures of offshore wind turbines have to resist hydraulic loads induced by currents and waves. Furthermore, the placement of a structure into a flow will cause a disturbance of the flow around it. As a result, bed shear stresses are amplified so that the sediment mobility around the structure increases. The emerging scour hole can then affect the integrity of the structure. In case of a monopile foundation, the structural stability might be influenced by an increased bending moment, a decreased axial and lateral bearing capacity or a change of the eigenfrequency of the pile (Achmus, Kuo, and Abdel-Rahman, 2010; De Vos, 2008; Van der Tempel, 2006). The degrading effects of scour have thus to be considered in the design process of an offshore foundation structure. The protection against the effects of scour can involve an optimisation of the structural design according to the expected scour depths or effective measures against the development of scour in form of a scour protection system.

A reliable prediction of scour development in marine environments and application-oriented design guidelines for an adaptive scour protection are, therefore, essential elements of foundation structure design, guaranteeing the further advancing expansion of offshore wind energy.

1.1 MOTIVATION

Seeking for higher load factors, the average distance to shore of offshore wind farms increased significantly over recent years, from 33 km in 2014 to 44 km in 2016 (WindEurope, 2017). This progressive expansion of offshore wind energy towards greater water depths de-

mands the scour prediction to account for a wider range of hydraulic conditions, as wind driven wave irregularity and directionality become important aspects of offshore sea states. In addition, as a result of climate change, the probability of extreme weather events with shorter return periods and intensified hydrodynamic loads acting on the offshore wind turbines is increasing. By comparing ten wave climate projections, Grabemann et al. (2015) evaluated the impact of climate change on North Sea wave conditions. They found an increase in mean and extreme wave heights for the eastern parts of the North Sea by the end this century.

In order to improve the scour prediction as a prerequisite for an optimised, more economical design of foundations structures, a wide range of site-specific hydraulic conditions have to be considered, including directional flow aspects. A literature review (chapter 2) reveals that available scour prediction approaches however often rely on simplified hydraulic conditions. By neglecting the influence of realistic offshore sea states and wave directionality on the scour development, those approaches are limited in their range of applicability. Concurrently, while numerous studies have been carried out on the progression of scour induced by unidirectional and steady currents, reliable approaches on the scour development in unsteady tidal currents are to this date limited, although tidal currents depict the decisive driving mechanism for scouring in most marine conditions.

A reliable scour prediction is important for the design process of an offshore foundation structure as it determines the imperative of an additional scour protection system. If the estimated, site-specific scour depths exceed defined threshold values, the installation of a scour protection system often becomes the most economical solution, as costs of structural enhancement or maintenance costs over the lifetime of the structure can be large and unpredictable. A flexible and sustainable scour protection system is required that covers the wide range of hydraulic and morphodynamical conditions offshore foundation structures are exposed to. Due to its cost-efficient production and undemanding installation procedure, a scour protection system made of widely graded broken stone material might depict a suitable alternative to a typical multi-layer setup. Installed as single-layer scour or bed protection, geometrical and hydraulic filter requirements might be met by adjusting the grain size distribution. In addition, if exposed to a flow, graded sediments tend to form a protective armor layer at their surface over time by selective erosion of finer grains. Whitehouse (1998) already pointed out potential implications of this characteristic material behaviour on the stability of a widely graded scour protection system:

> "Rock dump has been used in the North Sea to cover the Ekofisk-Emden pipeline and it is observed that the finer material will erode from the top layers of the rock protec-

tion at conditions less than the ultimate design condition. Providing the appropriate rock grading is used the upper layer of the bed protection scheme is likely to become armoured and perhaps somewhat more resistant with time."

However, available design approaches for granular scour protection usually consider uniformly graded materials, neglecting the characteristic properties and self-stabilising behaviour of widely graded materials. While it might be plausible to implement stability approaches for the incipient motion of non-uniform sediments in the design of scour protection, current approaches are derived from water-worked sediments in rivers, which significantly differ from the sharp-edged particles of broken stone materials. So far, no systematic research on the behaviour and stability of widely graded broken stone material exposed to flow has been carried out. Consequently, no guidelines for the design of a widely graded scour protection system in marine environments exist, leaving its promising potential as a more economical alternative to traditionally applied protection systems unused.

1.2 OBJECTIVES & METHODS

This thesis aims at contributing to the expansion of offshore wind energy by improving the design process of scour protection for offshore foundation structures. This is accomplished by addressing two major aspects of scour protection design. At first, insights into morphodynamical processes and scouring mechanisms around foundation structures in complex flows and realistic sea states are provided, allowing the refinement of scour prediction for foundation structures situated in offshore waters. The second step involves the analysis of fluid-sediment interactions and stability-affecting processes of widely graded broken stone material exposed to flow and an assessment of its protective performance as a scour and bed protection system in marine flow conditions. These two parts can be further separated into the following explicit objectives and their contribution to the process of scour protection design is illustrated in Fig. 1.1.

Improvement of scour prediction for offshore structures by a realistic representation of marine flow conditions:

a) Description of sediment transport processes and systematic analysis of scouring mechanism around offshore foundation structures in unsteady tidal flows. Comparison of scouring mechanisms, scour depths and rates to those induced by unidirectional currents to assess how the influence of continuously changing flow velocity and direction on the scour development can be incorporated into existing scour prediction approaches, which usually rely on time averaged, unidirectional flow com-

ponents. This is presented in Schendel et al. (2018) and results are summarized in chapter 3.1.

b) Advancing the knowledge of scouring processes induced by multidirectional waves as well as multidirectional waves combined with currents by systematically investigating the effects of wave directionality on scour depths and rates around an offshore foundation structure. Assessment of necessity to consider directional wave aspects into existing prediction approaches by comparison of scour depth and rates to those obtained by unidirectional waves. This objective is addressed in chapter 3.2.

Advancing of scour protection design for widely graded broken stone materials:

c) Description of erosive potentials and bed stability of widely graded broken stone materials subjected to unidirectional currents. Determination of incipient motion conditions for the selective erosion of individual grain sizes and selection of a suitable reference grain size by providing a comparison with available hiding functions. This is presented in Schendel, Goseberg, and Schlurmann (2016) of which a summary is given in chapter 4.2.

d) Assessment of sediment transport processes and armor layer development of widely graded broken stone materials as response to reversing flow conditions. Quantification of bed degradation processes and evaluation of bed stability against shear failure under reversing flow conditions as substitution to tidal currents. This is investigated in Schendel, Goseberg, and Schlurmann (2017) and summarized in chapter 4.3.

e) Elucidation of erosive behaviour of widely graded broken stone materials exposed to waves and assessment of its performance as scour and bed protection under random wave load. This is addressed in Schendel, Goseberg, and Schlurmann (2015) of which a summary is provided in chapter 4.1.

f) Formulation of application-orientated recommendations for the design of scour protection around offshore foundations with widely graded broken stone material based on existing and newly gained knowledge on the erosional behaviour of graded sediments. This is discussed and evaluated in chapter 5.

The individual objectives were approached by planning, conducting and analysing experimental model tests. In tests that dealt with the direct influence of a foundation structure on the scour development or scour protection stability around it, a monopile model was chosen as representative structure. Monopiles are the most common foundation structure for offshore wind turbines with a market share of above

80% (WindEurope, 2017). Due to their simplicity and symmetry, the usage of monopiles allowed to fully concentrate on effects related to the applied load conditions. Moreover, the abundance of available scour data for monopiles simplified the comparison and assessment of test results.
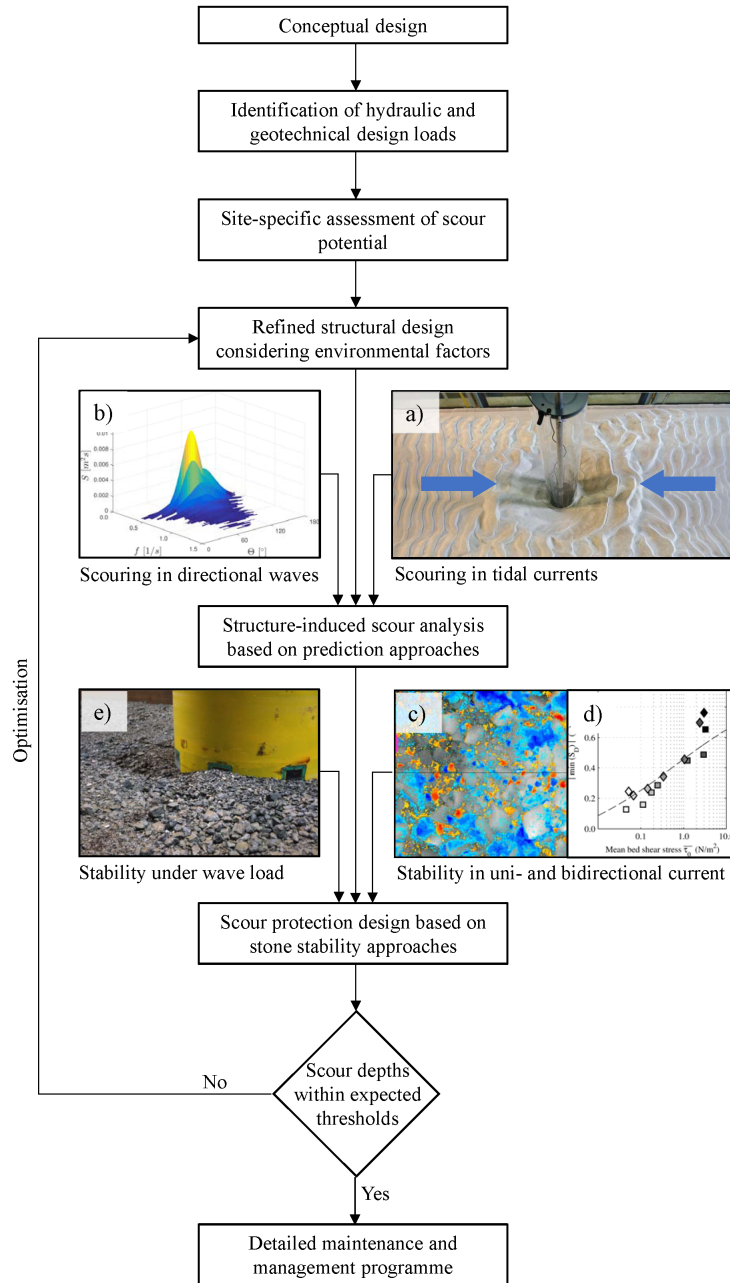
Figure 1.1: General methodology of scour protection design and contribution of this thesis to the design process.

While numerical models for the simulation of scouring and sediment transport processes became increasingly sophisticated in recent years (e.g. Baykal et al., 2017; Bihs, 2011; Caliskan and Fuhrman, 2017;

Fuhrman et al., 2014; Stahlmann, 2013), they are still limited regarding complex flow conditions, particularly regarding wave directionality or unsteady tidal currents, and the recognition of armor layer development in non-uniform sediments. Nevertheless, using the results from this thesis for validation, numerical models could depict a suitable tool for extending the results to a wider range of application in the future.

1.3 OUTLINE

The principal results of this thesis are submitted as a collection of international journal publications. These publications are complemented by sections, which either provide additional information, supplementary analysis or critical discussions of the results regarding their contribution to the objectives of this thesis as outlined above. In the following chapter 2, further background to the fields of bed stability, scouring and scour protection in form of a comprehensive literature review is given, laying a sound basis for the analysis and interpretation of the experimental results. This includes a summary of state-of-the-art approaches for scour prediction and the design of granular scour protection. In chapter 3, the experiments on the scour development in tidal currents as well as in multidirectional waves are presented, for the former in a summarized form of a submitted manuscript and for the latter as a detailed test description and in-depth analysis. The findings of both studies are evaluated regarding potential consequences for present scour prediction methods. Chapter 4 summarizes the findings of three published studies on the erosive behaviour and bed stability of widely graded broken stone materials subjected to different estuarine, coastal and marine flow conditions. Based on these findings, chapter 5 provides an extended discussion on ways to consider the characteristics inherent to widely graded materials in present scour protection design approaches, eventually leading to the formulation of explicit design recommendations. Finally, a summary and prospects for future investigations are given in chapter 6.

BACKGROUND & STATE-OF-THE-ART

The consideration of graded sediments for sediment transport processes has become common practice in hydraulic engineering, although there is still some disagreement and conflicting concepts regarding the erosion behaviour of graded sediments. More recently, the knowledge mainly gained in the field of river engineering has also been applied for coastal and marine engineering processes and is incorporated in several sediment transport formulae. While bed and scour protection systems in this environment typically consist of granular material, the unique characteristics of graded sediments, in particular the tendency to form an armor layer, are however not taken into account in scour prediction or scour protection design. Up to date, there are neither empirically derived stability approaches for scour protection design, nor are there concepts to adapt present approaches to the physical characteristics of graded sediments. In this context and as fundament for the analysis in the subsequent chapters, this chapter provides an overview of the characteristics of widely graded sediments exposed to hydraulic load and presents concepts for the stability assessment. Furthermore, recent developments and research on the topics of scouring and scour and bed protection design are given. The scope of this chapter lies on fully turbulent, hydraulically rough flow conditions, which typically prevail in the maritime environment. Descriptions of scouring processes and protection design focus on monopiles as foundation structure as well as coastal and marine flow conditions, i.e. relatively large water depths and combined wave and current regime.

2.1 FLOW RESISTANCE

2.1.1 *Characteristic grain sizes of natural sediments*

Natural sediments in alluvial channels or marine sea beds are characterized by a wide range of grain sizes. By discretization into representative fractions, the grain size distribution can be depicted by percentages of weight, presented as frequency histogram (cp. Fig. 14 in Schendel, Goseberg, and Schlurmann (2017)) or integrated to the commonly applied cumulative frequency curve (cp. Fig. 1 in Schendel, Goseberg, and Schlurmann (2017)). In the fields of sedimentology

and geology, grain sizes are often transformed to a logarithmic phi-scale in the form suggested by Krumbein (1936):

$$\Phi_i = -\log_2 d_i = \frac{\log d_i}{\log 2} \tag{2.1}$$

with d_i as the grain diameter of considered fraction i in millimetres, defined as $d_i = 0.5\,(d_i + d_{i+1})$.

For a given log-normal grain size distribution, the logarithmic transformation would result in a normal distribution, allowing a more convenient statistical analysis of grain sizes (Bunte and Abt, 2001). The spread of sorting of the grain size distribution can be described by its geometric standard deviation:

$$\sigma_g = \sqrt{\frac{d_{84}}{d_{16}}} \tag{2.2}$$

in which d_{84} and d_{16} are the grain diameters for which 84% and 16% of the distribution by weight are finer.

In phi-scale, the geometric standard deviation is given by:

$$\sigma_g = 2^{\sigma_\Phi} \tag{2.3}$$

$$\sigma_\Phi^2 = \sum_{i=1}^{n} (\Phi_i - \Phi_m)^2 \, \Delta p_i \tag{2.4}$$

with Φ_m being the arithmetic grain size, σ_Φ the standard deviation in phi-scale and Δp_i as the percental content of grain size fraction i.

Besides the median grain diameter d_{50}, several other characteristic grain diameters have been identified over the years, that are considered to be representative for the behaviour of the total sediment mixture. Among them, the arithmetic grain diameter d_m (often also denoted d_a) proposed by Meyer-Peter and Müller (1948):

$$d_m = \sum_{i=1}^{n} d_i \Delta p_i \tag{2.5}$$

The arithmetic grain diameter in phi-scale Φ_m can be calculated accordingly. The geometrical mean size can be derived from Φ_m by:

$$d_g = 2^{-\Phi_m} \tag{2.6}$$

To date, no agreement is reached on which statistical values should be used for the description of sediments in the engineering community. An overview of statistical parameters and characteristic grain sizes to describe the grain size distribution of natural sediments can be found in Zanke (1982) and Bunte and Abt (2001).

2.1.2 *Flow resistance in currents*

As a result of friction, a fluid interacting with a surface exerts shear stresses on the surface. This transmission of forces on the bed surface by shear stresses is essential for the distribution of flow velocity and sediment transport processes. In an open channel flow, shear stresses are distributed linearly between the bed and the water surface. Based on the equation of motion, the distribution of shear stress over the water column for a steady uniform flow is given by:

$$\tau\left(z\right) = \rho g\left(h - z\right) I \tag{2.7}$$

with I as the bed slope, ρ the fluid density, g the acceleration due to gravity, h the water depth and z as the distance from the bed.

For the shear stress maximum at the bed ($z = 0$), the equation reduces to:

$$\tau_0 = \rho g h I \tag{2.8}$$

Due to the no-slip condition at the wall, the near bed flow velocity is always zero. The transfer to the outer flow velocity, which is unaffected from the influence of the wall, is carried out in a velocity gradient of limited extend called boundary layer. The thickness of the boundary layer is determined by the surface roughness, Reynolds number and turbulence intensity of the flow and is often defined as the distance from the bed surface to the point at which the flow velocity has reached 99 % of the undisturbed outer flow velocity (Schlichting and Gersten, 2006; Zanke, 1982). Depending on the Reynolds number of the flow, the boundary layer can either be laminar or turbulent. For typical engineering applications in open channel flows, however, the boundary layer is usually turbulent as the overflown distance of the flow becomes very large.

The turbulent boundary layer itself can be divided in three sublayers: the viscous (laminar) sublayer near the bed, where the viscous shear stresses are dominant, the turbulent logarithmic sublayer near the undisturbed flow regime and a transition sublayer between the former two (Van Rijn, 1993). In the viscous sublayer, the shear stress distribution is proportional to the flow velocity gradient and is defined by Newton's friction law with:

$$\tau_v = \rho \nu \frac{\delta u}{\delta z} \tag{2.9}$$

where τ_v is the viscous shear stress, ν is the kinematic viscosity and u is the flow velocity at distance z from the bed.

In the outer layers, the viscous shear stresses are dominated by the turbulent shear stresses τ_t, which are generated by turbulent velocity

fluctuations in the horizontal u' and vertical flow direction w' (Zanke, 1982):

$$\tau_t = -\rho \overline{u'w'} \tag{2.10}$$

For a turbulent flow, the shear stress distribution over the water depth can thus be described as:

$$\tau(z) = \rho \nu \frac{\delta u}{\delta z} + \rho \overline{u'w'} \tag{2.11}$$

The influence of the viscous components on the total shear stresses depends on the hydraulic roughness of the flow. A turbulent flow is hydraulically smooth if the bed roughness heights are smaller than the thickness of the viscous sublayer. In contrast, if the roughness heights exceed the viscous sublayer the flow is considered hydraulically rough. In this case, the flow is fully turbulent and the shear stress is given by $\tau \approx \tau_t$.

Generally, the vertical velocity distribution in a steady, uniform and turbulent flow is described by the well-known log law:

$$\frac{u(z)}{u_*} = \frac{1}{\kappa} \ln\left(\frac{z}{z_0}\right) \tag{2.12}$$

where κ is the von Kármán's constant ($\kappa = 0.4$), u_* is the shear velocity defined as $u_* = \sqrt{\tau_0/\rho}$, and z_0 the roughness length, which can be assumed as $z_0 = k_s/30$ for hydraulically rough flow based on work by Nikuradse (1933), with k_s as the equivalent sand roughness by Nikuradse.

According to Smart (1999), the time and depth averaged flow velocity $\bar{U}$ can be estimated by integration of Eq. (2.12), if the logarithmic velocity profile is assumed to hold true throughout the water depth h, and if $h \gg z_0$. The result is a logarithmic flow resistance equation in a form suggested by Keulegan (1938):

$$\frac{\overline{U}}{u_*} = \frac{1}{\kappa}\left[\ln\left(\frac{h}{z_o}\right) - 1\right] \tag{2.13}$$

In turbulent flow, the bed shear stress, which represents the flow resistance, can be related to the depth-averaged flow velocity in a quadratic form through the drag coefficient C_D by:

$$\tau_c = \rho C_D \overline{U}^2 \tag{2.14}$$

By combining Eq. (2.13) and Eq. (2.14), C_D is given in a logarithmic form for a steady, uniform and fully turbulent flow as:

$$C_D = \frac{u_*^2}{\overline{U}^2} = \left[\frac{\kappa}{\ln\left(\frac{h}{z_0}\right) - 1} \right]^2 \tag{2.15}$$

Alternatively, the flow resistance can be expressed by other widely used resistance coefficients, including the physically derived Darcy-Weisbach roughness coefficient f_f, the Chezy roughness coefficient C and the empirical Manning-Strickler roughness coefficient n. Through Eq. (2.8), those resistance coefficients can be related by:

$$\frac{u_*^2}{\overline{U}^2} = \frac{f_f}{8} = \frac{g}{C^2} = \frac{n^2 g}{h^{2/3}} \tag{2.16}$$

Attributed to Manning-Strickler's resistance formulation, flow resistance approaches are also often expressed in a power law form. The applicability of either log law or power law based approaches is mainly dependent on the relative submergence height and is still discussed in literature. A comprehensive overview of flow resistance equations is given by Powell (2014). The author pointed out that for high relative submergence ($h \gg z_0$), which should be the case in offshore waters, flow resistance can be successfully estimated with log law based approaches, as the dominant source of energy loss is friction. For steep and rough streams with a large relative roughness, flow depth measurements often become inaccurate. As a result, several authors proposed nondimensional hydraulic geometry equations, that connect the mean flow velocity directly to the discharge (Aberle and Smart, 2003; Ferguson, 2007; Rickenmann and Recking, 2011).

2.1.3 *Flow resistance in waves*

Monochromatic wave parameters are often used in expressions for bed shear stress and sediment transport models. The maximum amplitude of the orbital flow velocity near the bed U_w can be derived by linear wave theory for monochromatic (regular) waves with small amplitude as:

$$U_w = \frac{\pi H}{T \sinh\left(\frac{2\pi h}{L}\right)} \tag{2.17}$$

where H is the wave height, T the wave period and L the wave length.

The wave length is depending on the relative water depth and might have to be determined iteratively for transitional waters. Alternately, the wave length can be calculated by the approximation method of Fenton and McKee (1990).

A natural sea state, however, is characterized by wave spectra (irregular waves), emerged from a superposition of waves of different height, length and direction. One of the most used formulations to describe the energy distribution of a wave spectrum is the JONSWAP spectrum, which was derived from North Sea data and applies to waves in continental-shelf waters (Soulsby, 1997). For a wave spectrum, the orbital velocity near the bed cannot be given in terms of a single velocity U. Instead, the root-mean-square value of the orbital velocity at the bed is usually used to describe the maximum near bed velocity of a time series (Soulsby, 2006). The root-mean-square velocity U_{rms} can be obtained by integration of the velocity frequency spectrum $S_u(f)$ over all frequencies:

$$U_{rms}^2 = \int_0^\infty S_u(f)\, df \tag{2.18}$$

For a Rayleigh distributed frequency spectrum, the amplitude of the orbital flow velocity U_w is then given by the following relation:

$$U_w = \sqrt{2}U_{rms} \tag{2.19}$$

As pointed out by Sumer and Fredsøe (2001a), U_w becomes identical to the maximum orbital flow velocity for monochromatic small-amplitude waves. Ockenden and Soulsby (1994) also found that the bedload transport under irregular waves can be simulated by equivalent monochromatic waves having an orbital velocity amplitude of $U_w = \sqrt{2}U_{rms}$, where U_{rms} is the root-mean-square of the orbital flow velocity in the irregular wave spectrum.

If it is necessary to calculate the orbital velocity from given spectral wave parameters, i.e. significant wave height H_s and peak period T_p, approximating formulas can be used. For a JONSWAP spectrum, Soulsby (2006) derived the following simple exponential approximation for U_{rms}:

$$U_{rms} = \left(\frac{H_s}{4}\right)\left(\frac{g}{h}\right)^{0.5} exp\left\{-\left[\frac{3.65}{T_z}\left(\frac{h}{g}\right)^{0.5}\right]^{2.1}\right\} \tag{2.20}$$

with T_z as the zero-crossing period, which can be approximated for a JONSWAP spectrum by $T_z = T_p/1.28$.

Similar to the drag coefficient under currents, bed shear stress under waves is usually obtained through a friction factor f_w, which re-

lates the bed shear stress to the maximum orbital velocity of the waves U_w at the bed (Soulsby, 1997):

$$\tau_w = \frac{\rho}{2} f_w U_w^2 \qquad (2.21)$$

According to Soulsby (1997) the wave friction coefficient depends on the hydraulic roughness, which is expressed as a function of the wave Reynolds number Re_w and the relative roughness r:

$$Re_w = \frac{U_w A}{\nu} \qquad (2.22)$$

$$r = \frac{A}{k_s} \qquad (2.23)$$

with $A = U_w T / 2\pi$ as the semi-orbital excursion.

Among the many available approaches, Soulsby (1997) proposed the following equation for the wave friction factor for turbulent rough flow, which also stand exemplarily for the typical power law based formulation:

$$f_w = 1.39 \left(\frac{A}{z_0} \right)^{-0.52} \qquad (2.24)$$

The definition of the wave friction factor has a large impact on the bed shear stress and is thus quite important when it comes to the stability assessment of scour protection. Because the boundary layer under waves is much thinner than under steady current (Nielsen, 1992), larger bed shear stresses are exerted on the bed and scour protection. The influence of several wave friction formulations on the bed shear stress was compared and discussed by De Vos (2008). For the given experimental conditions, the friction approach of Dixen et al. (2008) was found to perform best to determine the bed shear stress induced by waves.

2.1.4 *Flow resistance in combined wave and current conditions*

In the marine environment, hydrodynamic load on the sea bed is usually induced by an interaction of current and wave forces. Unfortunately, the combined load cannot be derived by a linear superposition of wave and current components. Instead, the mutual interaction can lead to a modification of wave lengths, resulting in refraction effects, and to increased bed shear stress components due to non-linear interaction between wave and current boundary layers (Soulsby, 1997). According to Soulsby et al. (1993), the boundary layer interaction must

be a nonlinear process, because the boundary layers are dominated by turbulent shear stresses, which are proportional to the square of flow velocities (cp. Eq. (2.14) and (2.21)). A comparison of several approaches for predicting the combined maximum and mean bed shear stresses is given in Soulsby et al. (1993), including the well-known approaches of Grant and Madsen (1979) and Fredsøe (1984). Based on a large set of laboratory and field data, Soulsby (1995) derived an empirical formulation for the cycle-mean bed shear stress by a two-coefficient optimisation (DATA2 formula):

$$\tau_m = \tau_c \left[1 + 1.2 \left(\frac{\tau_w}{\tau_c + \tau_w} \right)^{3.2} \right] \tag{2.25}$$

with τ_w as the bed shear stress induced by waves and τ_c as the bed shear stress in "current-only" conditions, respectively.

A corresponding expression for the maximum bed shear stress based on a vector addition of the wave induced bed shear stress τ_w and the calculated mean bed shear stress τ_m was also presented:

$$\tau_{max} = \left[(\tau_m + \tau_w \cos \alpha)^2 + (\tau_w \sin \alpha)^2 \right]^{0.5} \tag{2.26}$$

where α is the angle between wave and current direction, with $\alpha = 0°$ if the currents propagate in the same direction as the waves and $\alpha = 90°$ if they travel perpendicular to each other.

The calculation of the threshold of motion should be based on τ_{max}, while for the determination of sediment diffusion τ_m should be used (Soulsby, 1997). Because these formulae were only based on curve-fitting, Soulsby and Clarke (2005) derived a more physics-based approach for both rough and smooth flow. For a complete derivation as well as the algorithm for the application for laminar and turbulent smooth and rough flow it is referred to the mentioned publication at this point.

2.1.5 *Threshold of motion*

A particle in a sediment bed will have a critical condition at which it is unable to resist the hydrodynamic forces of the flow; thus, motion is initiated. The knowledge about this condition is a requirement for numerous hydraulic engineering applications, of which the design of bed and scour protection is only one. The particle entrainment is, however, a probabilistic process, as the instantaneous forces resulting from near bed turbulences are heterogeneously distributed over the bed surface. Consequently, the definition of the threshold of motion becomes more complex. Buffington and Montgomery (1997) divide the most common methods of defining the incipient motion condition

in four groups: (a) based on a selected reference value for bed load transport; (b) by visual observation; (c) based on the largest particle entrained for a certain load; (d) by theoretical calculation. The definition of a critical condition for incipient motion is generally associated with a subjective assessment. A discussion on the comparability of results obtained by either selecting a reference transport rate or visually detecting the largest eroded grain size is also given by Wilcock (1988). The critical condition is typically expressed in terms of:

- Critical bed shear stress or shear velocity or

- Critical flow velocity, often the depth-averaged or near-bed flow velocity.

According to Zanke (1982), approaches based on the determination of a critical shear stress should be preferred, as a critical depth-averaged flow velocity does not account for turbulence and bed roughness. In contrast, velocity based approaches are often more practical as shear stress can only be estimated by indirect methods in many cases (for a summary of indirect methods see Schendel, Goseberg, and Schlurmann (2016)). However, friction factors allow both approaches to be related to each other. As velocity and shear stress based approaches are widely used for the incipient motion determination, though not necessarily by the same communities (Recking and Pitlick, 2012), they are both addressed in the following section. Particles are entrained once the hydrodynamic forces of the flow exceed the resistance forces of the particle. The driving forces leading to the entrainment are thus established first.

Forces on particles

In river beds composed of loose sediment particles, the flow exerts lift forces and drag forces on each particle (Fig. 2.1). Frictional forces F_1 act on the rough surface of a particle by viscous shear in the direction of the flow, but not through the centre of the particle as only the top of the particle is exposed to the flow. Streamline separation and resulting wakes behind the top of the particle will induce a pressure gradient along the stream-wise axis of the particle, causing a pressure force F_2 acting through the center of the particle (Chien and Wan, 1999). Drag forces F_D are the resultant of these frictional and pressure forces and depend on the grain Reynolds number. At low Reynolds numbers, the viscous friction force will be dominant, whereas at high Reynolds numbers the pressure force will be much larger. At Reynolds numbers $Re \geq 10^3$ the friction forces become negligible and the drag force for a spherical particle with the diameter d is usually expressed by:

$$F_D = \frac{\rho}{2} C_D u_f^2 A_r \qquad (2.27)$$

with $A_r = \pi d^2/4$ as the cross-sectional area of the particle facing the flow, C_D as the drag coefficient, u_f as the flow velocity at the center of the particle.

The drag coefficient C_D is known to be a function of particle shape and the local Reynolds number, which compares the inertial to viscous forces. In addition, lift forces are introduced by a pressure gradient between the top and the bottom of a particle, acting through the center of a spherical particle in normal direction of flow. They can be described in a similar way to the drag forces by:

$$F_L = \frac{\rho}{2} C_L u_f^2 A_r \tag{2.28}$$

in which C_L is the lift coefficient.

For the particle to be entrained, the instantaneous fluid forces F_D and F_L have to overcome the vertically downward force of the submerged particle weight F_G, which is for a spherical particle given by:

$$F_G = \frac{\pi}{6} (\rho_s - \rho) g d^3 \tag{2.29}$$

where ρ_s is the density of the sediment.
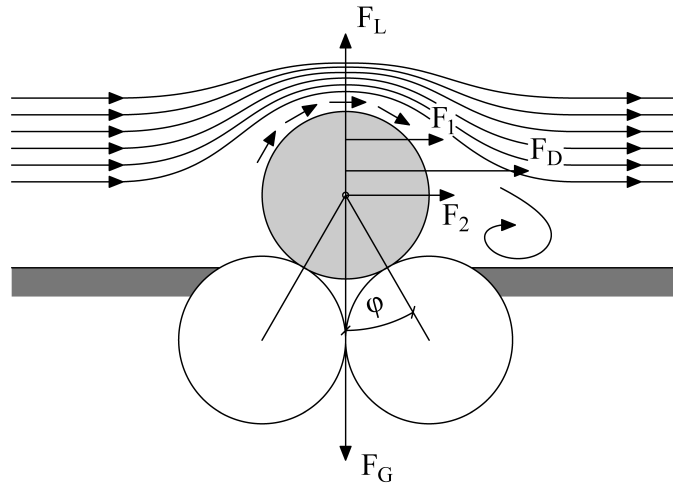
Figure 2.1: Forces acting on particles resting on a horizontal bed.

Critical shear stress

The critical condition for the incipient motion is reached when the forces acting on the particle exceed those stemming from the submerged particle weight. Taking the connection between flow velocity and shear stress into account, which is given through resistance equations (e.g. Eq. (2.14)), the equilibrium of forces acting on a particle

$F_G \leq F_D + F_L$ can be rearranged so that the critical condition can be expressed in terms of a critical shear stress:

$$\tau_{cr} = E \left(\rho_S - \rho \right) g d \tag{2.30}$$

here E is a dimensionless stability coefficient that incorporates the dependencies on the particle and flow characteristics near the bed.

One of the earliest approaches for the critical shear stress for uniform grains was proposed by Schoklitsch (1914):

$$\tau_{cr} = \sqrt{0.201 \gamma \left(\gamma_S - \gamma \right) \lambda d^3} \tag{2.31}$$

with λ as a coefficient for particle shape, that is $\lambda = 1$ for spheres, γ as the specific weight of the fluid and γ_s the specific weight of the particle.

Graf (1971) and Zanke (1982) give a comprehensive overview of earlier incipient motion approaches. Today, the approach proposed by Shields (1936) is widely used for the determination of critical bed shear stresses. For the case of a flat bed with uniformly sized grains, Shields (1936) found the critical condition for incipient motion to be a function of the grain Reynolds number Re_* and defined:

$$\theta_{cr} = \frac{\tau_{cr}}{\left(\rho_s - \rho \right) g d} = f \left(\frac{u_{*,cr} d}{\nu} \right) \tag{2.32}$$

where θ_{cr} is the critical Shields parameter and $u_{*,cr} d / \nu$ refers to the critical grain Reynolds number $Re_{*,cr}$.

For large values of Re_*, i.e. hydraulically rough flow, the Shields parameter becomes independent of the Reynolds number, so that incipient motion is only a result of inertia forces and not viscous drag forces (Zanke, 1982). In the experiments carried out by Shields (1936), the Shields parameter approaches a constant value of $\theta_{cr} = 0.06$ for $Re_* \geq 400$ (Graf, 1971). The definition of the incipient motion threshold by Shields (1936) was based on sediment transport rate measurements for several types of bed load with different grain weight, grain size and gradation as well as grain shape. The bed shear stresses at which the transport rates approach zero were considered as critical conditions. However, the exact extrapolation method was not given. According to Dittrich (1998), several authors have shown ongoing sediment transport below the Shields curve. By comparing the influence of different definitions for the initiation of motion, Delft Hydraulics (1972) (after Van Rijn, 1993) and Graf and Pazis (1977) clearly demonstrated that the threshold values given by Shields (1936) represent a frequent particle movement instead of a complete absence of motion. The values of the critical Shields parameter are therefore controversially discussed in literature and the values found by Shields (1936)

are usually considered to overestimate the critical shear stresses of embedded particles. Buffington and Montgomery (1997) presented a very comprehensive overview of incipient motion studies over eight decades. They reported a wide range of critical Shields parameters for the median grain size between 0.03 – 0.086 for high Reynolds numbers, strongly depending on the method used for the determination of incipient motion.

The stochastic nature of particle entrainment caused several authors (e.g. Gessler, 1971; Grass, 1970; Paintal, 1971) to modify the threshold given by Shields (1936) by a probabilistic approach. According to Grass (1970), particle entrainment can be characterised by the probability functions of instantaneously turbulent bed shear stresses and that of the resistance shear stress of the particle. The amount of overlapping of those probability functions is an indicator for sediment motion. Grass (1970) defined the threshold for incipient motion in terms of the standard deviation of those functions. In addition, Zanke (1990) extended the Shields approach by considering an additional risk of 10 % for the particles to be moved. Derived from experiments on sediment transport in steady uniform flow, Meyer-Peter and Müller (1948) presented an adjusted critical Shields parameter for both uniformly and nonuniformly sized sediment bed. For hydraulic rough flow, they proposed a critical Shields parameter of $\theta_{cr} = 0.047$ based on d_m (cp. Eq. (2.5)) for graded sediments, instead of d_{50}, which is often used for uniform sediments.

Because both sides of Eq. (2.32) are related to the shear velocity u_*, critical shear stresses can only be determined iteratively (Van Rijn, 1993). To overcome this impracticality, Bonnefille (1963) introduced the dimensionless particle diameter D_* as:

$$D_* = \left[\frac{\left(\frac{\rho_s}{\rho} - 1 \right) g}{\nu^2} \right]^{\frac{1}{3}} d_i \tag{2.33}$$

According to Van Rijn (1993), the critical Shields parameter can be parametrized in terms of D_* with:

$$\theta_{cr} = 0.24 D_*^{-1} \quad for \ 1 < D_* < 4$$

$$\theta_{cr} = 0.14 D_*^{-0.64} \quad for \ 4 < D_* \le 10$$

$$\theta_{cr} = 0.04 D_*^{-0.1} \quad for \ 10 < D_* \le 20 \tag{2.34}$$

$$\theta_{cr} = 0.013 D_*^{0.29} \quad for \ 20 < D_* \le 150$$

$$\theta_{cr} = 0.055 D_* \quad for \ D_* > 150$$

Soulsby and Whitehouse (1997) proposed an algebraic expression for the Shields curve based on D_* and improved it for very fine grain sizes. The expression has also been validated for a large set of wave and combined wave and current data, making it universally applicable for coastal environments:

$$\theta_{cr} = \frac{0.30}{1 + 1.2 D_*} + 0.055 \left[1 - exp\left(-0.020 D_*\right)\right] \qquad (2.35)$$

Critical flow velocity

Due to their simplicity, critical flow velocity based approaches are often considered for the determination of required stone sizes for bed stabilization concepts in hydraulic engineering. They consider either the near-bed or the depth-averaged flow velocity as decisive flow parameter, as the former is sometimes difficult to measure. According to Zanke (1982), one of the earliest studies for critical velocities of particles was carried out by Brahms (1754), who found the critical near-bed velocity $u_{b,cr}$ to be a function of the particle size d in the form $u_{b,cr} = ad^{0.5}$, with a being a constant. A well-known approach for the erosion and transportation of uniform sediments in loose beds is the diagram presented by Hjulström (1935). The proposed critical velocities represent the depth-averaged flow velocities at a water depth of 1 m. Zanke (1977) proposed an analytical estimation of the Hjulström curve by:

$$\overline{U_{cr}} = 2.8\sqrt{\gamma g d} + 14.7\frac{\nu}{d}c \qquad (2.36)$$

with c as the parameter for adhesion forces.

Most of the more recent approaches for the initiation of motion utilize a critical flow velocity that can be expressed in the form given by Isbash (1936), which was initially developed to assess the stability of dams:

$$\overline{U_{cr}} = E\sqrt{2g \left(\frac{\rho_s}{\rho} - 1\right) d} \qquad (2.37)$$

where E is again a dimensionless stability parameter.

Isbash (1936) proposed a value of $E = 0.86$ in case the stone is exposed to the flow and a value of $E = 1.2$ if the stone is embedded in between other stones. As the flow velocity is linked to the bed shear stress by a resistance equation (Eq. (2.14)), the formulation of

Eq. (2.37) is inevitably similar to the critical condition expressed in terms of critical shear stress (Eq. (2.30)). Recking and Pitlick (2012) showed that the equation developed by Isbash (1936) is consistent with the approach derived by Shields (1936) for predicting the motion of sediments. However, based on standard resistance equations, the Isbash formulation can result in an overestimation of rock sizes in riprap design in mountain streams. Additional approaches define E in terms of the ratio of water depth to grain size, examples are the approaches of Neill (1967) and Maynord (1987). An overview of equations and methods for estimating stone sizes in riprap design based on a critical velocity is provided by Melville and Coleman (2000).

2.2 BED STABILITY

River and sea beds are composed of a sediment mixture containing several grain sizes. A composition of finer grain sizes, within the sand and clay classes, can be found predominantly in estuarine and marine environments. In rivers and large gradient mountain streams, the sediment mixture becomes coarser and holds a large share of gravel sized particles. According to Dyer (1986), the gradation of the sediment can be considered well sorted if $d_{84}/d_{16} < 2$, and described as poorly sorted (or widely graded) if $d_{84}/d_{16} > 16$. The frequency distribution of grain sizes in natural streams is often expected to follow a log-normal (Gaussian) characteristic (Bunte and Abt, 2001), or in case of crushed stones for artificial bed protection, a Rosin-Rammler (Weibull) function (CIRIA, 2007). The determination of grain size distributions of water worked sediment beds is however being complicated by the intrinsic attempt of graded sediments to form a protective layer at the bed surface over time, known as *armor layer*. The armor layer is a result of repositioning processes and sorting mechanisms leading to a compositional change of the upper layer of the sediment bed. Over time, the grain size distribution of the armor layer becomes significantly coarser than that of the parent (or subsurface) material. As coarser grains are inherently harder to mobilize, the overall stability of the sediment bed is enhanced. Additionally, the increased roughness will alter the fluid-bed interaction and thus influence the effective shear stresses available to the bed surface. The armor layer is attributed a thickness corresponding to the diameter of the largest grain within the parental sediment mixture (Gessler, 1965). In contrast to uniformly sized sediments, the mobility of an individual particle within a sediment mixture is not just depending on the particle weight and the exerted hydrodynamic forces, but also on the interaction with surrounding particles and unequal exposure (Chin, Melville, and Raudkivi, 1994). This renders the determination of the threshold of motion for individual particles as well as the assessment of sediment transport rates and bed stability even more complex. On

the upside, the self-stabilizing characteristics of the armor layer might be exploited for scour and bed protection design with nonuniform granular material (riprap), particularly in a dynamically stable design that allows the limited movement of stones.

2.2.1 *Armor layer development*

If exposed to a flow, the finer particles of a nonuniformly sized sediment bed will erode earlier than the coarser fractions. Over time, this preferential erosion of finer particles will lead to an exposure of larger ones and subsequently lead to a concentration of coarse fractions in the top layer of the bed surface. By interlocking, the on the bed surface remaining fractions form a more and more compact sediment structure, which will protect the finer subsurface material from erosion. Until an equilibrium state is reached, at which the sediment transport approaches a minimum, the stability of the bed will successively increase as its surface will continue to coarsen (Dittrich, 1998; Jain, 1990). If the bed shear stress is increased above the equilibrium state, the armor layer recomposes and larger particles are set in motion until a new equilibrium state is reached asymptotically (Chin, Melville, and Raudkivi, 1994). Eventually, a critical condition is exceeded at which all particles will be in motion and no armor layer can develop. Chin, Melville, and Raudkivi (1994) also pointed out that, consequently, a sediment mixture has a given range of bed shear stresses over which an armor layer can develop, depending on the composition of the parent material. They added that a widely graded mixture will have a larger range of critical bed shear stresses at which armoring can occur than a well sorted mixture. Dittrich (1998) summarized grading criteria by several authors for the ability of the sediment mixture to form an armor layer. Among them Gessler (1965), who found a ratio of $d_{84}/d_{50} > 2$ for the sediment mixture necessary to armor and Little and Mayer (1976), who proposed a critical value of $\sigma_g \geq 1.3$.

Nevertheless, even at the state of equilibrium, all grain size fractions of the parental sediment mixture are still present in the armor layer (Gomez, 1984). Due to the stochastic distribution of turbulent shear stresses, the effective time-averaged shear stress available for some finer particles is smaller than the total averaged shear stress exerted by the flow (Gessler, 1965), which results in a *hiding* of those particles. According to Parker and Klingeman (1982) the hiding phenomenon can further be distributed in microscopic and macroscopic hiding. Microscopic hiding describes the decreased mobility of finer grains in a sediment mixture as they protrude less into the flow and are sheltered behind larger stones. Likewise, the mobility of larger grains is increased because they are more exposed to the flow than they would be in a uniformly distributed sediment bed. Thus, mi-

croscopic hiding depends on the relative placement of grains within the bed surface and equals the mobility of different sized grains in a sediment mixture exposed to flow. The mobility is further equalized by macroscopic hiding, which relates to the effect of the armor layer composition itself. The relative mobility of finer grains is of course reduced by their relative small presence within the armor layer (Parker and Klingeman, 1982).

The coarsening of the bed surface is initiated by one of two sorting processes, leading to either a *static* or a *mobile* armor layer. A static armor layer develops if fine grains are selectively washed out at the surface by a *downstream winnowing* process, leading to a coarse, yet immobile surface layer under a constant load (Gessler, 1971; Little and Mayer, 1976; Proffitt and Sutherland, 1983). As mentioned earlier, an equilibrium state will be attained over time for each incremental increase of exerted shear stress, until a critical shear stress is reached, above which no stable armor layer can be formed. Until then, the composition of the eroded bed load remains finer than that of the parent material. Static armor layer development can be found in river reaches, where upstream sediment supply is hindered, thus leading to an imbalance between sediment supply and bed load transport capacity (Efthymiou, 2012). In contrast, upstream sediment supply allows the sediment bed to form a sustained mobile armor layer. Here, the *vertical winnowing* process, in which finer fractions tend to fall in voids created by the entrainment of larger fractions (Gomez, 1984), is leading to an overexposure of larger fractions. As a result, the mobility between small and large fractions is equalized and the entire range of available grain sizes is mobile. As all fractions are transported at the same rate, the grain size distribution of the transported material has to be similar to that of the subsurface material. Experiments on the development of a mobile armor layer were carried out among others by Mao, Cooper, and Frostick (2011), Parker and Klingeman (1982) and Parker, Dhamotharan, and Stefan (1982).

2.2.2   *Stability concepts*

Hiding and exposure processes render the determination of bed stability for sediment mixtures more complex than for beds with uniformly sized particles. These processes are related to the particle characteristics, spatial distribution and even orientation of the particles within the bed surface, and thus, making a threshold of motion assessment beyond the sole consideration of forces acting on a single grain necessary. Numerous studies have thus been carried out to extend the concept of Shields (1936) regarding the fractional incipient motion for nonuniform sediments by defining hiding functions that describe how incipient motion for individual grain sizes d_i in a bed composed of nonuniform sediments deviates from those in uniform

beds (e.g. Ashida and Michiue, 1971; Egiazaroff, 1965; Einstein, 1950; Kuhnle, 1993; Parker, Dhamotharan, and Stefan, 1982; Patel, Patel, and Porey, 2014; Wilcock, 1993). Generally, these approaches assume that the self-stabilising effects of sediment grading can be represented by the size ratio d_i/d_R expressed by a power law function:

$$\frac{\theta_{cr,i}}{\theta_{cr,R}} = \left(\frac{d_i}{d_R}\right)^{b-1} \tag{2.38}$$

where d_R is a selected reference size fraction within the sediment mixture, $\theta_{cr,i}$ is the critical Shields parameter of the grain size of interest d_i, $\theta_{cr,R}$ is the critical Shields parameter of the reference grain size d_R, and b is the exponent of the power law function.

The dimensional form of Eq. (2.38) can be derived by considering Eq. (2.32) and reads:

$$\frac{\tau_{cr,i}}{\tau_{cr,R}} = \left(\frac{d_i}{d_R}\right)^{b} \tag{2.39}$$

with $\tau_{cr,i}$ being the critical shear stress of the grain size of interest d_i, $\tau_{cr,R}$ being the critical shear stress of the reference grain size d_R.

As pointed out by Komar (1987), the application of Eq. (2.38) is made difficult by the requirement to select a reference grain size for the normalization of the relationship, that is representative for the stability behaviour of the whole sediment mixture. While many authors used d_m (e.g. Egiazaroff, 1965; Hayashi, Ozaki, and Ichibashi, 1980) or d_{50} (e.g. Kuhnle, 1993; Parker, Dhamotharan, and Stefan, 1982) as reference grain size, more recent models (e.g. Patel and Ranga Raju, 1999; Shvidchenko, Pender, and Hoey, 2001) also acknowledge the standard deviation σ_g to be an important value. Nevertheless, to the author's knowledge, there is still no commonly accepted value to date. Due to the presence of the armor layer with its coarser composition, the reference grain size will also differ significantly whether it is based on the surface (Parker and Klingeman, 1982) or the subsurface material (Andrews, 1983). Based on their comprehensive literature review, Buffington and Montgomery (1997) indicated that scaling the critical shear stress with subsurface based reference grain sizes usually produces larger values of $\theta_{cr,R}$ than with surface based ones. They also added that the reference value should be based on the surface (armored) material, since the initiation of motion is eventually controlled by the grains on the bed surface. However, as the armor layer development is a transient process, the grain size distribution of the bed surface will change over time and in turn altering the reference value. This aspect becomes especially important for the determination of a stone size required to achieve a specified bed stability for granular bed or scour protection, which should be stable right after

the installation as well as later on. The grain size distribution of the fully developed armor layer might be estimated based on the parent (subsurface) material by approaches proposed by Günter (1971) or Schöberl (1979). Additionally, bed stability approaches are available for both a fully developed armor layer with maximum bed stability (e.g. Chin, 1985) and for an armor layer during the development (e.g. Parker and Klingeman, 1982).

Regardless of the definition of the reference grain size, the character of the hiding function (Eq. (2.38)) has been found to differ significantly between available approaches. The differences can certainly be attributed to the methods used to define the threshold of motion, the determination of the critical shear stress and the significantly different characteristics of the investigate bed material. With respect to sediment mobility and incipient motion threshold, available hiding functions are framed by two extremes, which are described by the concepts of equal and selective mobility. The concept of equal mobility, introduced by Parker and Klingeman (1982) for mobile armor layers, suggests the equalization of particle mobility by hiding and exposure processes that compensate the weight effects to a certain extent. As pointed out by Efthymiou (2012), this concept does not imply that there is a complete equalization of mobility over all grain sizes within the mixture but a strong tendency towards it. In contrast, the concept of selective mobility advocates the particle independent mobility, i.e. the stability concept introduced by Shields (1936). According to this concept, the critical shear stress of a particle is proportional to its mass. Consequently, coarser grain fractions in a sediment mixture require larger critical shear stresses to be entrained than finer fractions. Komar (1987) used this concept to explain the formation of coarse armor layers by downstream winnowing processes, which are initiated by the wide range of critical shear stresses between individual grain fractions. For a widely graded sediment, with a potentially large selective mobility, a suitable definition of the reference grain size and its critical shear stress is thus much more important than for a well sorted sediment. In mathematic terms, equal mobility is reached if the exponent b in Eq. (2.38) and Eq. (2.39) approaches zero, leading to $\tau_{cr,i} = \tau_{cr,R}$ and thus the entrainment of all fractions at the same critical shear stress $\tau_{cr,R}$. Accordingly, an exponent of $b = 1$ leads to $\theta_{cr,i} = \theta_{cr,R}$, implying that all fractions are entrained at the same dimensionless critical shear stress and exhibit a grain independent, selective mobility. According to Efthymiou (2012) the exponent b can be interpreted as a factor that represents the dominance of particle mass effects ($b \to 1$) over the mobility equalizing hiding effects ($b \to 0$). The influence of b on the mobility is also represented in the following Fig. 2.2.

For a systematic comparison of most existing hiding approaches differentiated by incipient motion definition, median grain size type,

(a) Plot of Eq. (2.39).   (b) Plot of Eq. (2.38).
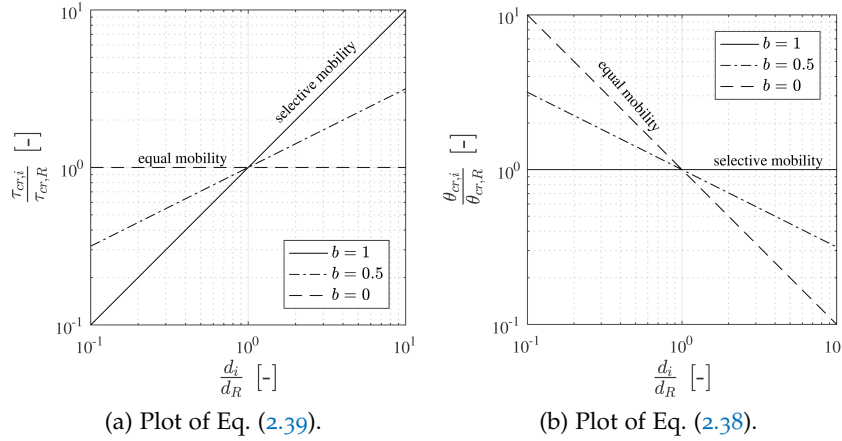
Figure 2.2: Comparison of stability concepts after Efthymiou (2012).

relative roughness and flow regime, the author again points to the work of Buffington and Montgomery (1997).

2.2.3 *Influence of sediment gradation*

Little and Mayer (1976) conducted a series of experiments on the effects of sediment gradation on armoring. For lognormal distributed sediments with geometric standard deviations in the range $1.3 < \sigma_g < 3.0$ they found that the armor layer composition becomes coarser with increasing σ_g of the parent material. A widely graded sediment contains more fine material than a well sorted sediment, meaning that for a given shear stress a larger amount of fine material will erode, leaving a coarse armor layer. In addition, they determined the d_{95} diameter of the parent material to be the maximum diameter at which armoring can occur. This implies that as long as the applied shear stress is smaller than the critical shear stress of d_{95}, a stable armor layer will eventually form. The critical shear stress of d_{95} might thus be a valuable stability criterion for the design of the required stone size for a bed of scour protection concept made from graded material.

Furthermore, Wilcock and Southard (1988) combined own experimentally obtained data with previously published ones to assess the influence of mixture sorting on the initial motion of individual fractions in a sediment mixture. They found that the sediment sorting has little effect on the critical shear stress of individual grains, as long as the mobility differences between grains are described in terms of relative grain d_i/d_{50}. Their analysis is based on the juxtaposition of $\theta_{cr,i}$ and d_i/d_{50}, which showed similar trends close to equal mobility and thus independence from σ_g. Eventually, they determined their findings to be generally valid, as the trends were also consistent with those for uniformly sized sediments.

Shvidchenko, Pender, and Hoey (2001) also conducted experiments with different graded sediment mixtures and compared the results to several data sets from literature. While the dimensionless critical shear stresses followed a similar trend for large fractions ($d_i/d_{50} > 1$) in all sediment mixtures, likewise to the results from Wilcock and Southard (1988), their trend varied for fine fractions. Shvidchenko, Pender, and Hoey (2001) attributed the variation partly to the effect of sediment gradation and showed that the exponent b in Eq. (2.38) systematically increases with increasing σ_g. In other words, the larger the gradation of a sediment mixture, the less the hiding effect and the higher the selective, grain independent mobility of finer fractions.

2.3   SCOURING AROUND PILES

A reliable prediction of expected maximum scour depths has to be an integral part of the design process. The scour depth determines whether the design of the structure can be adapted or what scour protection concept can be implemented to reduce its negative effects (Whitehouse, 1998). In addition, as pointed out by Whitehouse (1998), the assessment of scour should already be included in the early stages of the design process and be re-evaluated later on, because remedial measures and maintenance works can be expensive. Besides the maximum scour depth, an accurate prediction of scouring rates is also required to determine suitable time windows for the installation of the structure as well as for the remedial or maintenance works.

Numerous studies have been carried out on the scour development at piles under unidirectional, steady currents (e.g. Breusers, Nicollet, and Shen, 1977; Chiew, 1984; Kothyari, Garde, and Ranga Raju, 1992; Melville and Chiew, 1999; Raudkivi and Ettema, 1983; Sheppard, Odeh, and Glasser, 2004) or due to waves (e.g. Carreiras et al., 2000; Stahlmann, 2013; Sumer and Fredsøe, 2001b; Sumer, Fredsøe, and Christiansen, 1992). While the mechanics leading to scour are similar in flow and wave regimes, the interaction of both makes the scour problem considerably more complex in the marine environment than that at structures in rivers. Facilitated by the availability of more sophisticated wave-current flumes in recent years, there is also an increasing number of studies that take the time varying aspects of realistic sea conditions, i.e. combined random wave and tidal currents, into account (e.g. Eadie and Herbich, 1986; Qi and Gao, 2014; Rudolph and Bos, 2006; Sumer and Fredsøe, 2001a; Sumer et al., 2013). However, there is still a lack of knowledge regarding the influence of directional sea on the scour development as well as a fundamental problem with the access to field data from offshore sites to the public, which significantly complicates the valuation of laboratory obtained data.

This section focuses on the general processes of local scour around slender piles. Effects of diffraction at large piles, cohesive or layered sediments, global and contraction scour are not addressed. Information on these topics and further details on the scouring processes around a pile in fluvial or marine environment can be obtained from the comprehensive descriptions in Breusers and Raudkivi (1991), Hoffmans and Verheij (1997), Whitehouse (1998), Melville and Coleman (2000) and Sumer and Fredsøe (2002).

2.3.1 *Hydrodynamics near a pile*

The complex vortex system around a pile, which leads to the development of scour, can be separated into the following components: (a) the downflow at the upstream side of the pile, (b) the horseshoe vortex, (c) the lee-wake vortices and (d) the streamline contraction. The formation of the vortex system is not only depending on the approach flow characteristics and pile shape, but it also interacts constantly with the increasing depth and extent of the scour pit. At the upstream side of the pile, the vertical distribution of the approaching flow introduces a stagnation pressure gradient towards the water surface, leading to a downwards pointed flow (Dargahi, 1989). Consequently, the approaching flow separates three dimensionally upstream of the pile, creating the rotary horseshoe vortex that trails downstream along the sides of the pile. The horseshoe vortex is affected by the developing scour hole and its core becomes larger with increasing scour depth, while the induced bed shear stresses decrease with increasing scour depth eventually (Dey and Raikar, 2007).

Indicated by shear stress measurements by Hjorth (1975) or as observed by Ettema (1980) for steady flow conditions, the position of the scour initiation is located approx. 45° to the direction of approaching flow. At this position, according to the measurement of Hjorth (1975), time averaged bed shear stresses $\overline{\tau}$ can be up to 11 times larger than the bed shear stresses exerted by the undisturbed flow $\overline{\tau_\infty}$. The shear stress amplification around the pile is generally expressed by the factor $\alpha_{amp} = \overline{\tau}/\overline{\tau_\infty}$. In steady flow conditions, the size of the horseshoe vortex mainly depends on the boundary layer thickness of the approaching flow, the pile Reynolds number $Re_D = UD/\nu$ and the bed roughness (Roulund et al., 2005). With decreasing boundary layer thickness, the separation distance from the upstream side of the pile will be reduced, leading to a smaller horseshoe vortex (Sumer and Fredsøe, 2002). Likewise, a small Reynolds number will also result in a small horseshoe vortex. However, while this holds true in a laminar flow regime, it is noted by Sumer and Fredsøe (2002) that this relationship may be reversed in a turbulent flow, so that an increase of the Reynolds number will lead to a decrease of the horseshoe vortex. To describe the formation of the horseshoe vortex in the case of os-

cillatory (waves) flow, the Keulegan-Carpenter number *KC* is used as additional parameter:

$$KC = \frac{U_w T}{D} \tag{2.40}$$

in which T is the wave period, D is the pile diameter and U_w is the amplitude of the orbital flow velocity, which can be calculated for monochromatic waves based on Eq. (2.17) or in case of wave spectra with Eq. (2.19).

For short wave periods, and thus small values of *KC*, only a thin wave boundary layer is able to form with respect to the pile diameter. Consequently, with a less pronounced pressure gradient at the pile only a small horseshoe vortex can be expected to emerge. Experiments conducted by Sumer, Christiansen, and Fredsøe (1997) with Reynolds numbers in the order of $Re_D = O\left(10^3\right)$ indicate that no horseshoe vortex will develop below a limit of $KC = 6$. With larger wave periods, the pressure gradient will be maintained over a longer duration and the boundary layer separates upstream of the pile again. Thus, for each half cycle, a horseshoe vortex similar to that under steady current will form for larger values of *KC* (Sumer and Fredsøe, 2002). In case a current is superimposed on a wave, Sumer, Christiansen, and Fredsøe (1997) found that a horseshoe vortex develops at decreasing values of *KC* with increasing current velocity. However, the horseshoe will be mainly present during the half cycle in which the wave-induced flow propagates in the same direction as the current.

The lee-wake vortices are generated by a rotation in the boundary layer at the pile surface and its separation form the sides of the pile. As a result, a shear layer is formed, that will roll up into the lee-wake vortex (Sumer and Fredsøe, 1997). Vortex shedding can already be observed for flow Reynolds numbers $Re > 40$. With increasing Re the lee-wake transitions from a laminar to a turbulent state. According to Breusers and Raudkivi (1991), the sediment transport by these vortices is initiated by a vertical lift, that develops in the centre of the vortices due to a pressure gradient. A comprehensive overview of mechanism behind the vortex shedding as well as its dependency to different flow characteristics, the pile roughness and shape are given by Sumer and Fredsøe (1997). In the case of oscillating flow, the formation of the lee-wake vortices becomes essential for the scouring process and, like the horseshoe vortex, it additionally becomes a function of the KC number. The experiments of Sumer, Christiansen, and Fredsøe (1997) have shown, that vortex shedding at a pile occurs only for $KC > 6$, which is similar to but not the same as the threshold for the formation of a horseshoe vortex. At last, the streamlines around the pile are contracted and accompanied by enhanced flow velocities within a distance of one pile radius (Whitehouse, 1998). The com-

bined effect of the horseshoe vortex and the streamline contraction can lead to an amplification of the bed shear stresses near the pile by an factor of 4 in the case of waves. For steady currents, the amplification can even reach a factor of 10.

2.3.2 *Scouring induced by steady current*

Under steady currents the formation of a horseshoe vortex is decisive for the scouring process. The emerging scour hole develops in a conical shape around the pile, with steeper slopes at the upstream than at the downstream side of the pile. Thereby, the slope angle at the upstream side resembles that of the angle of repose of the sand. From the scour hole the sediment is transported downstream by the horseshoe vortex and eventually deposes in parts outside the hole. Assuming constant relative density, the main effects of flow, sediment and pile diameter on the local scour depth S in a steady current can be summarized in dimensionless terms by:

$$\frac{S}{D} = f\left(\frac{U}{U_{cr}}, \frac{h}{D}, \frac{U}{\sqrt{gD}}, \frac{D}{d}, \sigma_g, Re_D, T^*\right) \tag{2.41}$$

with T^* as the dimensionless time being an indicator for the scouring rate over time.

The first parameter on the right-hand side of Eq. (2.41) expresses the flow intensity, the second parameter the relative flow depth, the third parameter represents the pile Froude number and the fourth and fifth parameter account for the influence of the sediment size and grading. Instead of the pile Froude number, Ettema, Melville, and Barkdoll (1998) considered the Euler number U^2/gD more useful in describing the flow gradients around the pile.

With respect to the flow intensity, the sediment mobility can be categorised in either clear-water or live-bed condition. In clear-water conditions, in which the mean flow velocities are below the critical value for sediment motion ($U/U_{cr} < 1$ or $\theta/\theta_{cr} < 1$), the local scour depth increases almost linear with increasing flow velocity. As the threshold of sediment motion is exceeded ($\theta/\theta_{cr} > 1$), i.e. live-bed conditions, the constant sediment supply from upstream leads to a partial refilling of the scour hole. Consequently, beyond the threshold of motion, the scour depth decreases with increasing flow intensity at first but increases again until a second live-bed peak is reached (Melville and Coleman, 2000). At this second peak, flow velocities are large enough so that sheet flow conditions are approached. The influence of flow intensity on the scour depths was investigated intensively by many authors including Raudkivi and Ettema (1983), Chiew (1984), Baker (1986) and Sheppard and Miller (2006).

In laboratory experiments, sediments with particle diameters close to those in the field are often used to avoid cohesive sediment behaviour. Consequently, to ensure similitude of sediment mobility, flow velocities are scaled according to desired flow intensities, leading to Froude numbers that are significantly larger than those in the field. As Ettema, Melville, and Barkdoll (1998) point out, larger Froude numbers might induce steeper pressure gradients between the stream-wise sides of the pile, affecting the flow field in its vicinity. As a result, scour depths obtained in laboratory experiments might overestimate those in the field. The influence on the flow gradient might be best described by the Euler number, which represents the ratio of stagnation head to the pile diameter. In addition, Ettema, Kirkil, and Muste (2006) also attributed the increase of scour depths with larger Euler numbers to an increase of the shedding frequency and vorticity of the lee-wake vortex.

The relative flow depth (or pile height) influences the formation of the horseshoe vortex in a way that the size of the horseshoe vortex will be reduced with decreasing flow depth, resulting in a reduction of scour depth. For larger water depths, the scour depth will become almost independent of the water depth. According to Sumer and Fredsøe (2002), the influence of the relative flow depth on the scour depth can be expected to diminish for ratios larger than $h/D \geq 5$. Whereas Breusers, Nicollet, and Shen (1977) concluded, that already for $h/D \geq 3$ the influence of the relative water depth can be neglected. Nevertheless, the relative flow depth will be a more important factor for the scour development at bridge piers than for piles, which are used as support structures in relative deep offshore waters.

Graded sediments tend to develop a protective armor layer on the bed surface over time. The non-uniformity of the sediment should thus also be considered to have an effect on the scour depth. Ettema (1976) conducted experiments regarding the influence of sediment gradation on the scour depth for clear-water conditions and found for these conditions a considerable reduction of scour depths with increasing sediment grading. Baker (1986) complemented those findings with experiments under live-bed conditions. While the results also showed a general reduction in scour depths with increasing sediment gradation, they indicated a diminishing influence of sediment gradation for larger flow intensities. However, as the bed surface is coarsening with developing armor layer, the median grain size of the armor layer becomes inherently harder to mobilize than that of the subsurface sediment. As a result, the threshold peak at $U/U_{cr} = 1$ shifts to larger flow intensities with increasing sediment gradation. The classification in clear-water and live-bed conditions and its implications on the scouring process must thus be considered more differentiated in case of non-uniform sediments.

In addition to the gradation, the coarseness of the sediment also effects the scour depth. Melville and Sutherland (1988) combined data obtained by Ettema (1980) for clear-water and by Chiew (1984) for live-bed conditions. They derived a threshold value of $D/d \geq 25$ beyond which the scour depth is unaffected from the grain size of the sediment. Until this value, the scour depth decreases with larger grain sizes, as would have been expected. A more recent study by Sheppard, Odeh, and Glasser (2004) extended the data to much larger values of D/d, at which the scour depth started to decrease again. Based on the analysis of several field and laboratory data sets, Lee and Sturm (2009) confirmed the peak at $D/d \geq 25$ but also added that scour depths approach an almost constant value at around $D/d \geq 400$. Due to the well-known issue of geometric sediment scaling, the consideration of the effects of sediment size on the scour depth might be especially important when scaling from large diameter piles for offshore structures to small scale laboratory experiments.

Scouring is a time dependent process. Under clear-water conditions, the scour depth asymptotically approaches an equilibrium state. Under live-bed conditions, the scour depth increases more rapidly but oscillates around an equilibrium depth as bedforms propagate periodically into the scour hole from upstream (Melville and Coleman, 2000). The equilibrium depth at the end of the scouring process is usually of particular interest, as it resembles the conservative estimate for the stability design of structures exposed to scour. However, due to the very slow increase of scour depth under clear-water conditions, the equilibrium state may not be reached at all, e.g. in areas where the transient hydrograph only exhibits scour relevant flow velocities at very few occasions a year. The scouring process over time can be quantified by a representative time scale T_s. Sumer, Christiansen, and Fredsøe (1992) defined T_s as the time needed for the scouring process to reach 63% of the equilibrium scour depth. The time scale can be derived either by integration of the scour development over time (Fredsøe, Sumer, and Arnskov, 1992; Fuhrman et al., 2014) or by calculating the slope of the tangent through the start of the scour development (Sumer, Christiansen, and Fredsøe, 1992). In the steady current case the time scale is a function of the Shields parameter and the boundary layer thickness and is given in a normalized form T^* by Sumer, Christiansen, and Fredsøe (1992) as:

$$T^* = \frac{1}{2000} \frac{\delta}{D} \theta^{-2.2} \tag{2.42}$$

while the conversion to the dimensional formulation of the time scale is given by:

$$T_s = \frac{D^2 T^*}{\left(g \left(\frac{\rho_s}{\rho} - 1 \right) d^3 \right)^{0.5}} \tag{2.43}$$

with δ as the boundary layer thickness.

For clear-water conditions ($1 \geq U/U_{cr} \geq 0.4$), Melville and Chiew (1999) defined the time needed for equilibrium scour to develop t_e as:

$$t_e\ (days) = 48.26\frac{D}{U}\left(\frac{U}{U_{cr}} - 0.4\right)\ \ for\ \frac{h}{D} > 6 \qquad (2.44)$$

$$t_e\ (days) = 30.89\frac{D}{U}\left(\frac{U}{U_{cr}} - 0.4\right)\left(\frac{h}{D}\right)^{0.25}\ \ for\ \frac{h}{D} \leq 6 \qquad (2.45)$$

Here, t_e marks the time at which the increase of scour depth over the duration of one day does not exceed a value equivalent to 5% of the pile diameter.

2.3.3   *Scouring induced by waves*

In addition to the influences on the scour process under steady current conditions, the *KC* number (cp. Eq. (2.40)) becomes a major factor for the scour depth development under waves, as concluded by Sumer, Fredsøe, and Christiansen (1992) and Kobayashi and Oda (1994). For small values of *KC* (*KC* < 6), the thickness of the wave boundary layer is too thin to generate a strong horseshoe vortex at the upstream side of the pile. Similarly, no vortex shedding at the lee side of the pile emerges below *KC* = 6 (Sumer, Fredsøe, and Christiansen, 1992). As a consequence, only insignificant scour depths are to be expected, which are induced only by the general flow disturbance and streamline contraction at the sides of the pile. As the *KC* number increases, so does the scour depth until it reaches a constant value close to the equilibrium scour depth obtained for steady current conditions. It can thus be concluded, that for *KC* > 100 the driving force for the scour development is the horseshoe vortex, as the wave-induced flow approaches steady current conditions. For smaller values of *KC*, however, the major factor are the lee-wake vortices, that cause a net scour in each wave half cycle by transporting sediment downstream from the pile (Sumer and Fredsøe, 2001a). For irregular waves, Sumer and Fredsøe (2001a) found the scour depths to be best represented when the *KC* number is composed by U_w as given in Eq. (2.19) and T_p as the peak period.

Although storm generated sea states in the marine environment are characterized by multidirectional waves, the investigation on how wave spreading influences the scour depth and development is not much given attention so far. This may partly be attributed to the elaborate set-up and procedure of physical as well as numerical models dealing with multidirectional waves in combination with sediment transport processes. It may also be based on the anticipation that the effect of wave spreading on the equilibrium scour depth has to

be on the safer side. Given that the overall wave energy integrated over all directions in a directional wave spectrum should be identical to its underlying frequency spectrum, flow components (and thus *KC* numbers) in the main wave direction have to be slightly smaller than in unidirectional waves. Recently, Ong, Myrhaug, and Hesten (2013) and Myrhaug and Ong (2013) presented a stochastic method to estimate the equilibrium scour depths around piles in random two and three-dimensional nonlinear waves. In their model, the nonlinear wave-crest height distribution is calculated with the method provided by Forristall (2000), in which the wave-crest distribution is parameterised by a two-parameter Weibull function fitted to second-order simulations of JONSWAP spectra. The scour development is given by the approaches presented in Sumer and Fredsøe (2002) for waves and combined wave-current conditions. Furthermore, the authors assumed that mainly the 10% highest waves are responsible for the scour development. For large values of *KC*, they found the scour depths for three-dimensional waves to be slightly larger than those for two-dimensional waves and attributed this outcome to a smaller wave set-down effect of three-dimensional waves. In contrast, the scour depths are larger in two-dimensional waves than in three-dimensional waves for values of $KC \leq 2$. However, due to a lack in available field data, which provides both directional wave measurements and scour depth measurements, the results could not be validated.

2.3.4 *Scouring induced by combined waves and current*

The scour behaviour in combined wave and current situations is related to the parameter U_{cw}, which represents the ratio of undisturbed current U_c to wave generated flow velocity U_w and is given by Sumer and Fredsøe (2001a) as:

$$U_{cw} = \frac{U_c}{U_c + U_w} \tag{2.46}$$

Sumer and Fredsøe (2001a) carried out a systematic study on the influence of combined wave and current conditions on the scour process around a pile. In that study, irregular waves based on the JONSWAP spectrum were used. The authors concluded that in a wave dominated regime ($U_{cw} \to 0$) scour depths close to the waves only case are obtained, whereas towards a current dominated regime ($U_{cw} \to 1$), scour depths asymptotically approach values similar to the current only case. This behaviour is attributed to the lee-wake vortex system, which is stable on the downstream side but suppressed at the upstream side of the pile for large values of U_{cw} and for waves propagating in current flow direction. The results further indicate that for small *KC* numbers only a small superimposed cur-

rent could considerably increase the wave induced scour depths. At larger *KC* numbers, the influence of a current on the wave scour is less pronounced. The results of Sumer and Fredsøe (2001a) are also in general agreement with those obtained by Eadie and Herbich (1986), who found the scour development to be faster and the equilibrium scour depth larger than in the current alone case.

Rudolph and Bos (2006) complemented the data from Sumer and Fredsøe (2001a) with tests for small *KC* numbers in the range of $1 \leq KC \leq 10$. They proposed an improved model for the prediction of equilibrium scour depths based on a best-fit regression of self-generated data and data from Sumer and Fredsøe (2001a). Furthermore, Petersen, Sumer, and Fredsøe (2012) studied the time scale of scour development in combined waves and current conditions. Similar to the scour depths, they found that the time scale of the scouring process also increases significantly if a current is superimposed on a wave. Recently, Qi and Gao (2014) investigated the pore-pressure response and scour development induced by combined waves and current around large diameter piles ($0.44 \leq KC \leq 3.65$). The experimental procedure included the superposition of a current with both following and opposing waves. Regarding the scour development, the results showed generally larger scour depths under combined conditions than under the isolated load of either waves or current. The authors also reported the occurrence of larger maximum flow velocities in the case waves follow the current than in the case of opposing wave direction. Consequently, a directional dependency on the equilibrium scour depth and the time development was given.

Additionally, backfilling of an already established scour hole might occur in case of subsequently changing flow regimes, leading to alternating scour depths. Sumer et al. (2013) conducted a comprehensive series of tests on the topic of scouring and backfilling around a pile. That study found backfilling likely to occur if the flow regime changes from a steady current to either a wave or combined wave and current regime, or if small waves follow larger waves. While the equilibrium scour depth at the end of the backfilling process tends to be similar to that produced by a scouring process, the time scales of both processes are quite different. Depending on the *KC* number of the backfilling process, the time scale of backfilling is much larger than that of scour if $KC < O(10)$ but can be smaller for $KC \gg O(10)$.

2.3.5 *Scour prediction*

Given the mere number of available prediction models, particularly in the case of steady currents, the range of expected scour depths can be rather large for a certain boundary condition, further increasing the uncertainty of a reliable scour depth prediction. This state is also reflected by present guidelines for the design of offshore sup-

port structures, i.e. DNV-GL (2016), BSH (2015) or DIN (2016), which acknowledge the need of considering the effects of scour in the structural design, but at the same time can provide only rudimentary recommendations on expected scour depths, scour prediction or scour protection systems. For example, DNV-GL (2016) recommends the approach given by Sumer, Fredsøe, and Christiansen (1992) for predicting the equilibrium scour depth. Its application is however limited to cylindrical structures, non-cohesive soils, live-bed and "waves-only" conditions with $KC > 6$. It is thus for the experienced engineer to select appropriate scour prediction models for the structure of interest and for given boundary conditions or in some cases to consider additional and clarifying hydraulic model tests. However, it is highly recommended to evaluate the results of several approaches as input for structural design decisions and re-evaluate these decisions later in the design process.

Of those already mentioned in the previous sections, the most commonly applied approaches for the prediction of equilibrium scour depth around piles in steady current conditions are those by Breusers, Nicollet, and Shen (1977), Melville (1997), Richardson and Davis (2001) or Sheppard and Miller (2006). In case of wave only conditions the approach of Sumer, Fredsøe, and Christiansen (1992) is usually considered, while for combined wave and current conditions the approaches presented by Sumer and Fredsøe (2002), Rudolph and Bos (2006) or Zanke et al. (2011) are often referred to. The progression of scour depth over time can be estimated with models by Sumer, Christiansen, and Fredsøe (1992) for both current or wave conditions, or by Melville and Chiew (1999) for the current only case and clear-water conditions. If detailed hydraulic measurements are available, the scour development might also be appropriately predicted by using a time stepping prediction approach in the form presented by Harris, Whitehouse, and Benson (2010) or Raaijmakers and Rudolph (2008). Controlled by the angle of repose, which for most marine sands can be assumed to be around $\phi \approx 30°$, the extend of the local scour hole at equilibrium state might be estimated by $S/\tan\phi$ in case of a steady current (Whitehouse, 1998). In tidal currents (McGovern et al., 2014) or in waves (Sumer and Fredsøe, 2002), the slopes of the scour hole might be less steep, so that an additional security factor should be considered for planning the extend of a scour protection.

2.4 SCOUR PROTECTION DESIGN

While some aspects and concepts for the design of scour protection also apply for fluvial or coastal protection structures, this section focuses on scour protection measures suitable for offshore conditions.

Although scour protection measures usually account only for a relatively small fraction of the total costs of offshore foundation structures, a reliable system preventing the failure and damage of these structures is however indispensable for its stability. To assure the functionality and structural stability throughout their designated life-time, the degrading effects of scour have thus to be considered as integral part of the design. An economic and efficient design has to incorporate the mutual interaction of hydraulic, geotechnical and structural aspects (Schiereck, 2012). As a consequence, the scour protection concept might need to adapt iteratively throughout the design process of the foundation structure. This starts in the first conceptional design stage, where the identification of site-specific boundary conditions leads to first design values, and reaches up to the detailed engineering stage, in which the design is finalized and maintenance cost and a management program over the life-time of the structure are defined (Escarameia, 1998). Even after the installation, unexpected scour development identified through monitoring might require a re-evaluation of planned remedial works.

According to May, Ackers, and Kirby (2002), the scour protection concept might consist of scour reduction measures, structural measures, scour protection measures or a scour monitoring management, depending on design loads, structural design and cost-benefit assessment. Scour reduction measures refer to the optimisation of the flow pattern around a foundation structure, e.g. by collars (Dey, Sumer, and Fredsøe, 2006; McGovern et al., 2012) or sacrificial piles (May, Ackers, and Kirby, 2002), so that the actual formation of scour at the structure is hindered. On the other hand, structural measures improve the foundation structure's resilience by adapting its design, e.g. wall thickness or embedment depth, to the expected scour depth. Scour protection measures aim at reducing the transport potential of the sediment by stabilising the sediment near the structure. Scour protection measures include classical systems like granular scour protection (also denoted as rock armor or riprap), which is described in detail in the following section. Looking for an even more cost-effective alternative, the potential of geotextile sand-filled containers (Peters and Werth, 2012), rubber mattresses, artificial plants or rock filter bags as scour protection measure are also investigated and occasionally applied. The management of scour monitoring and the decision on whether remedial measures are required or not, can be determined by a risk based assessment of structural and financial consequences if defined scour threshold levels are surpassed. A reliable risk based assessment requires detailed knowledge of time-varying scour development for the identification of scour hazards and planning of effective remedial measures. Whitehouse, Harris, and Sutherland (2011) and Harris and Whitehouse (2012) outlined a risk based scour management plan for offshore wind turbine foundations, that provides a

framework for considering the consequences of scour on the design process by a reliable prediction of scour development through time.

Due to its flexibility and the broad experiences with its application, granular scour protection is often preferred over more recent alternatives and still the most applied scour protection system for foundation structures in marine environment (Whitehouse, Harris, and Sutherland, 2011). The following sections will thus focus on design aspects of granular scour protection.

2.4.1 *Failure mechanisms of granular scour protection*

A stable design of a granular scour protection has to account for several possible failure modes. Chiew (1995) and Chiew and Lim (2000) identified the following failure mechanisms a scour protection around a bridge pier is exposed to as:

- **Shear failure:** Dimensions of armor layer stones are not large enough to withstand the hydraulic forces acting on them, leading to their erosion. For the design of required armor stone sizes, the increase of hydraulic loads near the pile has to be considered. According to experiments carried out by Chiew (1995), the threshold for erosion at a pier is already reached at $U/U_{cr} = 0.3$, instead of the more commonly used value of $U/U_{cr} = 0.5$ (e.g. Breusers, Nicollet, and Shen, 1977). Several stability approaches are available for the determination of required armor stone sizes based on the threshold of motion criteria depicted in chapter 2.1.5, of which some are described in chapter 2.4.3.

- **Winnowing failure:** Wash-out of fine bed material through the voids of the armor and filter layer stones, potentially causing a sinking of the scour protection. For a pile exposed to a current, Nielsen et al. (2011) identified the horseshoe vortex as the primary driver for the winnowing process near the pile. If the horseshoe vortex is large enough it penetrates through the scour protection and exerts a bed shear stress to the underlying bed material, causing its erosion. Eventually, the sediment is transported through the scour protection by the upward directed flow at the separation point between the approaching flow and the horseshoe vortex. The winnowing process can thus be controlled by the thickness of the scour protection. A design approach for the estimation of expected winnowing depth in relation to scour protection thickness and pile diameter was presented by de Sonneville, Joustra, and Verheij (2014). With respect to the filter stability design, further approaches aiming to prevent winnowing are given in the next section.

- **Edge failure:** Development of scour at the edge of the scour protection, caused by a sudden change of bed roughness and

elevation height at the outer horizontal interface between scour protection and sand bed. The sediment motion is initiated by a local increase of turbulence in the approaching flow and in turn increased bed shear stresses. Subsequently, the sediment is carried away by occurring secondary flows. Petersen et al. (2014, 2015) conducted extensive experimental tests on the development of edge scour at stone covers in steady currents and wave conditions. They found the scour depth to be dependent on the pile diameter as well as on the thickness and width of the scour protection. To account for edge scour failure, the scour protection is typically extended by falling aprons that slide into the scour hole and suppress further edge scouring.

- **Bed-form induced failure:** Destabilisation of scour protection due to migration of large bed-forms under live-bed conditions. Experiments on bed-form induced failure of a granular scour protection were carried out by Lauchlan and Melville (2001), who found this failure mode to be dominant under live-bed conditions. They showed that the influence of bed-forms on the scour protection stability can be reduced if the protection is placed below the sediment bed level.

- **Sinking due to liquefaction:** The scour protection sinks into the seabed as a result of diminishing bearing capacity of the soil. Under waves, liquefaction might be caused by a build-up of pore pressure exceeding the overburden pressure (residual liquefaction) or a vertical pressure gradient in the soil during the passage of the wave through (momentary liquefaction). Both mechanisms are described in detail as part of a comprehensive state of the art review on liquefaction around marine structures by Sumer (2014).

2.4.2 *Principles of granular protection design*

Granular scour protection is designed to prevent the erosion of underlying bed material against waves and current-induced hydraulic loads, while maintaining permeability to avoid the build-up of a large pore pressure in the bed material and allow the rapid drainage of seepage water (Schiereck, 2012). The cost-effectiveness of granular scour protection, however, only comes into effect, if a practical and uncomplicated installation process can be ensured at the same time. In costal and marine engineering, this is typically achieved by a multi-layer setup of differently-sized granular material, consisting of a coarse, protective armor layer on top and one (or several) filter layer(s) beneath. The filter layer is designed in a way that the suction of the fine underlying bed material through the filter by winnowing processes is suppressed and sinking of the armor layer into the bed is

prevented. The dimension of the armor layer stones, that withstands the hydraulic load, is determined based on stability criteria specified by critical shear stresses or flow velocities (cp. chapter 2.1.5). A stability criterion can be defined according to a statically stable design, that produces conservative stone sizes, as it expects no stone movement under all circumstances. Thus, to reduce the required stone size, a dynamically stable design conventionally allows a limited movement of armor stones above a specified load. Stability approaches for armor layer stones for both, a statically and a dynamically stable design, are addressed in detail in the following sections.

From the viewpoint of production, the dimensions of armor layer stones are either given in terms of diameter or mass (weight). Instead of the median d_{50} diameter, the nominal dimension of an equivalent cube $d_{n,50}$ is usually used for the design. According to CIRIA (2007), the two values can be converted by $d_{n,50} = 0.84d_{50}$. Consequently, the relationship between diameter and stone weight is given by $M = \rho_s d_{n,50}^3$. Regarding the grading of armor stones, the EN 13383 provides a standardized grading system as requirement for a consistent production and quality control. According to CIRIA (2007), the system divides armor stones into:

- **Heavy gradings** for large sized armor stones, i.e. in armor layers for coastal protection applications. Normally individually handled.

- **Light gradings** for stones in armor and filter layers. Produced in bulk.

- **Coarse gradings** often applied for filter layers, typically smaller than 200 mm.

For each grading class, the available mass (or grain size) distributions have to meet grading requirements, that limit the grading curve at certain values, e.g. for heavy gradings at a cumulated mass passing less than 5%, 10%, 70%, 97% (CIRIA, 2007). An idealised grading curve between those limits can be interpolated by a Rosin-Rammler function for mass or grain size distributions.

Distinguished by the capability of restraining bed material from being wash-out, the layout of the filter layer can be designed in a way that the scour protection becomes geometrically closed or open. In a geometrically closed layout, the transport of bed material is prevented by selecting grain sizes for the filter layer that physically block the upwards movement of the bed material. This is typically accomplished by a multi-layer setup of varying grain sizes, leading however often to an uneconomically and unpractically large amount of filter layers (CIRIA, 2007; Schiereck, 2012). Geometrically open filters can provide a more economical alternative by additionally taking the hydraulic load into account. Principally, the hydraulic load acting at the

interface between filter and bed is controlled and consequently the amount of erosion of the bed material. By defining a critical value for the initiation of erosion, usually in terms of a critical flow velocity or critical hydraulic gradient, geometrically open filters can further be considered as stable or unstable. While geometrically open filters are applicable to be installed as a single layer, their design requires detailed knowledge of acting and critical hydraulic loads (Schiereck, 2012). For the design of geometrically closed filter three geometrically aspects of filter stability have to be considered: the internal stability, the interface stability between layers and the permeability that allows the seepage water to be drained rapidly. As long as both materials are well-graded, the criterion for interface stability between the filter layer and bed material is given by CIRIA (2007) as:

$$\frac{d_{15,f}}{d_{85,b}} < 5 \tag{2.47}$$

in which the index f denotes the filter material and the index b the bed material.

Eq. (2.47) is also known as the Terzaghi criterion and can be applied for the interface between the armor stones and the filter as well. The demands for the permeability of the filter are expressed by:

$$\frac{d_{15,f}}{d_{15,b}} > 5 \tag{2.48}$$

Finally, the grading of the filter layer itself should provide internal stability of the grain structure, and thus, avoiding internal segregation effects. The criterion given by CIRIA (2007) reads:

$$\frac{d_{60,f}}{d_{10,b}} < 10 \tag{2.49}$$

Geometrically open filters require the definition of a hydraulic filter criterion up to which the underlying bed material is stable. The filter criterion can be defined in terms of a critical hydraulic gradient in the filter. The hydraulic gradient is related to the flow velocity in the filter, which flows parallel or perpendicular to the interface between filter and bed. In case the flow is parallel, the critical gradient is defined within the filter layer, because the large difference in flow velocity between filter and bed layer will exert shear stresses on the bed material, similar to the process leading to incipient motion in open channel flows (Schiereck, 2012). On the other hand, for a flow perpendicular to the interface, the critical gradient is defined within the bed layer.

For conditions with steady flow parallel to the interface, de Graauw, Meulen, and Bye (1984) derived the following criterion for a critical hydraulic gradient I_c:

$$I_c = \left(\frac{0.06}{n_f^3 d_{15,f}^{4/3}} + \frac{n_f^{5/3} d_{15,f}^{1/3}}{1000 d_{50,f}^{5/3}} \right) u_{*,cr}^2 \tag{2.50}$$

where n_f is the porosity of the filter material.

Additional hydraulic filter criteria for a parallel and unidirectional flow acting on a bed or slope protection were proposed by Bakker, Verheij, and Groot (1994) or Hoffmans (2012). Wörman (1989) considered the influence of a pile on the flow within the surrounding scour protection and derived an approach for a critical filter thickness D_f, that is required to prevent erosion of bed material in a single-layer layout without additional armor layer:

$$D_f = 0.16 \frac{[(\rho_{s,f}/\rho) - 1]}{[(\rho_{s,b}/\rho) - 1]} \frac{n_f}{1 - n_f} \frac{d_{85,f} d_{15,f}}{d_{85,b}} \tag{2.51}$$

As pointed out by Schürenkamp, Bleck, and Oumeraci (2012) and de Sonneville, Joustra, and Verheij (2014), there is still a lack of approaches regarding design criteria for geometrically open filters. In particular, approaches that account for pile induced turbulences and oscillatory flow conditions. In light of this situation, Schürenkamp, Bleck, and Oumeraci (2012) and Sumer and Nielsen (2013) found a hybrid approach, consisting of a combination of geometrical and hydraulic filter criteria, the most reasonable alternative for designing a filter. In both publications, an application-oriented approach is presented and illustrated by an example for the design of a granular scour protection around an offshore wind converter foundation .

2.4.3 *Armor layer stone size determination*

In the context of river bed revetments, numerous approaches for the determination of stone sizes required to withstand shear failure are available (e.g. Escarameia and May, 1992; Maynord, 1993; Neill, 1967; Pilarczyk, 1995). A comparison of the approaches by Maynord (1993), Escarameia and May (1992) and Pilarczyk (1995) presented in CIRIA (2007) reveals rather small differences in determined stone size for normal levels of flow turbulence but significant differences for higher turbulence levels. While those approaches mainly use the median grain size diameter d_{50} (or $d_{n,50}$), some approaches relate to other characteristic grain sizes, i.e. d_{30} by Maynord (1987), d_{40} by Raudkivi (1976) or d_{80} by Zanke (1982) as presented in DVWK (1997). The selection of an appropriate reference grain diameter becomes more and more important with increasing gradation of the applied granular

protection material. Derived from an application-oriented engineering perspective, most of those approaches are based on critical flow velocities near the bed in form of Eq. (2.37), which in turn are determined assuming uniform flow conditions. Thus, those approaches might show limitations if applied for scour protections around bridge piers or piles, where local velocities are amplified and additional turbulences are introduced. Therefore, only approaches explicitly considering the flow disturbance near a pile are addresses in the following, which, as mentioned earlier, can be divided in statically or dynamically stable approaches.

Statically stable scour protection design

A description and comparison of approaches for the determination of stone sizes at bridge piers, and thus, "current-only" conditions, is presented in Melville and Coleman (2000). Among others, the comparison includes the well-known equations by Breusers and Raudkivi (1991), Chiew (1995) and Lauchlan (1999). For a typical range of flow Froude numbers, the comparison reveals again large discrepancy in determined stone sizes, and underlines the relevance of considering several approaches for the design of required stone sizes. Eventually, the stone size can be selected as an average value of considered approaches or as the most conservative stone size.

For wave and combined wave-current conditions present in the marine environment, less scour protection design approaches are available. Here, the required stone size is typically determined based on methods using the Shields concept (Eq. (2.32)) and an estimation of amplified bed shear stresses τ_{amp} around the pile. Accordingly, the required stone size d_{cr} is generally given as:

$$d_{cr} = \frac{\tau_{amp}}{g \left(\rho_s - \rho \right) \theta_{cr}} \tag{2.52}$$

Approaches based on this concept might however be prone to some uncertainties. Uncertainties can stem from the variety of possibilities to calculate wave and current friction factors, leading to significantly different bed shear stresses. The bed shear stress calculation is also affected by the disagreement regarding the definition of a suitable bed roughness description. With respect to the resistance of the armor stone layer, threshold criteria for incipient motion, i.e. critical shear stresses, are dependent on the considered reference grain size diameter and armor stone grading. Eventually, the application of design approaches is complicated by the mutual interaction of above factors (Whitehouse, 1998). The bed shear stress estimation is depending on the bed roughness, which is given by the armor layer stone size, which in turn is calculated based on the acting bed shear stresses. Therefore, Whitehouse (1998) suggests to derive the required stone

iteratively. As initial guess for the required armor stone size, Soulsby (1997) proposed the following stability criterion for $d_{cr} > 10mm$:

$$\text{Steady flow:} \quad d_{cr} = \frac{0.25\overline{U^{2.8}}}{h^{0.4}\left[g\left(\rho_s/\rho - 1\right)\right]^{1.4}} \tag{2.53}$$

$$\text{Waves only:} \quad d_{cr} = \frac{97.9U_w^{3.08}}{T^{1.08}\left[g\left(\rho_s/\rho - 1\right)\right]^{2.08}} \tag{2.54}$$

Eq. (2.53) and (2.54) assumes a critical Shields parameter of $\theta_{cr} = 0.055$ and a power-law based friction approach for steady flow conditions and a wave friction factor given by Eq. (2.24).

In the context of the OPTI-PILE project, den Boon et al. (2004) carried out physical model tests on the stability of a granular scour protection around a monopile under North Sea conditions. Based on a damage and failure assessment, den Boon et al. (2004) proposed a design approach for combined wave and current conditions. The criterion for the stability of the armor stone layer around a monopile was defined as:

$$Stab = \frac{\theta_{max}}{\theta_{cr}} \tag{2.55}$$

In Eq. (2.55), the acting shear stresses, in the form of θ_{max}, were derived based on the approach of Soulsby (1995), which is depicted by Eq. (2.25) and (2.26). For the critical Shields parameter, a value of $\theta_{cr} = 0.056$ was applied. For the tested multi-layer scour protection system, den Boon et al. (2004) considered the protective function to have failed when the filter is exposed over an area equal to the footprint of four armor stone ($4d_{50}^2$). The stability of the scour protection prior to failure was subdivided in two damage categories. As long as no stone movement occurred, the scour protection was viewed as statically stable, whereas the movement of some stones was allowed for the scour protection to be dynamically stable. They found the static stability to be exceeded above a threshold value for the stability parameter of $Stab = 0.415$. Consequently, for a statically stable scour protection design, this leads to a maximum acceptable load of $\theta_{max} = 0.415\theta_{cr}$. For a dynamically stable scour protection a less conservative threshold value of $Stab = 0.46$ was determined.

Probably the most wide-ranging static design approach for the calculation of the required armor stone size of a scour protection around a monopile foundation in combined wave and current conditions was derived by De Vos (2008) and De Vos et al. (2011). They conducted comprehensive physical model tests, which included the usage of three different armor stone gradings with stone sizes typical for scour protection of offshore foundations. In the test, the hydraulic load was

increased until movement of the stones was initiated. The initiation of movement was defined as the displacement of at least one stone over a distance equal to two times the d_{50} diameter. Based on the results, a practical linear relationship between the undisturbed wave and current bed shear stresses and the critical bed shear stress that initiates stone movement was derived. The direct correlation between undisturbed bed shear stresses and failure of the scour protection eliminates the need to determine an amplification factor for the bed shear stress near the pile. In its normalized form, the equation for the bed shear stress required to withstand the hydraulic load $\tau_{cr,pred}$, which replaces τ_{amp} in Eq. (2.52) accordingly, reads as:

$$\tau_{cr,pred} = 83 + 3.569\tau_c + 0.765\tau_w \qquad (2.56)$$

The wave bed shear stress τ_w was determined according to the wave friction approach by Dixen et al. (2008), while the current induced bed shear stress τ_c is based on the friction formulation given in Liu (2001). Furthermore, a critical Shields parameter of $\theta_{cr} = 0.035$ is assumed and it is suggested to use the $d_{67.5}$ diameter for Eq. (2.52) instead of the d_{50} diameter to account for armor layers with a wider stone grading. However, it has to be noted, that Eq. (2.56) was derived for regular wave conditions. In case of irregular waves, De Vos et al. (2011) recommends calculating τ_w by using the average of the 10% highest waves $H_{1/10} = 1.27H_s$ instead of the significant wave height H_s.

Dynamically stable scour protection design

In contrast to statically stable design approaches, dynamically stable scour protection design allows a limited movement of armor layer stones without risking the failure of the protective function. Thereby, a reduction of stone sizes can be achieved, leading to significantly lowered costs over the designated life-time of foundation structures. The design of a dynamic scour protection requires a suitable definition of damage and the formulation of an acceptable damage threshold, beyond which the scour protection will ultimately fail. De Vos et al. (2012) also underlined the importance of the time development of occurring damage, which might even converge to a stable equilibrium stage as found by van der Meer (1988) for the damage at breakwaters. Furthermore, Chiew (1995) revealed that a partial breakup of a riprap layer can lead to a re-armoring by the coarse riprap stones, avoiding total failure of the riprap layer.

In addition to their design approach for a statically stable scour protection (Eq. (2.56)), De Vos et al. (2012) also empirically derived a dynamically stable design formula. Similar to the experiments depicted in De Vos et al. (2011), the stability of a granular scour protection

around a monopile foundation in combined wave and current conditions was investigated, this time however, irregular waves (JONSWAP spectra) were used. The threshold criteria at which the scour protection has ultimately failed was adopted from den Boon et al. (2004), i.e. when the filter layer is exposed over an area larger than $4d_{50}^2$. Based on the method used by van der Meer (1988), a three-dimensional damage definition was proposed, that quantifies the emerging damage by relating the eroded volume V_e to a defined sub area times a chosen stone diameter. As reference sub area, De Vos et al. (2012) selected the area that corresponds to the cross-sectional area of the pile. The resulting damage number S_D is given by:

$$S_D = \frac{V_e}{d_{n,50} \frac{\pi D^2}{4}} \tag{2.57}$$

Because the eroded volume is a function of the $d_{n,50}$ diameter, a damage of $S_D = 1$ implies that the scour protection is eroded by a thickness of $d_{n,50}$ within the considered surface area.

Resulting from parameter regression, a prediction approach for the damage number as a function of the governing parameters for wave and current conditions was derived:

$$\frac{S_{D,max}}{N^{0.243}} = 0.00076 \frac{U_w^3 T_{m-1.0}^2}{\sqrt{gh}\,(\rho_s/\rho - 1)^{3/2}\,d_{n,50}^2}$$

$$+ a_1 \left(-0.022 + 0.0079 \frac{\left(\frac{\overline{U}}{w_s}\right)^2 \left(\overline{U} + a_4 U_w\right)^2 \sqrt{h}}{g d_{n,50}^{3/2}} \right) \tag{2.58}$$

where $S_{D,max}$ is the maximum value of S_D over all sub areas, N is the number of waves, w_s the fall velocity of the stone, $T_{m-1.0}$ the energy spectral wave period, which for a JONSWAP spectrum is given by $T_{m-1.0} = T_p/1.107$ and the parameter a_1 and a_4 represent the influence of the current flow velocity relative to the stone size and the current direction, respectively. For a description of these parameter and a detailed derivation of Eq. (2.58) it is referred to De Vos (2008) and De Vos et al. (2012) at this point.

Eq. (2.58) can be used to iteratively calculate the required stone size if an acceptable damage number is defined. The definition of an acceptable damage number is not trivial, as it considerably depends on the hydraulic conditions and scour protection concept. As pointed out by De Vos et al. (2012), for some cases even a value of $S_{D,max} > 1$ is suitable, especially if the formation of a stable equilibrium state over time can be expected. In general, the larger the selected value of $S_{D,max}$ the smaller the required stone size becomes. Eventually, it is the experienced engineer's responsibility to select an allowable damage, that is suitable for the considered scour protection concept.

2.5   KNOWLEDGE GAPS AND UNCERTAINTIES IN SCOUR PREDICTION AND PROTECTION DESIGN

In the marine environment, hydrodynamic load on offshore structures and the sea bed surrounding those structures is induced by a complex interaction of current and wave generated flows. The literature research presented in the previous section reveals that complex flow situations are still seldom taken into account for the prediction of scour development around offshore structure. Evidently, there is a lack of knowledge regarding the effects of realistic marine flow conditions on the scouring processes around offshore structures, despite the increasing availability of more and more sophisticated laboratories and numerical models that would allow investigations into such processes. This knowledge gap is particularly apparent for the scour development due to unsteady tidal currents and multidirectional waves, making a reliable prediction of scour depth for the design of offshore structures difficult. Although storm generated sea states in the marine environment are characterized by multidirectional waves, the investigation on how wave spreading influences the scour depth and development is not much given attention so far. This situation is reflected by the rudimentary recommendations on expected scour depths and progression provided by design guidelines.

The prediction of scour development, as a initial hazard assessment, is followed by the design of suitable protection measures. Here, granular scour protection is often preferred over other systems. Armor layer stone sizes for a granular scour protection have to be designed to withstand wave and current-induced hydraulic loads. The required stone sizes are typically determined based on methods using the Shields concept, comparing applied bed shear stresses with critical values. Unfortunately, large uncertainties in the estimation of bed shear stresses can stem from the variety of possibilities to calculate wave and current friction factors, leading to significantly different bed shear stresses. As the flow around a monopile is characterized by an increased turbulence and flow acceleration, the application of most friction factors, which were derived for uniform flow over a flat bed without the obstruction of a pile, might not be valid at all. This issue also translates to the amplification factor used to compensate for the lack of consideration of turbulence and flow acceleration. Furthermore, the inaccuracy of the bed shear stress estimation is increased by the disagreement in literature regarding the definition of a suitable bed roughness description.

Regarding thresholds for critical bed shear stresses several authors have shown ongoing sediment transport below the Shields curve. The values of the critical Shields parameter are therefore controversially discussed in literature and the values found by Shields are usually considered to overestimate the critical shear stresses of embedded

particles. The assessment of bed stability is especially complex for grain mixtures due to their tendency to from a protective armor layer at the surface. As extension of the Shields concepts, numerous hiding functions were defined to describe the incipient motion for individual grains within a bed composed of nonuniform particles. However, not only does the character of hiding functions differ significantly between available approaches, from equal to selective mobility, but the hiding functions were also derived for water-worked particles exposed to mostly stationary hydraulic flow conditions. To date, there is no systematic study available in which the validity of these hiding functions for widely graded broken stone material exposed to marine flow conditions is checked. Consequently, no guidelines for the design of a widely graded scour protection system in marine environments exist, leaving its promising potential as a more economical alternative to traditionally applied protection systems unused.

WAVE-CURRENT-INDUCED SCOURING PROCESSES AROUND A PILE

The reliable prediction of scour depth is of crucial interest for an economic and secure design as well as life-time management of structures in coastal and marine waters. The significance of scour for the design is reflected by the considerable amount of publications dealing with the emergence and characteristics of local scour in various hydraulic conditions (chapter 2.3). However, unresolved questions remain regarding the processes of scour induced by more complex flow conditions caused by the directional interaction of waves and tidal currents in the marine environment. Thus, systematic laboratory tests were carried out to assess the influence of tidal currents combined with directional random waves as decisive factors for the scouring process of a realistic sea state.

Hereinafter, the findings of the experiments regarding the influence of tidal currents on the scouring process are presented in summarized form of a submitted manuscript. The experiments on the effects of directional random waves are described in more detail and evaluated with respect to how the findings can complement the understanding of scouring processes and improve the prediction of scour as part of scour protection design for marine structures.

3.1 SCOURING INDUCED BY TIDAL CURRENTS

Schendel, A., Hildebrandt, A., Goseberg, N., and Schlurmann, T. (2018). Processes and evolution of scour around a monopile induced by tidal currents. Coastal Engineering, Vol. 139, pp. 65-84.

Results of systematic laboratory experiments are presented that focused on the initiation and development of scour around a monopile in tidal flow conditions. Continous scour depth measurements at multiple positions around the model pile allowed the quantitative elucidation of the scouring process over time. In previous studies (Escarameia and May, 1999; McGovern et al., 2014; Porter, Simons, and Harris, 2014), the simulation of tidal currents relied on either the periodical reversal of a constant flow velocity or on its erratic variation and thus was not capable to reproduce a realistic change of scouring rates over time. To ensure a more authentic representation of tidal currents, flow velocities were appropriately scaled from field measurements by continuously changing flow velocities and direction in this very study. Peak flow velocities of the tidal currents were adjusted to

satisfy clear-water and live-bed conditions, so that the dependency of scour to a large range of flow intensities could be systematically investigated. However, given the experimental setup, the rotary aspect of tidal currents was initially adapted by bidirectionally reversing currents.

Resonating with the flow velocity, constantly varying sediment infilling and displacement processes in the scour hole led to an unsteady time development of scour depth in tidal currents. The analysis of scouring rates revealed a periodically returning scheme of terminated scouring at times of changing flow direction, and a resumption of the scouring process in each tidal half cycle once a critical flow velocity is exceeded. The scouring process initially started with infilling, indicated by a negative scour rate, which was immediately followed by a fast increase of the scour rate and a deepening of the scour depth. This scheme was mostly pronounced in live-bed conditions, while the scour development in clear-water conditions was less erratic and much slower than in live-bed conditions.

In addition, baseline tests with unidirectional currents were conducted, in which the constant flow velocity was either based on the maximum peak or the root mean square velocity of the tidal currents. This comparison was aimed at giving valuable insights in the differences of scour development with respect to directional aspects and to assess how tidal currents with continuously changing flow velocity can be accounted for in scour prediction approaches. Generally, the design of scour protection also often relies on time averaged estimates of unidirectional flow velocities (cp. chapter 2.3 and 2.4). If based on the maximum peak velocity of the tidal signal, unidirectional flow induced scouring rates were significantly larger than under corresponding tidal currents. For this case, maximum scour depths were found to overestimate those generated by tidal currents of up to 62%, depending on the flow intensity. On the contrary, scour depths in tidal flows were considerably underestimated by those induced by unidirectional current, if unidirectional flow velocities were based on the root mean square value of the tidal signal. As a simple and thus practical value, a flow velocity close to $u_{max}/\sqrt{2}$ of the tidal signal, with u_{max} being the maximum flow velocity within the tidal current, was found to provide a good approximation of scour depths and rates in tidal currents by means of a constant flow velocity. Is was also shown, that an accurate prediction of the scour development over time is feasible by means of a time discretized prediction approach, in which the progression of scour depth is calculated by assuming quasi-steady flow conditions for defined time steps. The accuracy of this approach however relies heavily on the availability of detailed in situ flow measurements.

These findings thus emphasize the importance of selecting suitable flow velocities for the design of coastal and marine structures against

tidal currents as scour depths as well as scouring rates might significantly differ from those associated with unidirectional currents. An accurate assessment of scouring rates is also important for the estimation of time windows for the installation of those structures or for scour remedial measures and allows a more efficient management.

3.2   SCOURING UNDER COMBINED MULTIDIRECTIONAL WAVES AND CURRENTS

The progressive expansion of offshore wind energy towards deeper water depths demands an optimisation of foundation structure design to a wider range of load conditions. In offshore waters, wind driven wave irregularity and directionality become important aspects of realistic sea states. While it became common practice in physical modeling to approximate shallow water waves with unidirectional irregular waves, recent advantages in wave generation techniques and the increased availability of state-of-the-art wave basins allow the reliable reproduction of realistic multidirectional sea states (Kirkegaard et al., 2011). A limited number of studies regarding the interaction of directional waves with piles and resulting wave loads are already published. Yu, Zhang, and Zhao (1996) investigated the influence of directional wave spreading on wave forces on a pile and found them to be a function of the KC number and the amount of wave spreading. The run-ups and forces of waves on piles in multidirectional focused waves were examined by Li, Wang, and Liu (2012) and Li, Wang, and Liu (2014), respectively. The results showed larger wave run-ups in unidirectional waves than in multidirectional waves and that the spatial profile of the surface of a multidirectional focused wave affects its exerted force on the pile. Nielsen et al. (2012) carried out physical model tests on the effects of wave directionality and breaking of waves and their results indicated a reduction of slamming forces with increasing wave spreading. Most recently, Ji, Liu, and Jia (2015) presented results on the interaction of multidirectional irregular waves with a large pile for a wide range of directional wave spreading.

 Those studies provide valuable reference data for an optimization of the structural design of offshore foundations with respect to the influence of wave spreading. However, while the progression of scour in unidirectional waves has been already addressed by several studies (cp. chapter 2.3.3), there exist no experimental data on the scouring process induced by multidirectional waves to the author's knowledge. As mentioned before, this may be attributed to the elaborate set-up and procedure of physical model tests dealing with multidirectional waves in combination with sediment transport processes. Considering the lack of empirical data and the possibility of validation, the stochastic model by Ong, Myrhaug, and Hesten (2013) and Myrhaug and Ong (2013) as descibed in 2.3.3 provides a first useful estimation

of scour depths in random three-dimensional waves, which significantly differ from those in two-dimensional waves. In addition, studies on the influence of tidal currents on the scouring process (chapter 3.1) clearly demonstrate the influence of continuously changing flow directions on the scour progression. In order to improve the scour prediction and consequently optimize the design process of foundation structures in marine environments, directional flow aspects should therefore be considered.

Thus, a novel experimental study was carried out in the 3D wave and current basin of the Ludwig-Franzius-Institute for Hydraulic, Estuarine and Coastal Engineering, Leibniz Universität Hannover, Germany. The objectives of the study include:

- Deepening the understanding of scouring processes induced by multidirectional (short-crested) waves and multidirectional waves combined with currents.

- Systematically investigate the influence of wave spreading on the scouring process as a function of wave characteristics.

- Provide reference data for an improvement of scour prediction for coastal and offshore conditions by comparing the scour depths and rates to those in unidirectional (long-crested) waves.

3.2.1 *Experimental setup & procedure*

The 3D wave and current basin has a total length of 40 m, a width of 25 m and the maximum water level is limited to 1.0 m. On its long side, the wave basin is equipped with a multidirectional wave maker, consisting of 72 individual wave paddles, allowing a generation of regular and irregular waves with a propagation angle of up to ± 85° with respect to the main wave direction perpendicular to the wave maker. In addition to passive mesh screen wave absorbers surrounding the basin at the other three sides, the wave maker features an active real-time absorbtion system. A unidirectional current, perpendicular to the main wave direction, can be generated by a pump system consisting of four pumps with a combined maximum flow capacity of 5 m³/s, ensuring a mean flow velocity of up to 0.5 m/s at a designated water level of 0.6 m.

For tests associated with sediment transport processes, the wave basin also provides a modular sediment pit with a length of 9.15 m, a width of 6.65 m in main wave direction and an additional depth of 1.20 m. A sediment trap at the downstream side of sediment pit (with respect to the current direction) prevents any relevant recirculation of sediment by the current. For the scouring tests presented herein, a crystal quartz sand with a median diameter $d_{50} = 0.19$ mm, a geometric standard deviation $\sigma_g = \sqrt{d_{84}/d_{16}} = 1.4$ and a density

of $\rho_s = 2.65\,\mathrm{g/cm^3}$ was used as sediment. To guarantee a good compaction and to reduce entrapped air, the sand was installed in wet condition.

Assuming an approximate length scale of 1:75, a monopile structure was simulated by a transparent pile made of acrylic glass with a diameter of 80 mm. The pile was positioned in the centre of the sediment pit, resulting in a distance to the wave maker of 7.50 m. Visual information on the dimension of the wave basin and the experimental setup is shown in Fig. 3.1, which also introduces a local reference coordinate system.
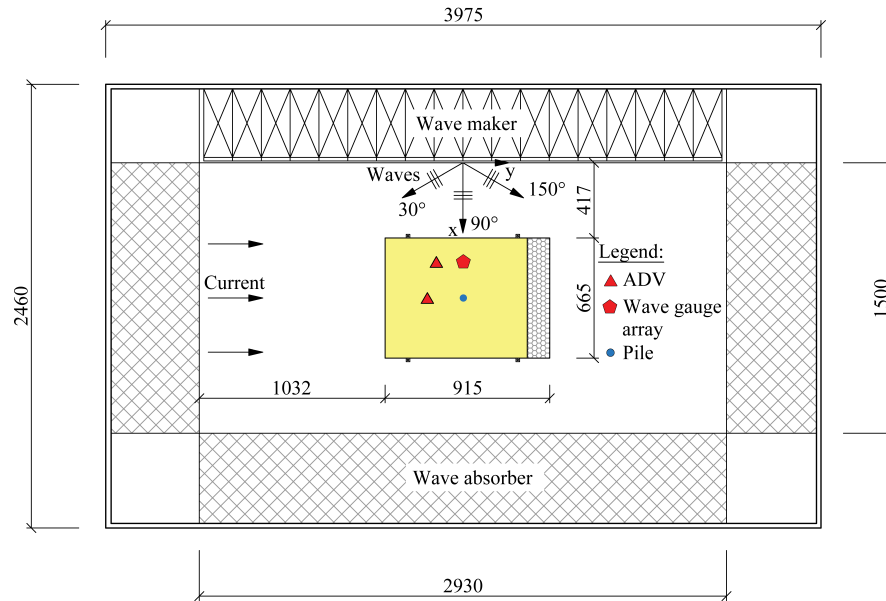
Figure 3.1: Experimental setup in top view with dimensions in centimetre.

Scour measurements were carried out by attaching a 1.0 mm fine grid to the pile, providing 0.5 mm intervals for scour recognition. The scour development was monitored by a camera (Basler, acA1920-25gc) placed inside the transparent pile. To follow the progressing scour depth, the camera was attached to a carriage system, enabling the automatic adjustment of its height and vantage point and thereby providing a high temporal resolution of the scour development at the pile. The pile including the camera system is presented in Fig. 3.2a.

The multidirectional waves were recorded by a CERC6 (Coastal Engineering Research Center) wave gauge array (Davis and Regier, 1977), consisting of six echo-sounder (General Acoustic, UltraLab ULS Advanced). The gauge spacing was adaptable and was matched relatively to the different wave lengths tested in this study by using similar principles as for a 2D reflection analysis (Mansard and Funke, 1980). The arrangement and general placement of the wave gauge array are illustrated in Fig. 3.2b.

(a) Image of transparent pile with camera system inside.

(b) Arrangement of measurement devices within the sediment pit. Dimensions given in centimetre.
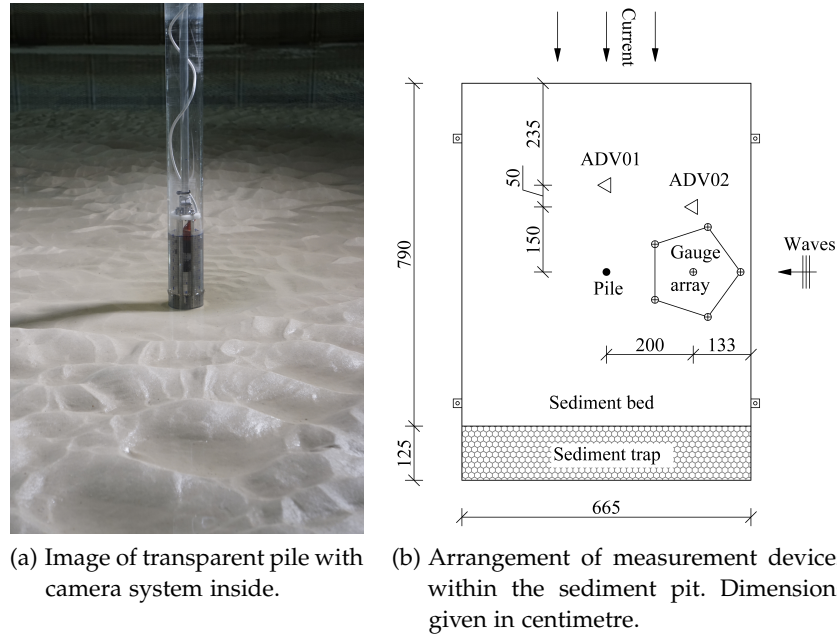
Figure 3.2: Camera equipped monopile and top view of measuring setup.

Wave and current induced flow velocities were measured by means of two Acoustic Doppler Velocimeter (ADV) (Vectrino+, Nortek AS, Norway). One was placed 2.0 m upstream (in current direction) from the pile at half water depth, the other was aligned with the wave gauge array at a distance of 10 cm above the sediment bed (cp. Fig. 3.2b). Both, the ADVs and the wave gauges sampled at 100 Hz. With the focus on the effect of wave spreading on the scouring process, the water depth was kept constant at 60 cm throughout the experiment.

As baseline tests, the scour development under unidirectional (long-crested) waves was investigated first. The tests included "waves-only" conditions as well as combined wave and current situations, in which the current flow direction was perpendicular to the main wave propagation direction (x-axis in Fig. 3.1). Irregular waves (JONSWAP spectra with a peak enhancement factor γ_J = 3.3, and spectral width parameters σ_a = 0.07 and σ_b = 0.09) were adopted for all tests as realistic representation of offshore North Sea conditions. Wave spectra were generated according to linear wave theory.

Wave parameters and current flow velocities were selected to cover a wide range of values for the KC number, U_{cw} and θ, which are essential governing parameters effecting the scouring process in combined wave and current conditions, as depicted in chapter 2.3. Test conditions and maximum scour depths for the unidirectional wave experiments are summarized in Table 3.1.

In Table 3.1, the maximum orbital wave velocity U_w is calculated from the root-mean-square (RMS) value of the orbital velocity near the bed U_{rms} according to Eq. (2.19) and as suggested by Sumer and

Table 3.1: Test conditions and maximum scour depths for unidirectional (long-crested) wave experiments.

Test	Number of waves N	Spetral wave height H_{m0}	Peak wave period T_p	Keulegan-Carpenter number KC	Maximum orbital velocity at the bed U_w	Undisturbed current velocity (at 10cm) U_c	Combined wave-current velocity U_{cw}	Shields parameter θ	Maximum scour depth S_{max}/D
	[-]	[m]	[s]	[-]	[m/s]	[m/s]	[-]	[-]	[-]
A01	5224	0.146	1.96	3.73	0.153	-	0	0.089	0.075
A02	6530	0.146	1.96	3.73	0.153	0.115	0.43	0.083	0.238
A03	6530	0.146	1.96	3.73	0.153	0.244	0.62	0.097	0.700
A04	6530	0.146	1.96	3.73	0.153	0.421	0.73	0.151	1.213
A05	5051	0.157	3.56	8.41	0.189	-	0	0.082	0.163
A06	4420	0.157	3.56	8.41	0.189	0.115	0.38	0.084	0.350
A07	6313	0.157	3.56	8.41	0.189	0.244	0.56	0.097	0.888
A08	5682	0.157	3.56	8.41	0.189	0.421	0.69	0.151	1.488
A09	5019	0.172	4.55	12.46	0.219	-	0	0.084	0.375
A10	6273	0.172	4.55	12.46	0.219	0.115	0.34	0.092	0.738
A11	6273	0.172	4.55	12.46	0.219	0.244	0.53	0.105	0.938
A12	5019	0.172	4.55	12.46	0.219	0.421	0.66	0.157	1.425

Fredsøe (2001a). The *KC* number is calculated using U_w and T_p with Eq. (2.40). For combined wave and current conditions, the parameter U_{cw} is determined by Eq. (2.46) with U_c being the time averaged current velocity near the bed determined in pretests. The Shields parameter θ is calculated based on the bed shear stress approach by Soulsby and Clarke (2005). While for all tests depicting "waves-only" conditions a laminar flow regime was found, indicated by wave Reynolds numbers $Re_w \leq 1.5x10^5$, the flow was turbulent in the case of combined wave and current conditions. The definition of Re_w is given by Eq. (2.22).

To reduce the increasing influence of wave reflection over time, in particular during tests with larger peak wave period and thus longer wave lengths, the generated JONSWAP spectra were limited to approximately 600 waves. These spectra were repeated up to 10 times, including breaks for wave motion damping, until either an equilibrium scour depth was achieved or at least 6000 waves were applied. As it was intended to keep the number of waves between tests comparable, the duration of a test increased with larger peak wave periods.

The procedure for each series of tests can be described as follows:

1. Run a test with wave only conditions until the scouring process reaches an equilibrium stage.

2. Superimpose the current with the smallest flow velocity to the waves and run the combined wave and current test until a new equilibrium stage is reached (or 6000 waves were generated).

3. Increase the current velocity a second and subsequently a third time and run each test until a new equilibrium stage is achieved.

4. Level the bed and repeat this procedure for new wave parameters.

This procedure is in general agreement with that from Sumer and Fredsøe (2001a), allowing a direct comparison of results.

During the tests the scour development was recorded visually by the camera placed inside the pile, with a set of pictures taken every 3 min. A set of pictures consisted of eight pictures successively taken in radial intervals of 45° around the pile. The maximum scour depth at a time was defined as the absolute maximal scour depth within the eight depths in a single set of pictures.

3.2.2 *Generation and analysis of multidirectional (short-crested) waves*

The directional spectrum $S(f, \Theta)$ required for the generation of multidirectional waves is obtained by extending the unidirectional frequency spectrum $S(f)$ with a directional spreading function $D(f, \Theta)$:

$$S(f, \Theta) = S(f) D(f, \Theta) \tag{3.1}$$

Integrated over the complete range of directional distribution, the total wave energy inhered in the directional spectrum has to be identical to that of the frequency spectrum, given that:

$$\int_{\Theta_{min}}^{\Theta_{max}} D\left(f,\Theta\right) d\Theta = 1 \tag{3.2}$$

where Θ_{min} and Θ_{max} represent the minimum and maximum angle of wave spreading, respectively.

In this study, the directional spreading was limited to a range of $\Theta_{range}\pm 60°$ with respect to the main wave direction (90°), as waves propagating beyond that range were not able to approach the pile directly.

Focusing on the influence of wave spreading on the scouring process, the same JONSWAP spectra were applied for the multidirectional as for the unidirectional tests, ensuring identical total wave energy between both cases. The test conditions for the multidirectional tests are summarized in Table 3.2.

Following Eq. (2.18) and given that the total wave energy of the directional spectrum is independent from wave spreading, similar values of U_w for unidirectional and multidirectional spectra should be expected. However, for the multidirectional tests, U_{rms} had to be extracted as the resultant of the orbital velocity components in streamwise (x) and lateral direction (y) of wave propagation. The amplitude of the resulting maximum orbital velocity U_w well agreed with those from the unidirectional wave tests.

Two different target spreading parameters, $s = 10$ and $s = 50$, were selected, representing a wide and narrow spreading sea, respectively. The spreading parameter s is defined by a Mitsuyasu-type directional spreading function as:

$$D\left(f,\Theta\right) = cos^{2s}\left\{\frac{\Theta - \Theta_0\left(f\right)}{2}\right\} \tag{3.3}$$

in which Θ_0 is the main wave direction, i.e. 90° in this study.

The analysis of the multidirectional waves was carried out with the WaveLab3 software package (available from Aalborg University), applying the Bayesian Direct Method (BDM) with 90 discrete directions in the spreading function for each individual generated spectrum (600 waves).

In the following, the analysed wave spectra, unidirectional (2D) and multidirectional (3D), are compared with target spectra to allow for an assessment of accuracy and performance of wave generation. Indicated by Fig. 3.3, the frequency spectra agreed well with the target values, although slight differences in wave energy for the peak wave period were present, particularly for spectra with larger peak period ($T_p = 3.5$ s und $T_p = 4.5$ s). Considering only the generated waves, the

Table 3.2: Test conditions and maximum scour depths for multidirectional (short-crested) wave experiments.

| Test	Number of waves N	Spetral wave height H_{m0}	Peak wave period T_p	Keulegan-Carpenter number KC	Maximum orbital velocity at the bed U_w	Undisturbed current velocity (at 10cm) U_c	Combined wave-current velocity U_{cw}	Shields parameter θ	Spreading parameter s	Maximum scour depth S_{max}/D
	[-]	[m]	[s]	[-]	[m/s]	[m/s]	[-]	[-]	[-]	[-]
A13	5215	0.143	1.95	3.58	0.147	-	0	0.086	8.90	0.038
A14	6519	0.143	1.95	3.58	0.147	0.115	0.44	0.079	8.90	0.275
A15	6519	0.143	1.95	3.58	0.147	0.244	0.62	0.089	8.90	0.875
A16	6519	0.143	1.95	3.58	0.147	0.421	0.74	0.147	8.90	1.375
A17	5183	0.159	3.56	8.81	0.198	-	0	0.086	9.21	0.213
A18	6479	0.159	3.56	8.81	0.198	0.115	0.37	0.090	9.21	0.588
A19	6479	0.159	3.56	8.81	0.198	0.244	0.55	0.103	9.21	1.038
A20	5183	0.159	3.56	8.81	0.198	0.421	0.68	0.156	9.21	1.425
A21	4960	0.172	4.40	12.49	0.227	-	0	0.088	9.87	0.300
A22	6200	0.172	4.40	12.49	0.227	0.115	0.34	0.098	9.87	0.625
A23	6200	0.172	4.40	12.49	0.227	0.244	0.50	0.111	9.87	1.038
A24	4960	0.172	4.40	12.49	0.227	0.421	0.65	0.162	9.87	1.388
A25	5224	0.144	2.00	3.75	0.150	-	0	0.086	31.34	0.088
A26	4951	0.158	3.56	8.72	0.196	-	0	0.085	43.50	0.238
A27	4974	0.171	4.55	12.74	0.224	-	0	0.086	31.26	0.413
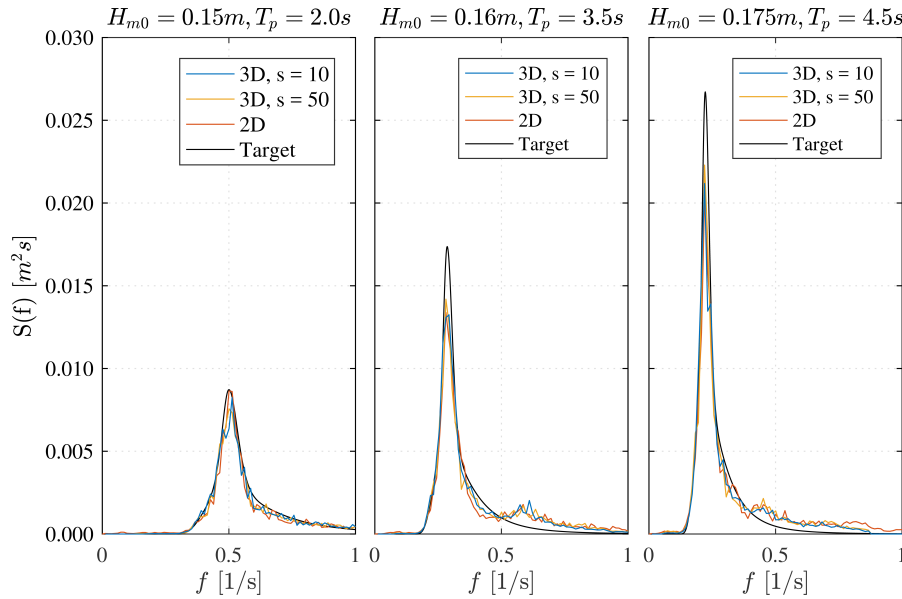
Figure 3.3: Comparison of analyzed frequency spectra of multidirectional (3D) and unidirectional (2D) waves with target spectra. Target values for the JONSWAP spectra are given by the figure title.

frequency spectra of unidirectional and multidirectional waves were almost identical.

The juxtaposition of directional spreading distributions in Fig. 3.4 revealed a good agreement with the target distribution for an intended wider spreading parameter of $s = 10$, but also a too large wave spreading for a narrower value of $s = 50$. As presented in Table 3.2, the analysis yielded spreading parameters in the range of $s = 31 - 44$ instead, despite thoroughly calibration of wave generation. However, it has to be noted, that the generated waves with peak wave periods of up to 4.5 s depict the specified limits in terms of wave maker performance.

Ultimately, Fig. 3.5 shows the radial distribution of frequency spectra to provide visual reference to wave spreading in the wave basin and to further illustrate the differences between a wide ($s = 10$) and a narrow ($s = 50$) wave spreading.

3.2.3 *Scour depths in unidirectional waves combined with current*

Equilibrium scour depths obtained in the present study are presented in Fig. 3.6 as a function of U_{cw}. The measured data are plotted against results from Sumer and Fredsøe (2001a) and Rudolph and Bos (2006) for similar KC numbers (cp. chapter 2.3.4). Current only scour depths are extracted from previous studies described in Schendel, Hildebrandt, and Schlurmann (2016) and in chapter 3.1, contributing a scour depth of $S/D = 1.43$ for a current velocity of $U_c = 0.46$ m/s.
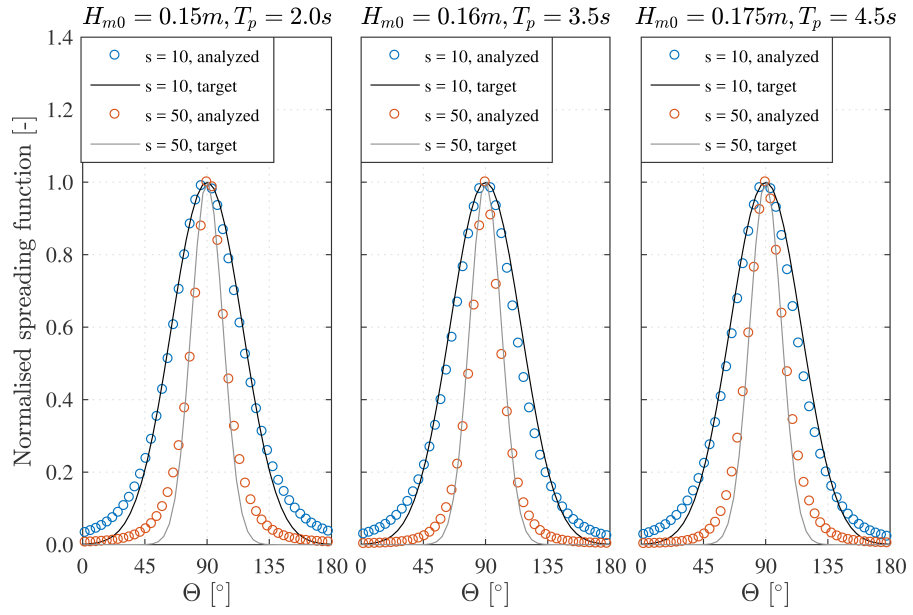
Figure 3.4: Comparison of analyzed directional spreading distributions of multidirectional (3D) waves with target spectra. Target values for the JONSWAP spectra are given by the figure title.
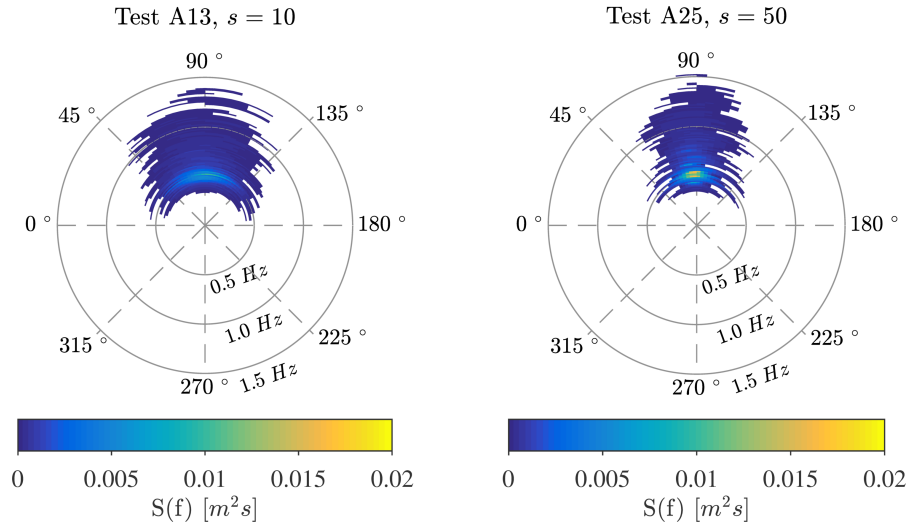

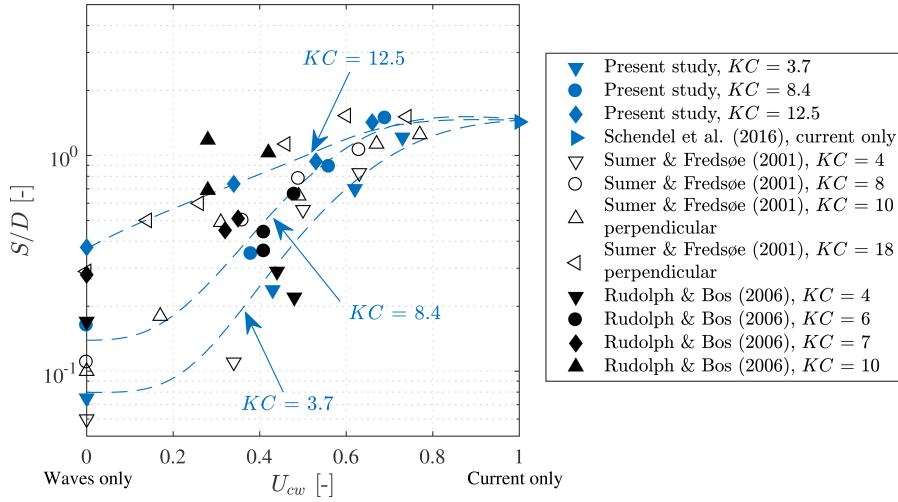Figure 3.5: Directional wave spreading for multidirectional waves. Incident waves are coming from 90°.

Figure 3.6: Equilibrium scour depths for unidirectional waves combined with current against dimensionless flow velocity U_{cw}. Dashed lines indicate trends of identical KC number.

While some scattering of scour depths was obvious, which was expected given the prevailing uncertainties coming from model and scale effects, the results were in general agreement with those from Sumer and Fredsøe (2001a) and Rudolph and Bos (2006). Consequently, similar conclusions can be drawn regarding the scouring process in combined waves and current conditions. In current dominated conditions, i.e. $U_{cw} \rightarrow 1$, scour depths approached values similar to those obtained for current only conditions, whereas in wave dominated situations, i.e. $U_{cw} \rightarrow 0$, scour depths close to those in "waves-only" conditions were observed. While scour depths generally increased with KC number over the whole range of U_{cw}, the influence of KC on the scour depths was significantly larger in the wave dominated than in the current dominated regime. Furthermore, the dependency of scour depths on U_{cw} became more pronounced for small KC numbers. As pointed out by Sumer and Fredsøe (2001a), this indicates that for small KC numbers only a small superimposed current can considerably increase the wave induced scour depths.

The prediction of scour depth in combined wave and current condition is often carried out by referring to the approach proposed by Sumer and Fredsøe (2001a), which reads:

$$\frac{S}{D} = \frac{S_c}{D} \left[1 - exp \left\{ -A \left(KC - B \right) \right\} \right]; \; for \; KC \geq B \tag{3.4}$$

with S_c as the scour depth in the case of "current-only" conditions and:

$$A = 0.03 + 0.75 U_{cw}^{2.6} \tag{3.5}$$

$$B = 6\,exp\left(-4.7U_{cw}\right) \tag{3.6}$$

Fig. 3.7 evaluates the accuracy of this approach for the prediction of scour depths obtained in the present study and for those given in Sumer and Fredsøe (2001a) by comparing the measured scour depths to predicted values. The scour depths measured in the present study are predicted as good as those from Sumer and Fredsøe (2001a). While most scour depths are predicted with an accuracy of ±20%, the approach fails to accurately estimate smaller scour depths, implying the need for an improvement for that particular range of scour depths. Given this consistency with results from literature, the obtained scour depths can thus serve as reliable reference for future tests in the 3D wave and current basin and for the upcoming analysis of multidirectional wave induced scour.
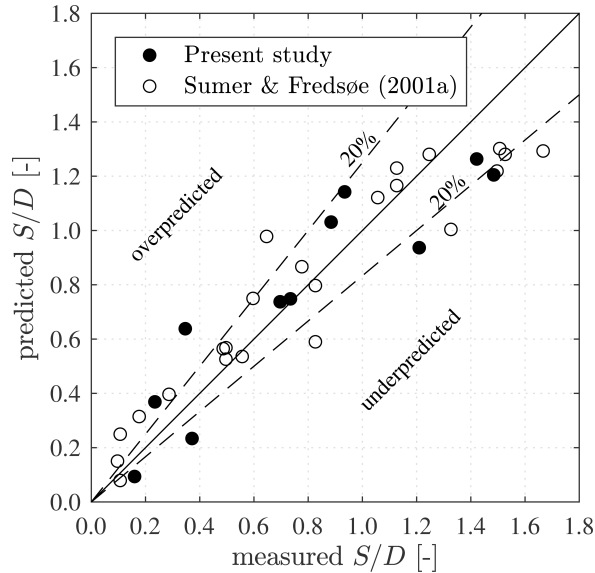
Figure 3.7: Comparison of measured and predicted equilibrium scour depths. Predicted scour depths are estimated by the approach of Sumer and Fredsøe (2002).

3.2.4 *Scour depths in multidirectional waves combined with current*

Exemplarily, Fig. 3.8 presents the scour development over time for a wave spreading ($s = 10$) with a constant value of $KC = 3.6$ and successively increasing current velocity. In Fig. 3.8, the upper panel visualizes the scouring process by interpolating the measured scour depths to a scour pattern, that consists of the scour depths at all positions around the pile at every time step of measurement. In addition, the lower panel of Fig. 3.8 illustrates the scour development over time for the stream-wise (0° and 180°) and lateral (90° and 270°) positions

Figure 3.8: Test A13-A16: Scour progression over time. Upper panel: Pattern of occurring displacement processes around the pile. Lower panel: Scour development at the stream-wise and lateral positions around the pile, referring to the direction of current.

at the pile, referring to the direction of the current. As depicted in Fig. 3.8, the position of the maximum scour depth at the pile relocated to the upstream side of the pile, similar to the behaviour in unidirectional waves, once an additional current was superimposed to the waves. From that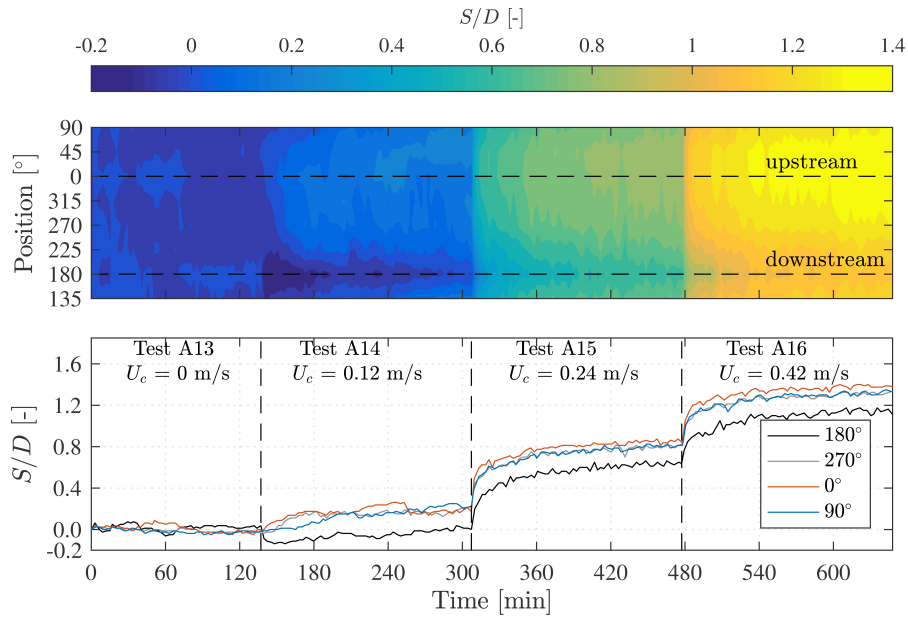 moment on, the position of maximum scour depth around the pile was thus determined by the direction of the unidirectional current.

Furthermore, for comparable *KC* numbers and values of U_{cw}, the imbalance of scour depth between the upstream and downstream side of the pile was more pronounced for multidirectional than for unidirectional wave conditions. As a distinct characteristic of unidirectional current induced scour around a pile, this imbalance implies a more current dominated scour behaviour for multidirectional than for unidirectional wave conditions, if superimposed with a current of similar magnitude.

As expected, the scour depths increased immediately with every step-wise increase of current flow velocity, and subsequently, followed a steady and logarithmic growth towards an equilibrium stage. Additionally, to elucidate the dependency of the scouring process on the *KC* number, Fig. 3.9 contrasts the progression of maximum scour depth over time for tests with similar values of U_{cw} but different *KC* numbers. The depicted scour depths are related to the initial scour depth at the start of each test, allowing the evaluation of scour progression as the explicit result of a superimposed current. The scour
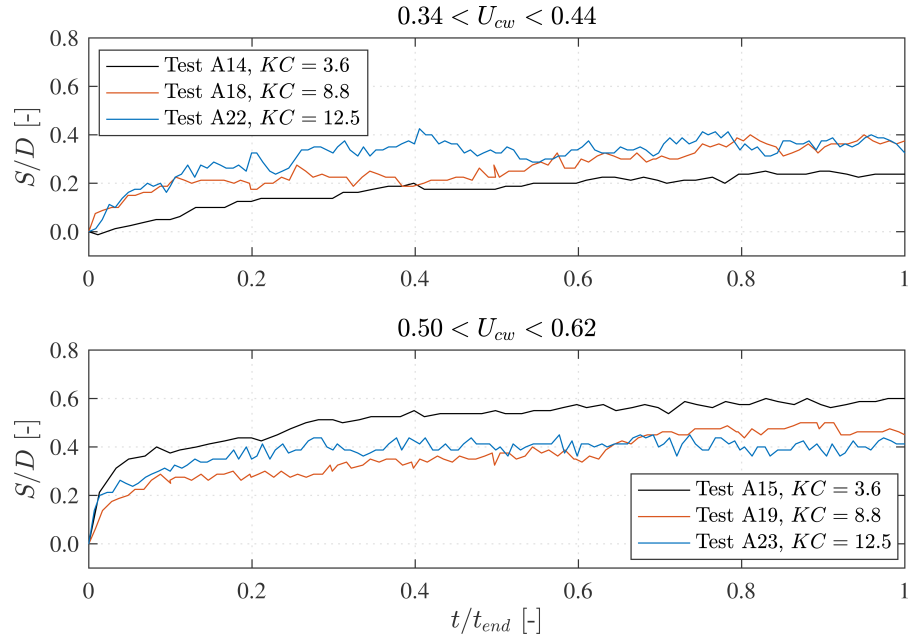
Figure 3.9: Progression of maximum scour depth S/D over dimensionless time t/t_{end}, where S/D refers to the increase of scour depth during the considered test.

depths further represent the maximum scour depths around the pile for each time step of measurement.

For smaller values of U_{cw}, i.e. in wave dominated regime, the increase of maximum scour depth as well as the scouring rate correlate positively with increasing KC number. However, for values of $U_{cw} > 0.5$, the influence of waves on the scouring process did not only diminish, but instead, even reversed. As the flow condition became current dominated, the increase of scour depths and the scouring rates lessened with increasing KC number. Considering the test procedure with successively increasing current velocity, this caused an equalization of absolute scour depths towards the equilibrium scour depth in "current-only" conditions. In addition to the increase of scour depths, the smaller the KC number, the more resembled the scour progression over time that in unidirectional current.

Regarding the influence of wave spreading on the scour depth, Fig. 3.10 presents the maximum scour depths obtained in wave only conditions as a function of KC number and spreading parameter s. While the general influence of wave spreading on the scour depths appeared to be relatively small, a clear tendency for scour depths to decrease with increasing wave spreading was still evident. The dependency of scour depth on wave spreading was particularly prominent for small KC numbers. However, given the limited number of data points combined with the general uncertainties naturally coming with hydraulic model tests, especially if they are dealing with the stochastic nature
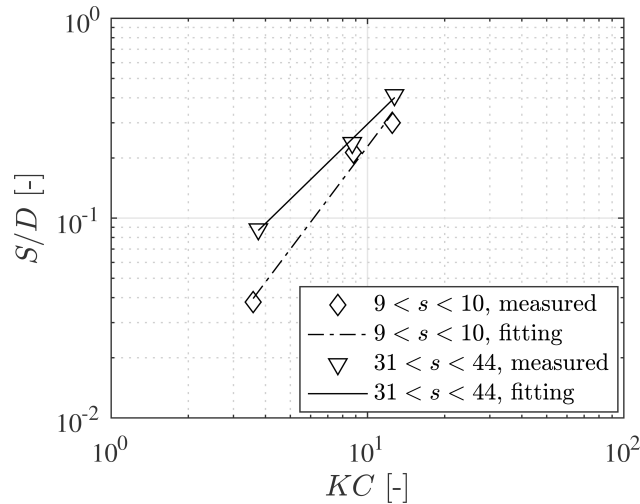
Figure 3.10: Comparison of maximal scour depths over *KC* for multidirectional "wave-only" condition.

of sediment entrainment, further tests are required to validate these findings.

Comparison to unidirectional waves

While the findings on the scour development in multidirectional waves alone provide already valuable insights in the scour processes in complex flow conditions, the direct comparison to scour induced by unidirectional waves might additionally allow the definition of application-oriented reference values for present scour prediction approaches. Typically, these approaches (cp. chapter 2.3.4 and 2.3.5) do not account for directional waves, let alone directional waves superimposed with a current. The comparison might thus provide useful indications on whether and to what extend wave directionality should be considered in engineering practice.

In case of small values of U_{cw}, i.e. in wave dominated regime, the results indicated a slightly faster progression of scour depth towards an equilibrium value for multidirectional waves than for unidirectional waves, regardless of applied *KC* number. As expected, the differences in scouring rate declined for higher values of U_{cw}, once the current flow velocity was sufficient, so that the time progression resembled that in unidirectional current conditions and the individual characteristics of wave-induced scour were suppressed.

Compared to "wave-only" conditions, the time scale, as representative quantification of the scouring rate (cp. Eq. (2.43)), increased significantly once a current was superimposed on the waves. However, with further increasing current flow velocity, the time scale decreased again, similar to the behaviour in "current-only" conditions, indicating a faster scour progression for larger values of U_{cw}. For the given range of U_{cw} the results regarding the time development in combined
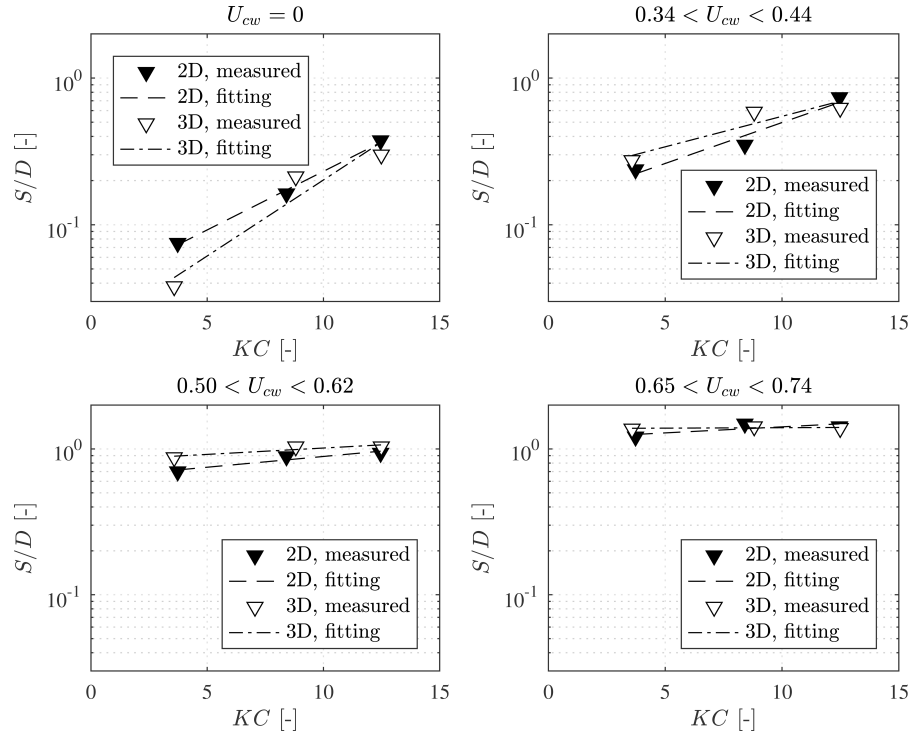
Figure 3.11: Comparison of final scour depths for multidirectional (3D, $s = 10$) and unidirectional (2D) waves against KC number.

current and wave conditions are thus in agreement with those from Petersen, Sumer, and Fredsøe (2012). While these trends apply regardless of wave directionality, the time scale in unidirectional waves was generally slightly more dependent on U_{cw} than that in multidirectional waves, particularly for large KC numbers. However, it has to be noted, that the determination of time scales could be influenced by the successive load conditions coming with the test procedure.

Fig. 3.11 compares the maximum scour depths for uni- and multidirectional waves as a function of the KC number and U_{cw}. The scour depths followed the same trend for multidirectional (3D) and unidirectional (2D) waves, namely that the influence of the KC number on the scour depths declined with increasing value of U_{cw}. For values of $U_{cw} > 0.65$, scour depths even remained almost constant regardless of the KC number. Obviously, only slight differences in maximum scour depth between multidirectional and unidirectional waves have been measured.

While the scour depths were larger by a factor of 1.33 (averaged over KC) for unidirectional compared to multidirectional waves in case of "waves-only" conditions, they were smaller by a factor of 0.88 for values of U_{cw} in the range of $0.34 - 0.44$ and smaller by a factor of 0.85 for values of U_{cw} in the range of $0.50 - 0.62$. In current dominated conditions with values of $U_{cw} > 0.65$, and thus, diminishing influence of waves, the differences in scour depths were negligible.

This finding is in agreement with results obtained with the stochastic prediction method by Ong, Myrhaug, and Hesten (2013) and Myrhaug and Ong (2013), who also found decreasing differences between two and three-dimensional wave induced scour depths with increasing current. However, regardless of the considered value of U_{cw}, the stochastic model showed larger scour depths in three-dimensional than in two-dimensional wave conditions for values of $KC > 2$. In the study presented herein, overall larger scour depths are found in unidirectional than in multidirectional waves for wave only conditions (cp. Fig. 3.11). Although a trend towards similar scour depths with increasing KC number is evident, this contradicts the results given by the stochastic model.

3.2.5 *Conclusions & Discussion*

Findings regarding the scouring process induced by multidirectional waves and its differences to scouring in unidirectional, long-crested waves can be summarized as follows:

- In "wave-only" conditions, scour depths have been measured in unidirectional waves that were on average 33% larger than those in multidirectional waves for comparable values of KC number. Furthermore, the scour depths displayed a growing dependency on KC numbers with increasing wave spreading.

- For combined wave and current conditions that were still wave dominated ($U_{cw} < 0.5$), scour progressed faster over time when exposed to multidirectional than to unidirectional waves. The time scale was, however, less depending on U_{cw} for multidirectional than for unidirectional waves. In combined current and wave conditions, wave directionality led to slightly larger scour depths, reversing the ratio of scour depths found for "wave-only" conditions.

- With flow conditions further approaching current dominated regime ($U_{cw} \rightarrow 1$), differences regarding the scouring rates and depths resulting from the wave directionality were declining and the scour characteristics resembled more and more those in unidirectional currents.

Concluding, the results thus indicate a reduction of scour depths as a consequence of directional distributed wave energy. By definition, the total energy of the directional wave spectrum has to be identical to the wave energy inherent to the underlying unidirectional frequency spectrum. As the wave energy distributes over several directions, the amount of energy and consequently the erosive potential in main wave direction must be smaller than that in a comparable unidirectional spectrum. In addition, given the short-crested nature,

waves approach the pile simultaneously from more than one direction and are unsymmetrical on two sides of the pile at any time. This minimizes the accumulating effects of a constantly recurring, bidirectional vortex system around the pile on the scour development. In combined current and wave conditions, the wave directionality thus leads in turn to larger scour depths compared to long-crested waves, as the influence of the unidirectional current on the scour process is relatively increased.

However, differences in scour depth between uni- and multidirectional waves remain relatively small, even more so considering the still limited number of data points and the general uncertainties inherent to hydraulic testing, not least attributed to disproportionally sediment scaling. Therefore, scaling the result to prototype dimensions could be subject to uncertainties and a design process for offshore structures based solely on the results of this study is thus not recommended without additional scrutiny. From engineering perspective, and for current dominated regimes, a conservative prediction of maximum scour depths for combined current and wave conditions might consider values obtained for current only conditions. However, it is important to note, that the critical thresholds for the expected scour depth and the required stone size for a granular scour protection are not induced by the same flow condition. While the development of critical scour depths is a time-dependent transport process, the initiation of stone movement is an instantaneous incipient motion problem instead. The design of scour protection is thus much more determined by wave-induced bed shear stresses. Consequently, despite relatively small predicted scour depths in "wave-only" conditions compared to current flow conditions, the size of required stone sizes for a stable scour protection might be rather large.

While the effects of short-crested waves on the scour development around a pile have been demonstrated, the direct influence of short-crested waves on the flow and vortex system around the pile and its interaction with the scour development has yet to be investigated systematically. Future model tests should incorporate a wider range of wave spreading and wave parameter. Large scale tests could also be rewarding by enabling the detailed analysis of the flow field, but could be difficult to accomplish because multidirectional wave basins are usually limited with respect to available wave heights and periods.

STABILITY OF WIDELY GRADED BROKEN STONE MATERIAL UNDER COASTAL AND MARINE FLOW

A series of experiments was carried out to elucidate the erosive behaviour and stability-affecting processes of widely graded quarry-stone material subjected to coastal and marine flow conditions. By deepening the understanding of armoring processes in oscillating flow conditions, providing a quantification of bed stability and assessing the performance as scour protection, the results lay out a sound basis for the inherent characteristics of widely graded material to be considered in scour protection design, and potentially progressing it towards an even more efficient process.

To account for a wide range of marine and coastal flow conditions, the multi-phase test program included experiments with spectral wave load (Schendel, Goseberg, and Schlurmann, 2015), unidirectional flow (Schendel, Goseberg, and Schlurmann, 2016) and reversed flow conditions (Schendel, Goseberg, and Schlurmann, 2017) as substitution for tidal currents. The grain material used in all of these experiments was a widely graded quarry-stone mixture composed of granodiorite (Jelsa quarry in Norway) with a homogenous grain size distribution in the range of 0.063 mm - 200 mm, a median grain diameter $d_{50} \approx 30$ mm and a geometric standard deviation of $\sigma_g \approx 6 - 7$ (cp. Fig. 4.1). The material was provided by an industry partner, and thus, its properties resembled the actual composition intended to be applied as scour and bed protection around coastal and marine structures. Fabricated as broken stone material with sharp edges, the particle shape distinguished clearly from the water-worked surfaces of natural sediments in rivers, from which most current bed stability approaches are derived.

In the following, the author's publications dealing with the erosion stability of this granular material under various flow situations are summarized and evaluated with respect to the overall objective of this thesis and especially towards possible implications regarding the design of scour and bed protection. An extended critical discussion on how the characteristic material properties can be considered in current scour protection design, and moreover, explicit, application-oriented recommendations for the design of scour protection with widely graded are then given in the following chapter 5.
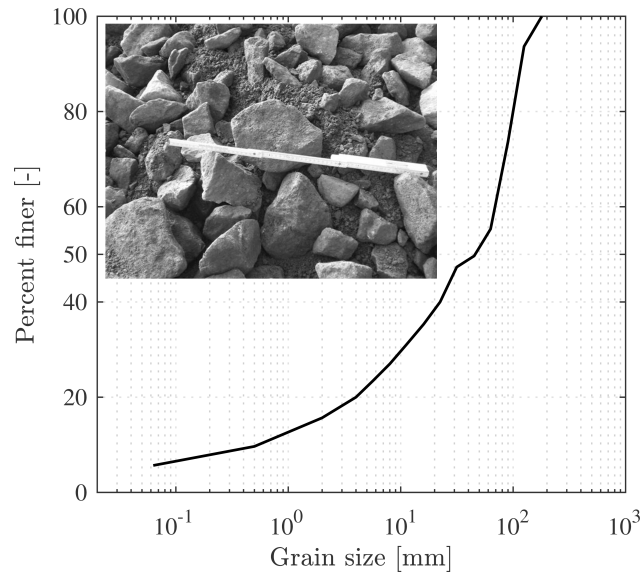
Figure 4.1: Representative grain size distribution of widely graded broken stone material as applied as scour and bed protection.

4.1   EROSION STABILITY OF WIDELY GRADED MATERIAL UNDER WAVES

Schendel, A., Goseberg, N., and Schlurmann, T. (2015). Experimental study on the erosion stability of coarse grain materials under waves. Journal of Marine Science and Technology, Vol. 23(6), pp. 937-942.

This publication describes large-scale hydraulic model tests carried out to assess the general suitability and performance of a widely graded granular scour protection under random wave load. To minimize possible scaling effects, particularly with respect to the characteristics of the granular material, the hydraulic model tests were performed at a length scale of 1:4 in the Large Wave Flume (GWK) of the Forschungszentrum Küste (FZK) in Hannover, Germany. However, from Figure 1 in Schendel, Goseberg, and Schlurmann (2015) it is evident that the scaling of the granular material from the prototype material was not evenly for all grain fractions. As it was technical not feasible to produced the required amont of fine grains (over 200 t of granular material were used), finer fractions in model became relatively larger compared to the prototype material.

With the focus on the stability against shear failure, an experimental setup consisting of a monopile foundation surrounded by a single layer scour protection was chosen, preventing winnowing effects or a destabilisation due to bed form migration. In addition to commonly applied scour measurement techniques, i.e. underwater cameras and echo sounder, a state-of-the-art high-resolution 3D laser scanner was used to measure the spatially distributed damage after a certain number of waves. Spectral wave loads (JONSWAP) were based on typical

North Sea wave conditions with subsequently increasing significant wave heights, substantiating the application-oriented approach of the tests.

The results provided insights in the behaviour of widely graded material under wave load, which differs decisively from unidirectional flows in river channels by the presence of horizontally and vertically oscillating flow components. Two additional stability-affecting aspects that might need to be considered in the scour protections design with widely graded grain material were revealed: the development of a protective armor layer under spectral wave load and the possibility of material segregation in the vicinity of the monopile.

Taking into account that the number of waves was insufficient to reach equilibrium state, only relative small scour depths could be measured. The scour development however did at least converge towards a constant depth, indicating a declining damage over time instead of a progressive failure mechanism for which damage increases exponentially. This allows the definition of a threshold criterion in form of an acceptable damage for a dynamically stable scour protection design (De Vos et al., 2012).

In addition to the analysis given in Schendel, Goseberg, and Schlurmann (2015), further information on applied load conditions are presented in Table 4.1 to provide reference for an extended damage assessment. The flow parameters in Table 4.1 are based on acoustic doppler velocimeter (ADV) measurements, which were carried out 34 m upstream of the monopile but whose analysis initially was not part of Schendel, Goseberg, and Schlurmann (2015).

Table 4.1: Test conditions, where the maximum horizontal flow velocity U_w is based on measurements at 10 cm above the bed, and τ_w the wave induced bed shear stress is based on Eq. (2.21) and Eq (2.22). The damage number S_D is given by Eq. (2.57).

Spectrum	H_s	U_w	KC	τ_w	$\lvert \min(S_D) \rvert$
	[m]	[m/s]	[-]	[N/m²]	[-]
1	0.7	0.30	2.3	2.75	0.298
2	1.0	0.43	3.4	4.65	0.899
3	1.3	0.56	4.5	6.67	1.962

Following the concept of De Vos et al. (2012) for the damage assessment of a dynamic scour protection design, the volume of eroded material V_e can be related to a specified sub area times the d_{max} diameter of the granular material, allowing the quantification of damage by a non-dimensional number:

$$S_D = \frac{V_e}{d_{max}\frac{\pi D^2}{4}} \tag{4.1}$$

In accordance with the approach of De Vos et al. (2012), the sub area is chosen to resemble the cross-sectional surface of the pile. However, d_{max} as reference grain diameter is assumed to better represent the stability characteristics of the widely graded material than the $d_{n,50}$ diameter used by De Vos et al. (2012). The distribution of damage numbers in the vicinity of the monopile at the end of the tests is depicted in Fig. 4.2. The elicitation of scour in terms of defined damage numbers helps quantifying the residual stability as a performance index of the widely graded scour protection, and thus, can provide a decision-making tool for the scour protection maintenance management over the life-time of the structure.

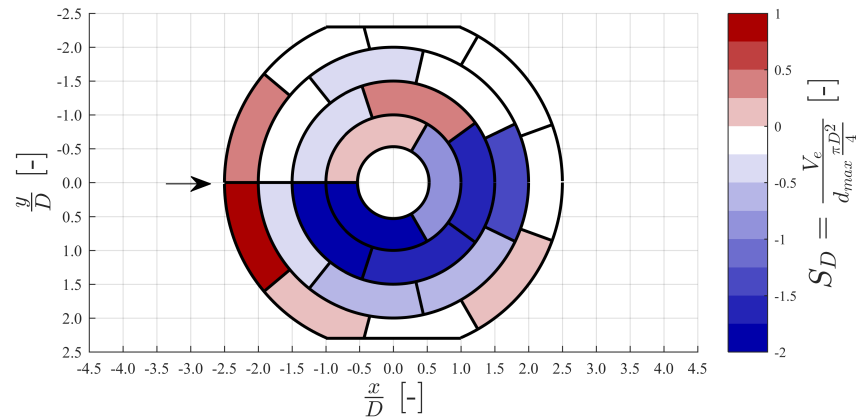Figure 4.2: Distribution of damage at the end of the tests, where negative values of S_D refer to scour and positive values to accumulation of material. Arrow indicates direction of wave propagation.

Fig. 4.3 correlates the damage at the end of each wave spectrum to the wave induced bed shear stress. Here, $|min(S_D)|$ resembles the maximum damage number over all sub areas at the end of a wave spectrum.
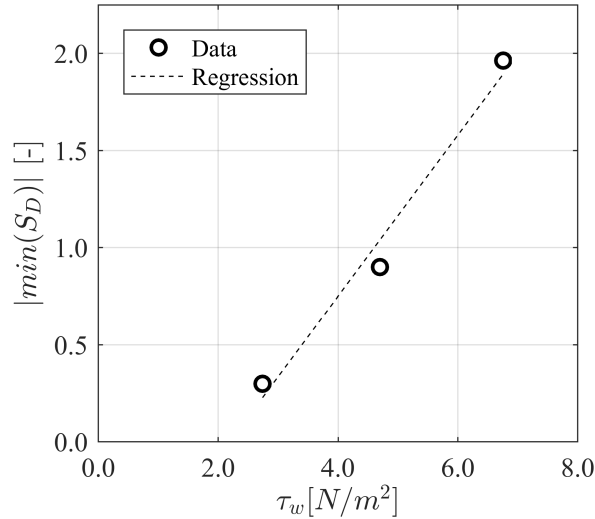
Figure 4.3: Development of maximum damage over the surface of the scour protection versus the applied maximum wave induced bed shear stresses.

The final value of $|min(S_D)|$ = 1.96 implies a maximum damage equal to the height of two times the d_{max} diameter of the widely graded material. As this material is intended to be used mainly in a single-layer scour protection a layer thickness considerable larger than two times the d_{max} stone diameter can be assumed. Eventually, for the investigated conditions, no overall failure of the protective function could thus be observed.

4.2 EROSION STABILITY OF WIDELY GRADED MATERIAL UNDER UNIDIRECTIONAL CURRENT

Schendel, A., Goseberg, N., and Schlurmann, T. (2016). Erosion stability of wide-graded quarry-stone material under unidirectional current. Journal of Waterway, Port, Coastal, and Ocean Engineering, Vol. 142(3).

In this paper, experimental model tests are presented that addressed the erosional behaviour and the bed stability of widely graded broken stone material subjected to unidirectional currents. The experiments were carried out in a close-circuit flume, in which the granular material was built-in at ground level and subsequently exposed to incrementally increasing unidirectional flow. For each incremental velocity step, the flow velocity was maintained until an equilibrium state was reached and sediment transport could no longer be observed. Eroded bed load was collected and detailed near-bed flow field measurements were performed, allowing the determination of critical threshold values for the initiation of motion as basis for a quantified assessment of bed stability. High-resolution digital eleva-

tion models (DEMs) derived from 3D laser scans helped to assess the flow-induced changes of the bed surface and their effect on the bed roughness. While the model tests were performed in a scale of 1:1 with respect to rock sizes, flow velocities and shear stresses, the water depth was much smaller compared to that in offshore conditions. The distorted scale of the water depth might lead to significant scale effects. The scale of the largest turbulence structures in the flow might be different, which could influence the winnowing processes. Moreover, as the gradient of flow velocities is more pronounced obtained bed shear stresses might be larger. This might give extra destabilizing forces on the bed material, as discussed in (Steenstra et al., 2016).

Indicated by a strong dependency of critical bed shear stresses to individual grain sizes, a highly selective mobility of finer grain fractions was found. Shvidchenko, Pender, and Hoey (2001) attributed this behaviour to the effect of sediment gradation on the hiding process, which they assumed becomes less effective with increasing gradation due to the relatively large amount of finer particles in the sediment mixture. In this study, however, the analysis of the DEMs clearly demonstrated the occurrence of hiding and exposure processes during the experiments. For the design of a scour protection with widely graded material, this finding is of major importance as it implies the necessity to account for a wide range of critical shear stresses between individual grain sizes, and thus, stresses the role of selecting a suitable reference grain size to represent the stability behaviour of the material. Therefore, the suitability of several reference grain sizes was assessed by providing a comparison with available hiding functions. While the usage of d_{50} and d_a as reference size failed to represent the material characteristics adequately, the use of d_σ (based on σ_g) as reference size performed well when compared with results from previous studies. Consequently, given the formulation of hiding functions (Eq. (2.38)), the critical shear stress of all fractions finer than d_σ will be increased relatively to that of d_σ. Because d_σ resembles a much larger grain size than d_{50} or d_a, the increase of critical shear stresses will apply to wider range of grain fractions.

At the end of each incremental increase of flow velocity, a stable and immobile static armor layer formed, indicated by observed downstream winnowing processes and the composition of the eroded bed load, which remained finer than that of the parent material throughout the experiments. The armor layer demonstrated a very compact grain structure, so that the coarsened bed was able to provide the required resistance against the applied hydraulic loading. This behaviour might thus add to the potential of the widely graded material to be used in a dynamic design of scour protection, which allows the limited movement of stones to reduce the required stone size and decrease the cost. Following the erosion of finer fractions and the for-

mation of an armor layer, the remaining coarse bed could assure the protective function of the cover layer.

4.3 EROSION STABILITY OF WIDELY GRADED MATERIAL IN RE-VERSED CURRENTS

Schendel, A., Goseberg, N., and Schlurmann, T. (2017). Influence of reversing currents on the erosion stability and bed degradation of widely graded grain material. International Journal of Sediment Research, Vol. 33(1), pp. 68-83.

As a subsequent investigation to Schendel, Goseberg, and Schlurmann (2015, 2016), this paper focuses on the response of a widely graded material bed to reversing flow conditions as found in tidal currents and expands the knowledge on its erosive behaviour by the quantification of local bed degradation processes. For this purpose, complex tidal currents were initially substituted by bidirectional and periodically reversing currents with incrementally increasing flow velocity every tidal cycle. The applied flow velocities and the experimental setup were identical to those presented in Schendel, Goseberg, and Schlurmann (2016), allowing the comparison of processes involved with armor layer development and revealing differences regarding the bed stability against shear failure.

Given the rough and inhomogeneous bed surface, dissimilar local near-bed flow velocities and turbulence intensities depending on the flow direction were measured. Thus, despite identical approach flow velocity, exerted bed shear stresses did not only vary spatially over the bed surface but were also strongly dependent on the flow direction, causing anisotropic erosion potentials between flow directions. For the design of scour and bed protection in environments with changing flow directions, this additionally raises the question of how to account for the anisotropic bed roughness and flow resistance.

Furthermore, a rearrangement of the formerly established static armor layer occurred with changing flow direction, indicated by the resumption of sediment transport. Following the re-allocation of sheltered and exposed areas within the bed surface as a result of reciprocal effects between flow and the bed, previously protected grain fractions became exposed again and were thus re-entrained despite being exposed to the same flow velocity as before. It might therefore be concluded that with an increasing number of periodically changing flow direction an even coarser static armor layer will form than under unidirectional flow, in case no additional sediment is supplied.

The anisotropic behaviour was also found to affect the erosion stability in a way that the bed load composition was slightly coarser in the succeeding reverse flow direction than in the initial direction, leading to a higher bed stability in the initial flow direction. In compar-

ison to the stability of widely graded material under unidirectional current, larger critical bed shear stresses were determined for the reversing current case and consequently a higher stability can be assumed. The increased stability was attributed to the formation of a more compact and dense surface structure, stemming from the continuous repositioning and subsequent interlocking of stones. A quantification of bed degradation by adapting the approach and failure criterion of De Vos et al. (2012) was applied to further assess the bed stability and to provide insights in the progression of damage as basis for a definition of acceptable damage threshold. The progression of bed degradation with increasing bed shear stresses was found to be a function of the median grain diameter d_{50} of the parent material.

In conclusion, the obtained insights in the erosion behaviour of widely graded broken stone material under reversing current conditions as well as the evaluation of bed stability contribute to the derivation of a holistic design approach for a widely graded scour protection system.

SCOUR PROTECTION DESIGN WITH WIDELY GRADED MATERIAL

5.1 DESIGN RECOMMENDATIONS

The small amount of bed degradation, which additionally was very heterogeneously distributed over the bed surface, indicates an normal bed resistance to shear failure of widely graded quarry-stone material against unamplified current load (Schendel, Goseberg, and Schlurmann, 2016). In oscillating flow conditions (Schendel, Goseberg, and Schlurmann, 2017), first results suggest a complex fluid-bed-interaction, due to a relocation and balancing of sheltered and exposed areas, leading to bidirectional displacement processes. The selective wash out of fine sediment fractions, as a result of downstream winnowing processes, leads to the development of a static armor layer, which is characterized by a coarser grain size distribution than that of the subsurface material. As coarser grains are inherently harder to mobilize, the overall bed stability is further enhanced.

By proving effective resistance against hydraulic load conditions found in marine and estuarine environment, the potential as bed and scour protection system for offshore structures seems promising with respect to the shear failure mechanism. However, with the erosional behaviour of graded sediment significantly differing from that of uniformly sized sediments, traditional stability approaches like Shields (1936) and even improved hiding functions based on mean grain diameters (see chapter 2.2.2) do not adequately reflect the material behaviour.

With expected effects on required stone sizes and connected costs for installation and maintenance, it seems only reasonable to consider the self-stabilising features of graded sediments within the stability assessment of scour protection design. The material of interest, as described in chapter 4, is characterized by a grading of $\sigma_g \approx 6 - 7$ and a ratio of d_{85}/d_{15} larger than 30. This is considerably wider than the grading of usually applied rock protection, which can be classified according to CIRIA (2007) as wide graded if $1.5 < d_{85}/d_{15} < 2.5$ and very wide graded if $2.5 < d_{85}/d_{15} < 5$. Consequently, several design aspects need to be re-examined to account for the extremely wide graded material composition and to ensure a stable scour protection.

Thus, this chapter intends to provide application-oriented recommendations for the design of scour protection with widely graded material by discussing the feasibility of linking available (chapter 2.2) and newly gained (chapter 4) knowledge on the erosional behaviour

of graded sediments to present design methods for scour protection around offshore foundations. Instead of aiming at the definition of a complete new and customized design process for widely graded materials, the given recommendations follow a practical approach of expanding available design concepts at this point. Until further studies provide sufficient data for the derivation of a holistic design concept, these recommendations might already improve the scour protection design by highlighting interfaces within the design, at which the influence of sediment gradation is particularly crucial.

In addition, while the recommendations focus on the determination of required stone sizes for a statically stable protection against shear failure as part of the actual design stage, other failure modes (e.g. filter stability) are not considered at this point. Furthermore, this section does not intend to answer unresolved but not less important questions regarding the economical and ecological footprint of widely graded materials applied as scour protection in marine environment compared to other protection systems. In particular, the following aspects regarding the influence on the scour protection design will be discussed:

- **Identification of interfaces** within present scour protection design, which are crucial for the implementation of graded material characteristics.

- **Discussion and recommendations** on suitable adjustments to identified interfaces regarding graded material characteristics.

- **Implementation** into present scour protection design and **assessment** of influences on required stone size based on a case study.

- **Limitations** of the extended design approach.

5.1.1 *Identification of interfaces*

The stability assessment, as integral part of scour protection design, is traditionally based on the determination of a certain stone size with a resistance large enough to withstand the given hydraulic loads. The integration of graded sediments into the scour protection design might thus be directly linked to this dependency on a single stone size. Obviously, a re-evaluation of the fixation on a single representative stone size would be reasonable, considering the differences in material composition and erosional behaviour between uniform and graded sediments. In a first step, before additional model tests can deliver a more comprehensive stability criterion suited for graded materials in the future, preferably obtained in large-scale tests with a scour protection setup, a more adequate representation of graded ma-

terial properties than the often-applied median diameter d_{50} should be used.

In this context, options of expanding the typically scour protection design for graded materials are presented for both parts of the resistance-load comparison, including the modification of bed roughness, effective and critical shear stresses. Fig. 5.1 gives an overview over possible interfaces for the calculation of required stoned sizes within a static scour protection design based on the critical shear stress concept by Shields, which should be adjusted to account for graded materials characteristics.
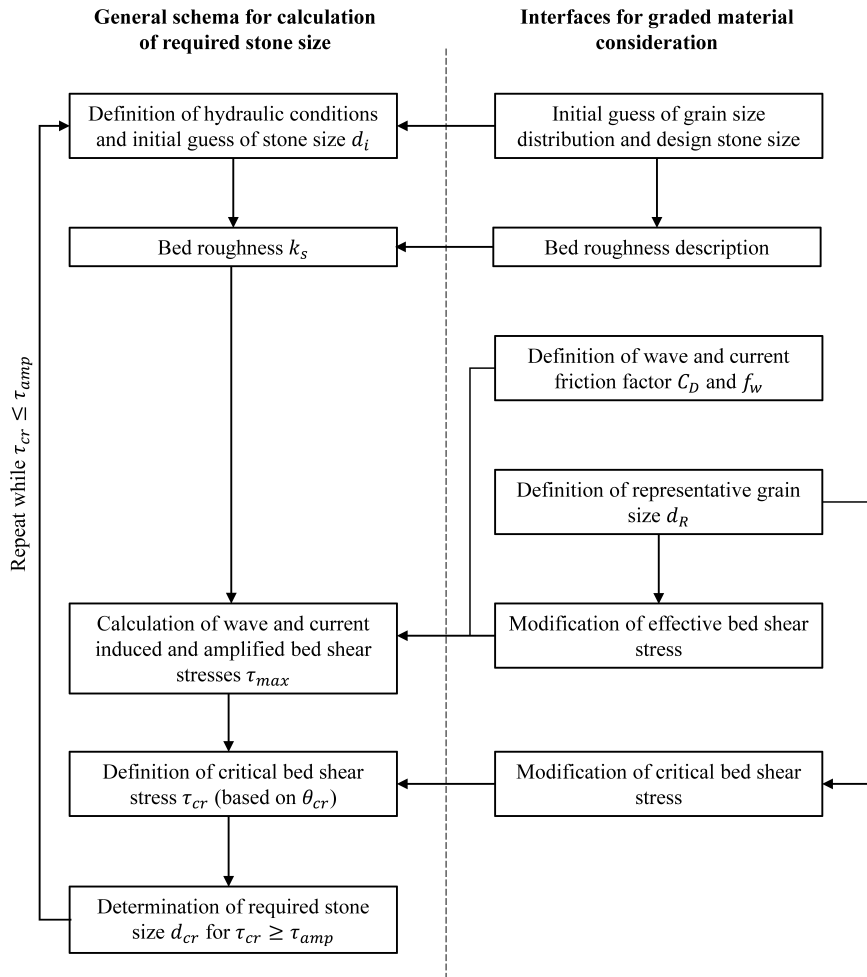
Figure 5.1: Identification of interfaces for the consideration of graded material properties within the determination process of required stone size for a static scour protection.

Since graded sediments develop a stabilising armor layer over time, several phases with different stability should be considered throughout the design process. While the material will be loose during the installation, a varying stability with developing armor layer might occur once the material is installed and exposed to flow. In addition, the

composition of the armor layer might be repeatedly changing with varying sediment supply coming from the surrounding sea bed. Thus, the presented options for implementing graded material behaviour in recent scour protection design include stability approaches for an already armored bed, in addition to approaches for loose material beds.

Selection of bed roughness parameter

An accurate description of bed roughness is essential for the estimation of acting shear stresses, which in turn determine the required stone sizes in a scour protection design. Here, the selected bed roughness effects the shear stress through the definition of a dimensionless friction (or drag) factor (cp. Eq. (2.15)). As pointed out in chapter 2.1, numerous definitions for wave and current induced friction factors (including the well-known Darcy-Weisbach, Chezy or Manning coefficients) are available, in which the bed roughness is usually expressed by values of the equivalent sand roughness k_s after Nikuradse (1933) or by the roughness length z_0, the height above the bed at which the logarithmic velocity profile tends to zero. Based on the work of Nikuradse (1933), the dependency between z_0 and k_s for a hydraulically rough flow regime is given by $z_0 = k_s/30$, which should be almost always the case due to the coarse stone size used in scour protection applications. A comparison of several approaches for the wave friction factor and a discussion on their influence on the scour protection design is given in De Vos (2008). As much smaller boundary layers develop under waves than in tidal currents, due to the substantially shorter flow periods of waves, significantly larger bed shear stresses can be expected for waves than for currents for a comparable free stream velocity (Nielsen, 1992). The influence of the current friction formulation on the overall bed shear stress and the required stone diameter might thus be of minor importance for design-relevant marine conditions. Nevertheless, a summary of logarithmic and power law based friction factors for high and low relative submergence is given by Powell (2014).

Traditionally, the equivalent sand roughness k_s is described by multiples of a characteristic grain size, e.g. d_{50}, d_{65}, d_{84} or d_{90}. With regard to different hydraulic conditions (relative submerge height) and bed material properties, empirical approaches are available in literature that vary in a wide range between $2.5\,d_{50}$ (Engelund and Hansen (1967) for a flat sand bed) to $3.5\,d_{90}$ (Charlton, Brown, and Benson (1978) for gravel bed rivers). Reviews and summaries on the relation between grain size and equivalent sand roughness are given in Van Rijn (1982), Dittrich (1998) and López and Barragán (2008). For coarser beds, which are characterized by an inhomogeneous bed structure, packing and the protrusion of large stones into the flow, a grain size coarser than the average grain size, i.e. d_{84} or d_{90}, is usually

selected as being representative for the bed roughness (Powell, 2014), although the selected grain size seems quite arbitrary. Recently, by assuming a lognormal grain size distribution, Cheng (2015) derived that the representative grain size diameter is increasing with the grading, which is expressed by the geometric standard deviation σ_g. For a selected representative grain size, his analysis also suggested an increasing bed roughness k_s with increasing σ_g. Exemplary, for a value of $\sigma_g = 3$, the bed roughness k_s would be best represented by a factor of $4.3\,d_{84}$ or $3.2\,d_{90}$. Assuming a very widely graded sediment with a geometric standard deviation of $\sigma_g > 5$, as it is the case for the scour protection material at the basis for this evaluation, the results would even suggest a representative grain size d_{99} and value for $k_s > 5\,d_{90}$. However, the grain size distributions reported for the widely graded scour protection material can hardly be expressed by a lognormal distribution .

With recent advances in photogrammetric techniques and access to laser scanning technology, the description of bed roughness in terms of statistical parameters of the random bed surface elevations became more popular (e.g. Aberle and Nikora, 2006; Aberle and Smart, 2003; Bertin, Groom, and Friedrich, 2017; Mao, Cooper, and Frostick, 2011; Marion, Tait, and McEwan, 2003). In particular, the standard deviation of bed surface elevations has to be emphasized as promising parameter. Smart, Duncan, and Walsh (2002) and Aberle and Smart (2003) proposed a flow resistance equation by introducing the standard deviation of the bed elevations as roughness parameter. They found, that using the standard deviation as roughness parameter improves the flow resistance estimation compared to a bed roughness characterization based on a single grain size. While these models can account for the irregularity of the bed surface, they require detailed measurements of the bed surface elevation, preferable obtained by digital elevation models, to yield reliable estimates of bed roughness. Thus, at this state, a bed roughness estimation based on statistical parameters seems rather unpractical for the initial stage of scour protection design.

With the abundance of available roughness definitions and friction factor approaches, it is evident, that there is no consensus on a universal description, suitable for a wide variety of bed characteristics. Furthermore, friction factor approaches and bed roughness parameters are usually derived for natural river beds consisting of water-worked sediments with round edges. As broken quarry-stone material is used for scour protection, the applicability of those approaches might be questionable. Studies on the influence of artificial broken material on the bed roughness as well as on bed stability, given by a potential increase of grain interlocking, are still limited. Maynord (1991) evaluated resistance equations of logarithmic and power law form for riprap beds made of gravel or crushed stone particles. For

small scale roughness (high relative submergence), which should be the case under offshore conditions, flow resistance was correctly determined by using a standard logarithmic approach and a bed roughness of $k_s = 2\,d_{90}$. Overall, a power law approach based on d_{90} is recommended for small scale and intermediate scale roughness. However, the considered riprap materials are characterized by a relatively small geometric standard deviation of $\sigma_g > 2.2$, compared to the wide-graded material used in Schendel, Goseberg, and Schlurmann (2015, 2016, 2017).

Gessler (1990) re-evaluated tests of Little and Mayer (1976), who conducted a study on armoring with crushed materials, to obtain friction factors for armored river beds. Based on the calculated controlling roughness, Gessler (1990) derived Shields parameters for the tests of Little and Mayer (1976) and compared them to those for tests of Gessler (1965) and Proffitt (1980). He found a 33 % smaller Shields parameter for beds with crushed materials compared to beds with rounded material. While this difference might be explained by the different grain shape, Gessler (1990) found the difference to be based on the grain weight instead, which is for the same sieve size systematically lower for crushed than for rounded materials. Nevertheless, the results of Gessler (1990) were adopted by DVWK (1997) with a recommended increase of roughness for crushed materials of $k_{s,crushed} = 1.3\,k_{s,round}$.

The definition of an appropriate roughness parameter is further complicated by the fact that graded sediments tend to develop a coarse armor layer over time (cp. chapter 2.2) if $\sigma_g > 1.3$ (Little and Mayer, 1976). Assuming a dependency of roughness to armor layer composition (Gomez, 1993), the roughness becomes a temporally variable quantity depending on sediment supply and flow regime and direction. Given the common approach of relating the bed roughness to a certain grain size, one might try to estimate the roughness of an armored bed based on its grain size composition. The approach of Günter (1971) allows an estimation of the grain size distribution of a maximum coarse static armor layer based on the composition of the initial sediment bed. However, exposed to similar flow conditions, the composition of static armor layers is coarser than that of mobile armor layers. Furthermore, Mao, Cooper, and Frostick (2011) found, that due to a more complex particle arrangement and poorer interlocking, mobile armor layers exhibit a larger vertical roughness than static armor layers, which feature a more coherent surface structure. As the random surface of armored beds is additionally strongly characterized by the formation of irregular bed structures, a bed roughness description only by means of grain size composition would be subject to significant inaccuracies.

The aforementioned approaches provide valuable information on the range of expected roughness and on the influences, that have to be

considered when dealing with graded sediments. The applicability of those approaches for the exceptional characteristics of the considered widely graded quarry-stone material remains arguable, especially if they are derived on empirical basis. Thus, additional information on the roughness of this very material might be obtained from the results of the tests presented in Schendel, Goseberg, and Schlurmann (2016). Here, based on velocity measurements conducted over the statically stable armor layer at the end of the tests and by assuming a logarithmic velocity profile, roughness lengths were determined. Averaged over all measurement positions and applied loads, values of k_s between 81 mm and 153 mm were found for the individual experiments. Following the single grain size approach, these values resemble factors of $k_s = 0.8 - 1.5\,d_{84}$ or $k_s = 0.7 - 1.3\,d_{90}$. No increase of roughness with increasing load could be found, which might be attributed to the fact, that exerted flow velocities were not large enough to entrain the larger fractions, which in turn are responsible for the roughness as derived before. It should also be noted, that these roughness values are based on selective velocity measurements over a very irregular bed with high spacious variability of surface elevations.

Recommendation: The very complex fluid-sediment interactions of graded sediments, expressed by hiding and exposure processes, armor layer development and particle arrangement (clustering), which are also very depending on sediment composition and hydraulic regime, render an recommendation for the bed roughness difficult.

At present, and despite the fact that the bed roughness of gravel beds is obviously not only dependent on their grain size composition, a roughness assessment based on a single representative grain size might be the most practical approach. Based on the variety of approaches, a bed roughness formulation based on d_{90} seems reasonable for a widely graded quarry-stone material. As a conservative value, which considers the exceptional sediment grading, the influence of particle shape and a possible increase of roughness with developing armor layer, a bed roughness in the range of $k_s = 2 - 3\,d_{90}$ is thus recommended. A value of $k_s = 3\,d_{90}$ is in agreement with the value proposed by Van Rijn (1982) and later adopted by CIRIA (2007) for graded sediments. The difference in obtained roughness, and thus bed shear stress, compared to the usually applied approaches based on d_{50} (De Vos et al., 2011, 2012; den Boon et al., 2004; Soulsby, 1997) will get larger with increasing material grading, as d_{90} and d_{50} are diverging more and more.

Selection of design stone size

The design process, first and foremost, requires the definition of a suitable stone size for which the stability of the scour protection is designed for, and of which the critical Shields parameter in Eq. (2.52)

is dependent. It goes without saying, that this stone size should represent the overall stability behaviour of the applied material. As mentioned before, the erosion stability of gravel beds in rivers and streams is usually assumed to be controlled by a mean grain size of the bed surface (cp. chapter 2.2.2). Similarly, the design of required stone sizes for armor stones or riprap is typically related to the d_{50} diameter or to the nominal dimension of an equivalent cube $d_{n,50}$ (CIRIA, 2007).

While the selection of an appropriate reference stone size might be trivial for uniform sediments, it becomes more and more important with increasing grading as the critical shear stresses between individual fractions can vary significantly according to the stability concept of Shields (1936). On one hand, a design towards a stable d_{50} diameter for a widely graded material would result in uneconomically large maximum stone sizes d_{max}. On the other hand, choosing d_{max} as representative stone size could lead to an unmanageable large amount of erosion of finer grain material and might also prevent the development of the protective armor layer.

In addition, as graded sediments are subjected to a transient armoring process, the grain size composition of the bed surface changes over time. The relative size of the grain fraction considered for the design might thus considerably coarsen over time, along with the grain size distribution of the surface material, until an equilibrium state with maximum bed stability is reached. Therefore, it might be necessary to consider at least two distinct states of bed stability for the design: (a) stability shortly after the installation of the material, taking into account the composition of the parent material and (b) maximum stability under the expected design load, considering a fully developed armor layer with a composition significantly coarser than that of the parent material. For production purposes, the corresponding stone size of the parent material then needs to be re-calculated, if the required stone size is designed towards maximum bed stability.

The differences in grain size distribution between a fully developed armor layer and the parent material can be estimated by approaches proposed by Günter (1971) or Schöberl (1979). Alternatively, as will be shown in the following section, stability approaches for fully developed armor layer can be used that are based on the composition of the parent material. If designed against the same hydraulic load, the coarsening of graded materials over time thus entails smaller required stone sizes for widely than for uniformly graded materials, regarding the production relevant initial material composition.

Despite that the stability of armored beds is most often only related to mean grain diameters, a considerably influence of the coarser fractions on the armor layer development and thus stability may be assumed. Chin, Melville, and Raudkivi (1994) found that the formation of the armor layer is strongly dependent on the coarser 16 % of the initial grain size distribution. They defined a stability approach that

makes use of the ratio d_{max}/d_{50}, with d_{50} as the median grain diameter of the parent material. Recently, MacKenzie and Eaton (2017) compared the stability and morphodynamical implications of two nearly identical sediments, slightly differing only regarding their d_{90} grain size. The results suggest that channel stability is controlled mainly by the coarsest grains on the bed surface instead of the median surface grain size. As mentioned earlier, Little and Mayer (1976) found the d_{95} diameter of the parent material to mark the upper limit of potential critical shear stresses, meaning that as long as the applied shear stress is smaller than the critical shear stress of the d_{95}, a stabilising armor layer will form eventually. With the intention to design the required stone size for the state of maximum bed stability, i.e. a fully developed armor layer, the d_{95} diameter might thus prove to be a reasonable choice for a representative grain size. To account for a sediment gradation that is typical for well-graded riprap protection, Breusers and Raudkivi (1991) suggested a representative grain size that is approximately equal to the d_{67} diameter of the mixture. This diameter was later adopted by De Vos et al. (2011) for their proposed static design approach.

Yet again, those studies can only provide a first indication regarding the definition of a representative stone size and their applicability for the extremely widely graded material of interest remains questionable. The comparison conducted by Schendel, Goseberg, and Schlurmann (2016) of critical shear stresses with several available stability approaches revealed that the stability of widely graded material might be best represented by the d_{σ} diameter of the parent material composition. This representative diameter was introduced by Patel and Ranga Raju (1999) as the product of the geometric mean size and the geometric standard deviation of the material. For the widely graded material in Schendel, Goseberg, and Schlurmann (2016) this diameter resembled values that were approximately equal to the d_{95} diameter of the parent material. However, it has to be noted, that the exerted shear stresses were insufficient to entrain grain sizes larger than the d_{50} diameter, so that the state of maximum bed stability of the tested material was not reached.

Recommendations: Although still limited in amount and considered sediment gradings, available studies generally acknowledge the importance of coarser fractions for the armor layer development and stability behaviour of widely graded grain material. The usage of d_{90} of the parent, production-relevant grain size distribution as the representative stone size might depict a good compromise between a design value that allows the development of an armor layer and, at the same time, ensures economical sized maximum stone sizes. If needed, e.g. for a comparison with required stone for a more uniformly graded granular scour protection, further relevant grain di-

ameter can be calculated by assuming a Rosin-Rammler distributed grain size composition.

Modification of critical and effective shear stress

According to the stability concept of Shields (Eq. (2.52)), the design of a required stone size involves the definition of a critical Shields parameter depicting the critical condition for incipient motion of the considered grain fraction. For rough turbulent flow, commonly a value of $\theta_{cr} = 0.055$ is quoted as critical Shields parameter, reflecting the critical condition for the median grain size d_{50} in a nearly uniformly graded sediment. Although this value has been constantly revaluated over the years and generally found to overpredict the grain stability (Buffington and Montgomery, 1997), it was adopted in many scour protection approaches including Soulsby (1997) and den Boon et al. (2004). Given the uncertainty related to the definition of a universally valid value for θ_{cr}, CIRIA (2007) recommended the usage of more conservative values of θ_{cr} for the design of armor stones and riprap, i.e. $\theta_{cr} = 0.030 - 0.035$ as criterion for initiation of motion and $\theta_{cr} = 0.050 - 0.055$ if limited stone movement is allowed. To account for the effects of material gradation, De Vos et al. (2011) applied a value of $\theta_{cr} = 0.035$ combined with a d_{67} diameter as reference grain size instead of a d_{50} diameter, probably assuming a grain independent mobility and consequently a constant critical Shields parameter for all grain sizes.

However, in a sediment bed consisting of differently sized grains, the stability of any individual grain size considerably differs from that in a uniform bed of this very grain size (cp. chapter 2.2.2). As pointed out by Buscombe and Conley (2012), due to hiding and exposure effects, graded sediments are more equally mobile than that predicted by determination of the critical Shields parameter for each grain size, so that the behaviour of graded sediments cannot be assessed by just applying knowledge obtained from the uniform case. To account for the effects of sediment grading, hiding functions in the form of Eq. (2.38) are used that adjust the critical Shields parameter for the considered grain size by relating it to the critical Shields parameter of a reference grain size.

As derived in the previous section, the d_{90} diameter of the parent material composition might be most suitable to represent the stability characteristics of the widely graded material of interest. Therefore, a hiding function should be selected that preferably considers the d_{90} diameter as reference value. Hiding functions based on a different reference grain diameter will entail an additional step in the design of the required stone size as the initially unknown value of the reference diameter has to be calculated based on the d_{90} diameter and the given grain size distribution first. The selection of an appropri-

ate hiding function should also account for the state of armor layer development the hiding function was derived for, i.e. state of maximum bed stability or not, and if a static or mobile armor layer was considered. It goes without saying, that the hiding function should also be derived for material characteristics close to the intended material composition. For a comprehensive overview of available hiding functions, it is again referred to Buffington and Montgomery (1997).

A comparison of hiding functions that are empirically derived for sediments with similar grading or median grain diameter to the widely graded material of interest is given in Schendel, Goseberg, and Schlurmann (2016). Averaged over the three experiments conducted by Schendel, Goseberg, and Schlurmann (2016) with widely graded broken stone material, hiding functions related to either the d_{50} or the d_σ diameter of the parent material can be obtained:

$$\theta_{cr,i} = 0.020 \left(\frac{d_i}{d_{50}} \right)^{-0.389} \tag{5.1}$$

$$\theta_{cr,i} = 0.013 \left(\frac{d_i}{d_\sigma} \right)^{-0.389} \tag{5.2}$$

While the critical Shields parameter for a reference grain size d_{50} is considerably smaller than the commonly used values of $\theta_{cr} = 0.055$ or $\theta_{cr} = 0.030$ as suggested by CIRIA (2007), its value $\theta_{cr} = 0.020$ still lies within the boundary spanned by the approaches reported in Buffington and Montgomery (1997). The critical Shields parameter for a reference diameter d_σ reaches those of Patel, Patel, and Porey (2014) and Wilcock, Kenworthy, and Crowe (2001). The small exponent in Eq. (5.1) and (5.2), however, implies a higher selective, grain independent mobility than in most other studies (e.g. Parker and Klingeman (1982)), meaning that critical shear stresses will vary significantly between considered grain fractions, but still less than implied by the Shields curve. Additionally, the results of Schendel, Goseberg, and Schlurmann (2017) indicate slightly larger critical reference Shields parameter under reversed flow conditions, while maintaining a similar grain independent mobility as under unidirectional current.

As alternative to the correction of critical shear stresses by a hiding function, the effects of hiding and expose on the stability of individual stones in a nonuniform sediment bed can also be considered by correcting the effective shear stress acting on the stones. According to the findings of Day (1980), the effective shear stress should be adjusted because the individual stones are exposed to a different form drag as the larger stones are more exposed to the flow and the smaller stones are sheltered behind the larger ones. In contrast to the modification of the critical Shields parameter θ_{cr} by hiding functions, the modification of the effective Shields parameter θ implies reducing its

value for smaller stone sizes and increasing it for larger ones. Stemming from the description of bed load transport of nonuniform sediments, several approaches incorporating a modification of the effective Shields parameter are available, including those proposed by Day (1980), Van Rijn (2007) and Buscombe and Conley (2012). A modification of the effective Shields parameter might be particularly crucial in high shear stress regimes such as sheet flows (Hassan, Kroekenstoel, and Ribberink, 2001), where the effective Shields parameter is several times larger than its critical counterpart. For issues related to incipient motion conditions, such as the design of required stone sizes for scour protection, the adjustment of critical shear stress might be more suitable, also because most hiding function recognise the armor layer development as additional stabilising factor. As it has been shown by Schendel, Goseberg, and Schlurmann (2015, 2016, 2017), the development of an armor layer can be assumed under most flow conditions inherent to estuarine and coastal environments.

Recommendations: For the moment, until more sophisticated, empirically supported design approaches are available, the design of required stones sizes based on Eq. (5.1) and (5.2) should allow a more appropriate stability assessment for a widely graded scour protection than by applying a constant, grain independent critical Shields value of $\theta_{cr} = 0.030$ or even $\theta_{cr} = 0.055$, that does not take the stabilising characteristics inherent to widely graded materials into account. Nevertheless, the utilization of Eq. (5.1) and (5.2) for the design of required stone sizes of a widely graded grain material comes along with several uncertainties. In the experiments of Schendel, Goseberg, and Schlurmann (2016) only grain sizes smaller than the d_{50} diameter of the parent material were eroded, restricting the validity of Eq. (5.1) and (5.2) to ratios $d_i/d_{50} < 1$. An application of those equations for a d_{90} diameter thus assumes the extrapolation of their validity to ratios $d_i/d_{50} > 1$, which might be a reasonable assumption considering the trends of other hiding functions, but cannot be proven with concrete data at this point. Furthermore, as the given assessment of bed stability was empirically derived for a very specific material composition, it should not be universally applied for materials with characteristics significantly deviating from those used in Schendel, Goseberg, and Schlurmann (2015, 2016, 2017). Instead, additional scrutiny in form of systematic tests for the specific material of interest should be sought.

5.1.2 *Implementation & Application*

Based on an exemplary case study, the implementation of the recommendations outlined above into the design process of required stone sizes for a static scour protection system is described. To assess the influence of the resulting, novel design approach on the required stone size for a widely graded grain material, a comparison to traditional,

grain independent approaches, which are based on the mobility description of uniformly graded sediments, is added.

For the case study, a scour protection around a monopile ($D = 6$m) situated in typical North Sea wave and flow conditions is considered. Hydraulic conditions are based on a 50-year extreme event hindcasted by DHI (2007) for the location of the FINO 1 research platform. The water depth at this location is approximately 30 m. A widely graded grain material is intended to be applied as statically stable, single layer scour protection around the monopile. In accordance with the material characteristics outlined in Schendel, Goseberg, and Schlurmann (2016), the grading of the widely graded material is given by $\sigma_g = 6$, and the grain size ratio d_{90}/d_{50} is specified with $d_{90}/d_{50} = 2.5$. The knowledge of the ratio d_{90}/d_{50} is required for the application of Eq. (5.1) as design approach, which is given the preference over Eq. (5.2) for this case study as it simplifies the comparison to traditional approaches using d_{50} as the reference grain diameter. If the grain size ratio is unknown, it can be determined assuming a Rosin-Rammler shaped grain size distribution. The required design values are summarized in Table 5.1.

Table 5.1: Design values for a 50-year extreme event at FINO 1 platform. Hydraulic conditions are based on hindcast modeling by DHI (2007).

Hydraulic conditions:		
JONSWAP wave spectrum		
Significant wave height H_s	8.5	m
Wave period T_p	12.3	s
Orbital flow velocity U_w [a)]	1.14	m/s
Tidal flow velocity U	1.3	m/s
Water depth h	30	m
Water density ρ	1030	kg/m³
Kinematic viscosity ν	10^{-6}	m²/s
Wave-current misalignment α	0	°
Graded material properties:		
Stone density ρ_s	2650	kg/m³
Ratio d_{90}/d_{50}	2.5	
Grading σ_g	6	

[a)] Calculated with Eq. (2.20).

The improved design process for the calculation of the required stone size of a widely graded scour protection is depicted in Fig. 5.2. Here, *Step 1* involves the definition of the considered design stone size that is assumed to be representative for the material stability. Following the recommendation for widely graded material given in

the previous section, a value of $d_{cr,i} = d_{cr,90}$ is selected. In addition, a suitable roughness description as well as friction factor definition has to be specified. Again, in line with the suggested description given in the previous section, the bed roughness is defined as $k_s = 3\,d_{90}$. To allow a dedicated assessment regarding the influence of the bed roughness on the required stone size, stone sizes were also calculated for a bed roughness of $k_s = 2.5\,d_{50}$.
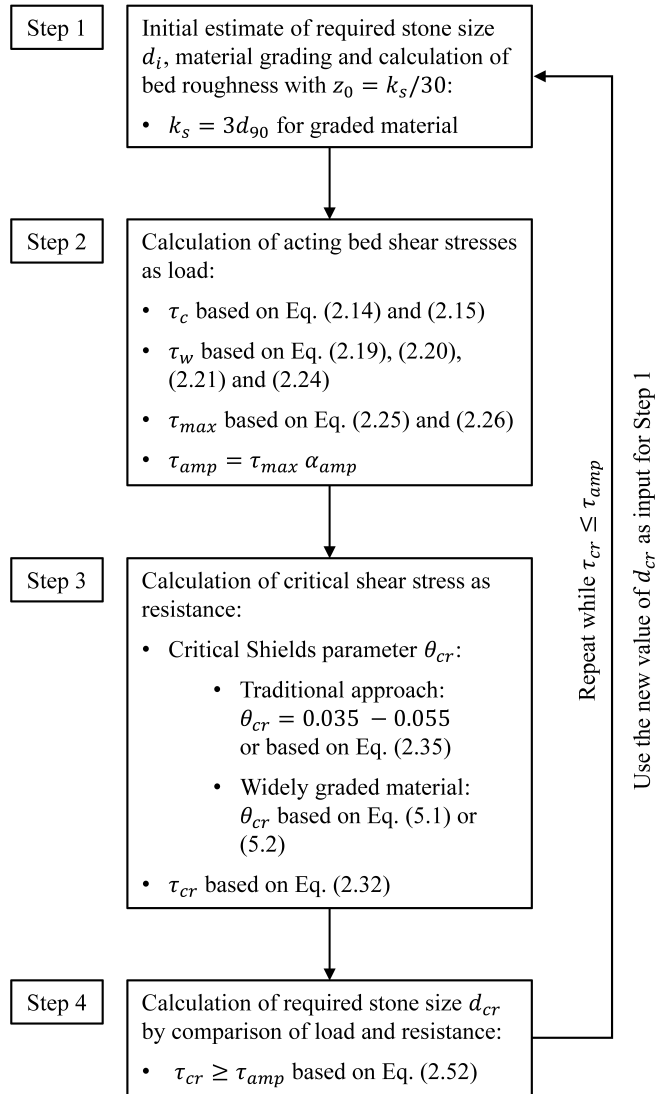

| Step 1 | Initial estimate of required stone size d_i, material grading and calculation of bed roughness with $z_0 = k_s/30$:

• $k_s = 3d_{90}$ for graded material |

| Step 2 | Calculation of acting bed shear stresses as load:

• τ_c based on Eq. (2.14) and (2.15)
• τ_w based on Eq. (2.19), (2.20), (2.21) and (2.24)
• τ_{max} based on Eq. (2.25) and (2.26)
• $\tau_{amp} = \tau_{max}\,\alpha_{amp}$ |

| Step 3 | Calculation of critical shear stress as resistance:

• Critical Shields parameter θ_{cr}:
  • Traditional approach: $\theta_{cr} = 0.035 - 0.055$ or based on Eq. (2.35)
  • Widely graded material: θ_{cr} based on Eq. (5.1) or (5.2)
• τ_{cr} based on Eq. (2.32) |

| Step 4 | Calculation of required stone size d_{cr} by comparison of load and resistance:

• $\tau_{cr} \geq \tau_{amp}$ based on Eq. (2.52) |

Repeat while $\tau_{cr} \leq \tau_{amp}$

Use the new value of d_{cr} as input for Step 1

Figure 5.2: Design process for calculation of required stone sizes for statically stable scour protection composed of widely graded grain material.

The current friction factor is calculated based on Eq. (2.15) and the wave friction factor determined using the approach proposed by Soulsby (1997) given by Eq. (2.24). However, similar to the approach of Swart (1974) the wave friction factor is limited to a maximum value of $f_w = 0.3$ for values of $A/z_0 \leq 1.57$. This limitation becomes nec-

essary as the wave friction factor would otherwise rapidly increase with every iteration, leading to extremely large bed shear stresses and consequently unrealistically large required stone sizes.

Based on the friction factors, the load in form of acting bed shear stresses is calculated in *Step 2*. The decisive bed shear stress for combined wave and current conditions τ_{max} is determined based on the approach of Soulsby (1995), and further amplified using an amplification factor of $\alpha_{amp} = 2.2$, which was obtained by experiments by Sumer, Fredsøe, and Christiansen (1992) for a wave load with a *KC* number of around 10. For the load in this case study, the selected amplification factor should be on the safe side as the chosen wave conditions result in a *KC* of only approx. 2.5. The critical shear stress in *Step 3* is either calculated by applying a traditional stability approach or by using the hiding function given by Eq. (5.1), and thus, accounting for the equalization of grain mobility due to hiding and exposure processes inherent to widely graded materials. For the traditional approach, one of two constant critical Shields parameters is used, i.e. $\theta_{cr} = 0.035$ or $\theta_{cr} = 0.055$ as recommended by CIRIA (2007) for the initiation of motion and limited stone movement, respectively.

Eventually, the required stone size can be calculated using the Shields concept given in Eq. (2.52). The design of the required stone size is an iterative process, as the calculated acting bed shear stress is dependent on the bed roughness, which in turn is a function of the required stone size. Consequently, the design process depicted in Fig. 5.2 has to be repeated until a stone size is obtained for which the critical conditions $\tau_{cr} \geq \tau_{amp}$ is fulfilled. In Table 5.2, the comparison is made between the required stone sizes $d_{cr,90}$ calculated with the traditional approach and with the hiding function in Eq. (5.1).

Table 5.2: Comparison of required stone sizes $d_{cr,90}$ in [m] for a considered design stone size $d_i = d_{90}$. For the traditional approach, a) corresponds to a constant $\theta_{cr} = 0.055$ and b) to $\theta_{cr} = 0.035$.

Traditional approach with $k_s = 2.5\,d_{50}$		Traditional approach with $k_s = 3\,d_{90}$		Approach based on Eq. (5.1)	
a)	b)	a)	b)	$k_s = 2.5\,d_{50}$	$k_s = 3\,d_{90}$
0.57	1.41	1.44	2.32	1.41	2.32

The generally large stone sizes depicted in Table 5.2 are attributed to the fact that the d_{90} grain diameter is considered as design value, instead of the usually considered median diameter d_{50}. Furthermore, the critical Shields parameter of $\theta_{cr} = 0.035$ as well as the hiding function in Eq. (5.1) conservatively assume incipient motion conditions, and thus, the complete absence of stone movement. In engineering practice, the required stone sizes would be reduced by tolerating a

limited movement of stones or by increasing the thickness of the scour protection.

As expected, the required stone size also correlates to the definition of bed roughness, regardless of the applied stability approach. A bed roughness parameter defined as $k_s = 3\,d_{90}$ leads inevitable to larger stone sizes than a bed roughness parameter $k_s = 2.5\,d_{50}$. At first glance, the required stone size seems to remain independent of the applied stability approach, as stone sizes calculated by the traditional ($\theta_{cr} = 0.035$) and the new approach (Eq. (5.1)) are identical. However, this is a remarkable coincidence caused by the initially defined grain size ratio $d_{90}/d_{50} = 2.5$. For this ratio, Eq. (5.1) results in a critical Shields parameter of $\theta_{cr} = 0.014$, which happens to be 2.5 times smaller than $\theta_{cr} = 0.035$ used for the traditional approach, compensating the influence of the stability approach on the stone size. For a material gradation deviating from this specific ratio, there is however a distinct difference in required stone size.
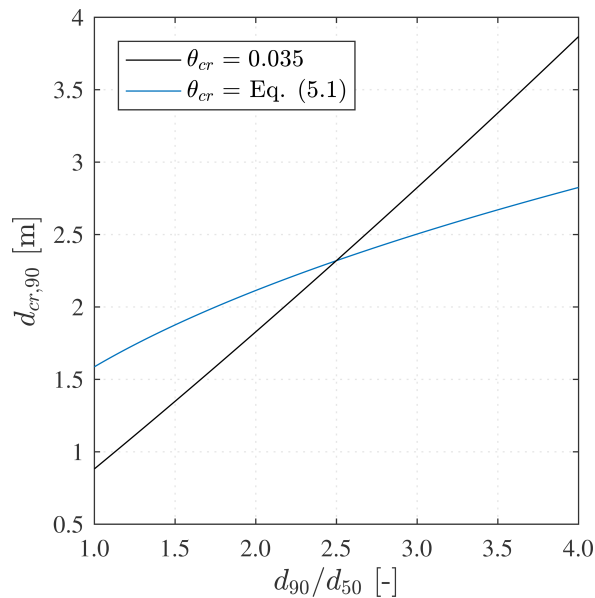
Figure 5.3: Comparison of calculated required stone sizes $d_{cr,90}$ as a function of the ratio d_{90}/d_{50} and based on design conditions given in Table 5.1.

To illustrate the different effect of material gradation on required stone sizes depending on whether the traditional ($\theta_{cr} = 0.035$) or the extended approach (Eq. (5.1)) is used, Fig. 5.3 shows calculated required stone sizes $d_{cr,90}$ as a function of the grain size ratio d_{90}/d_{50}. For grain size ratios $d_{90}/d_{50} < 2.5$, the traditional approach underpredicts the required stone sizes, while for grain size ratios $d_{90}/d_{50} > 2.5$, it significantly overpredicts the required stone sizes compared to the extended approach given by Eq. (5.1). Following similar trends as depicted in Fig. 2.2, the comparison therefore confirms a less selective grain mobility than would be predicted by a traditional approach

based on uniformly graded material. As an application-relevant consequence, Fig. 5.3 indicates that the larger the intended material gradation the more economical the scour protection can be designed using the extended approach in Eq. (5.1), as required stone sizes can be reduced significantly compared to the traditional approach.

5.1.3 *Limitations*

In this chapter, sensitive points within the design process of a statically stable granular scour protection are revealed, that are particularly critical regarding the influence of material gradation on required stone sizes. For scour protection made of widely graded materials, these interfaces need to be modified to account for the stability behaviour inherent to widely graded materials exposed to flow. Based on the insights gained in the experimental studies described in chapter 4, explicit recommendations are given on how to integrate the characteristics of widely graded materials in the current design process, eventually leading to an improved design approach. However, this also implies that the application of the extended design approach is limited to material properties and hydraulic conditions investigated in those studies. In addition, the given recommendations solely focus on the aspects of shear failure as critical failure mechanism for the scour protection, excluding other possible failure modes like winnowing caused by insufficient filter stability. Widely graded grain materials contain very small grain size fractions that might reduce the permeability and consequently could lead to an increased pressure build-up particularly under vertical wave motion. The wide sediment gradation could also affect the internal stability of the grain structure in a way that segregation effects could occur. Without further tests aimed directly at those failure mechanisms, it therefore cannot be ruled out, that other failure mechanisms yield to be more decisive regarding the scour protection stability than the considered shear failure. Apart from technical aspects, the design process of a scour protection does also involve the consideration of economical, logistical, and ecological factors. It would just not be plausible to design the stability of a scour protection, whilst the economic viability of widely graded material is not proven or as long as an ecological impact of the inevitable erosion of finer grain particles on the surrounding environment cannot be dismissed.

Furthermore, as already pointed out, the hiding functions given in Eq. (5.1) and (5.2) are derived from tests in which only grain sizes smaller than the d_{50} diameter were entrained and the state of maximum bed stability could not be reached. The experiments were also conducted without additional upstream sediment supply, allowing the formation of a static armor layer, but at the same time representing unrealistic marine and coastal morphodynamic conditions. While

the results of Schendel, Goseberg, and Schlurmann (2015) revealed a scour pattern around the monopile similar to that in sand, the actual influence of the structure on the flow characteristics, and thus, on the load exerted to the scour protection was not determined. Instead, until a direct correlation between bed shear stress and failure of the scour protection can be derived from further tests, the increase of shear stresses near the pile has to be estimated by an amplification factor, following common engineering practice.

Anisotropic erosion potentials between flow directions as a result of a rough and inhomogeneous bed surface were demonstrated by Schendel, Goseberg, and Schlurmann (2017) for reversed current situations. As this point, it is still unclear how to account for diverse bed resistance within the design of a stable bed and scour protection. A first approach might involve the usage of a mean bed roughness value derived from the statistical description of spatial-temporal roughness attributes. This approach however would require a substantial database for a wide variety of material compositions and flow conditions in order to provide values that can be used in the design process of scour protections, where the actual bed surface structure is not known.

Although the potential for a dynamically stable scour protection has been proven, as the limited erosion of finer grain fractions results in a stabilization of the bed surface, the improved design approach only considers a statically stable system defined by a critical threshold for the initiation of movement. The formulation of a design approach for a dynamically stable protection additionally requires the definition of suitable damage criteria and stability thresholds. No critical failure of the protective function (Schendel, Goseberg, and Schlurmann, 2015) or critical amount of bed degradation (Schendel, Goseberg, and Schlurmann, 2017) has been found, rendering the definition of those values difficult. Again, further tests are needed, incorporating higher load conditions beyond the state of maximum bed stability for the widely graded material. Further limitations stemming from the experimental procedure are discussed in the publications introduced in chapter 4.

6

SUMMARY & OUTLOOK

This thesis concerns the design of offshore foundation structures against the structural deteriorating effects of scour. It was aimed at reducing uncertainties in the dimensioning process of those structures by providing insights in previously neglected aspects of scour prediction and scour protection design. In the context of the progressing expansion of offshore wind energy towards unexploited waters and considering the already showing consequences of climate change on extreme weather events, more severe and complex hydraulic conditions have to be taken into account for an accurate prediction of scour development. Concurrently, a flexible but also economic scour protection system is needed that provides sufficient resilience against those loads and is easily applicable independently from site-specific conditions.

Thus, a series of novel experimental studies was carried out to systematically investigate (a) the morphodynamical seabed response around a foundation structure to complex marine flows and (b) the stability of widely graded broken stone material and its potential as alternative bed and scour protection system.

6.1 WAVE-CURRENT-INDUCED SCOURING PROCESSES

As tidal currents decisively depict a determining factor for scour in marine conditions, laboratory experiments were conducted that focused on the emergence and development of scour around a monopile structure in tidal flow conditions. To achieve a more realistically representation of tidal currents than by previous studies, tidal signals were appropriately scaled from field measurements, resulting in bidirectionally reversing flow with continuously changing velocities. Novel insights on the intrinsic progression of sediment displacement and time scale of the scouring process around a monopile were presented as a function of flow intensity. Because of constantly varying sediment infilling and displacement processes, the time development of the maximum depth under tidal flow was found to be unsteady and was characterized by periods of stagnating and decreasing scour depth. Following the oscillating velocities of a tidal current, the development of scour depths depicted a returning, distinct scheme with every tidal half cycle, especially in live-bed conditions.

It can be assumed that the variability of scouring rates within the course of a tidal half cycle cannot be represented appropriately by

modelling techniques that considerably simplify unsteady tidal currents; for example, a square tide or a step-wise adjustment of flow velocities. Accordingly, it is impossible to describe the characteristic morphodynamical processes by using a constant and unidirectional velocity value, as it is often required as many hydraulic test facilities are restricted to unidirectional current generation. However, maximum scour depths in tidal currents might be estimated by a unidirectional current within a reasonable degree of certainty, if a suitable reference velocity is selected. A good approximation of scour depth and rate with unidirectional currents was found by applying a velocity close to $u_{max}/\sqrt{2}$ of the tidal signal, i.e. it's true RMS value.

Furthermore, to account for typical offshore sea states, novel laboratory experiments regarding the influence of wave directionality on the scouring process at a monopile foundation were carried out. The test program included experiments with multidirectional waves as well as superimposed with oblique currents and were complemented by tests with unidirectional waves to provide additional reference for comparison. For all tests JONSWAP wave spectra were generated and a transparent pile was used as substitute for an offshore monopile foundation. Despite identical total wave energy between the multi- and unidirectional wave spectra, distinct differences in scour depth and rate could be observed, which inevitably can only be attributed to the influence of wave spreading on morphodynamical processes around the pile. In general, smaller scour depths have been found due to multidirectional than induced by unidirectional waves. The reduction of scour depths might be ascribed to the combining effects of energy dispersion, leading to reduced erosive potential in the main wave direction, and to the asymmetrical and simultaneous approach of waves towards the pile, hindering the formation of a recurring, bidirectional vortex system around the pile. Nevertheless, further tests have to be carried out that focus on the flow regime around the pile to fully uncover responsible morphodynamical processes leading to the differences in scour depth and rate.

The experiments on tidal and multidirectional wave induced scour advance the knowledge of scouring processes in the marine environment. In addition, with respect to the scour prediction for offshore structures, the following conclusions can be drawn:

- Flow directionality stemming from tidal currents or multidirectional waves should be considered for the assessment of scour progression over time, as scouring rates are significantly affected in both cases compared to a unidirectional flow. The accurate assessment of scour rates becomes important for the estimation of time windows available for the installation of offshore structures and its scour protection systems. Furthermore, the accuracy of numerical and hydraulic models greatly depends on a precise description of expected scouring rates.

- In tidal currents, maximum scour depths will be vastly overestimated if they are predicted based on peak tidal flow velocities alone, possible leading to an uneconomic structural design of offshore foundations. Instead, a flow velocity close to the true RMS value of the tidal signal is found to represent maximum scour depth best. Due to its simplicity, this approach provides application-oriented relevance.

- A reduced scour potential due to wave directionality has been been found in wave only conditions, which in turn lead to larger scour depths in combined current and wave conditions. The largest scour depths, however, were measured in conditions approaching the current only case, regardless of the amount of wave directionality. Thus, in a current dominated regime, superposition with waves reduces the scour depths that would be obtained in current only conditions.

6.2 BED STABILITY AND SCOUR PROTECTION DESIGN

As imperative for a reasonable assessment of its scour protection capabilities for offshore foundation structures, the erosive behaviour of widely graded material subjected to marine flow conditions has to be understood. Therefore, a coherent series of hydraulic experiments was carried out to shed light on the material's stability response to a wide range of marine flow conditions, including unidirectional and bidirectionally reversed current as well as spectral wave load.

- Under successively increasing current load the widely graded material showed a highly selective mobility of finer grain fractions, as opposed to the concept of equal mobility. As each grain fraction will be entrained by a different shear stress, this finding implies a wide range of potential critical conditions for the bed stability, depending on the selected representative grain size. The suitability of several representative reference grain sizes was evaluated by comparing the results to different hiding functions. It was found that hiding functions, which use the d_σ (approximately equal to d_{95} in this study) as reference size, represent the material behaviour well.

- In oscillating currents, the assessment of bed stability is additionally complicated because exerted bed shear stresses were found to be strongly dependent on the flow direction, causing anisotropic flow resistance and erosion potentials. As a consequence, larger critical bed shear stresses were measured for the oscillating than for the unidirectional current case. In addition, the progression of bed degradation with increasing flow velocity was determined and was found to be dependent on the size of the median grain diameter.

- Eventually, the material behaviour was tested under spectral wave load. As under current flow conditions, the development of a protective armor layer was observed, but also the possibility of material segregation in the direct vicinity of the monopile structure. Induced by the vortex system, an inhomogeneous level of armor layer development and consequently bed stability around the monopile structure was thus given. The scour development approached an equilibrium state over time, which indicates the possibility to define threshold criteria for acceptable damages for a dynamically stable scour protection system in future studies.

These findings help setting a sound basis for the inherent characteristics of widely graded material to be considered in scour protection design for marine and offshore structures. First application-oriented recommendations are given by incorporating those findings into present scour protection design methods. The recommendations involve the identification of sensitive interfaces within the design process of required stone sizes for granular scour protection systems, that are particularly critical regarding the influence of material gradation. Subsequently, suitable adjustments to the definition of bed roughness, the selection of a representative stone size and eventually a modification of critical shear stresses by means of hiding functions are discussed in detail. The application of the proposed stability approach was demonstrated by a case study, in which the required stone size for a granular scour protection at an offshore structure situated in the North Sea was exemplary designed. If determined by the proposed stability approach, required stone sizes significantly differed from those calculated with traditional stability criteria, depending on the selected material gradation.

6.3 future work

As facilities and numerical models are getting more and more sophisticated, the justification for a simplified representation of hydraulic flow conditions is not valid anymore. To fully understand scouring processes at foundation structures and to further minimize uncertainties regarding the scour prediction, future experiments should thus strive towards the most realistic representation of flow conditions given in the field. Regarding the scouring process in tidal currents, this involves the consideration of rotary flow aspects, tidal range and the oscillating boundary layer. To further elaborate the influence of wave spreading, experiments incorporating a wider range of spreading parameters should be sought. Eventually, for the assessment of the scour development over the life-time of the foundation structure, tests combining the directional aspects of tidal currents and short-crested waves should be aimed for. In these long-term tests, scour

depth and rate affecting backfilling processes can be reproduced by subsequently changing flow regimes. Given the restrictions set by model and scaling effects and the great effort generally coming with laboratory experiments that deal with scouring, the synergy of physical and numerical experiments as well as in-situ monitoring is of particular importance and should continue to be pursued in the future. Here, an easier and less restricted access to monitoring data would be desirable.

While the erosion behaviour of widely graded broken stone material has been investigated for several different load conditions, the state of maximum bed stability was never reached. To define definite critical conditions and to provide information on the material behaviour after initial damage occurred, the material has to be exposed to more severe hydraulic conditions in future tests. Furthermore, the role of material composition on the bed stability must be further elucidated by testing a wider variety of material gradation. Eventually, this will allow the determination of a representative grain size as basis for a specific stability criterion in form of a hiding function. Furthermore, a suitable description of bed roughness and friction factors is necessary for the calculation of acting bed shear stresses. As indicated in this thesis, the bed roughness is depending on the flow direction and the stage of armor layer development. Therefore, a detailed analysis of the near-bed flow field induced by marine flow conditions should be carried out.

Given that large turbulence intensities and nonuniform flow fields are induced by the very rough structure of the bed surface, a stability assessment based on the Shields concept might involve great uncertainties. The Shields parameter is derived for uniform flow conditions and is based on time- and spatially-averaged shear stresses, neglecting a locally increase of load due to turbulence. Alternatively, the stone stability can be assessed by parameters that take the effects of turbulence (Hoffmans, 2010; Hofland, 2005), pressure gradients due to flow acceleration (Dessens, 2004) or of both aspects combined (Steenstra et al., 2016) into account. Further detailed measurements of near-bed turbulence are however required, in particular in the direct vicinity to the structure the scour protection is intended for.

Regarding the stability of widely graded material and its performance as a scour protection system, the experiments presented in this thesis focused on shear failure. Other failure modes, particularly insufficient filter stability, could however prove to be more critical to the design of scour protection. Experiments addressing the internal erosion and interface stability for different layer thicknesses under horizontally and vertically oscillating flow are thus required.

Considering the proven potential of the widely graded material to be used as scour protection, two follow-up research projects have already been granted to further expand the knowledge on the ma-

terial's stability and allow the definition of a comprehensive design approach. Funded by the EU's Horizon 2020 Research and Innovation Programme, the first project will involve large scale laboratory experiments with combined wave and current loading. These experiments focus on the derivation of a design approach for a dynamically stable scour protection, but are also intended to provide data on viscous scale effects inside the porous scour protection as well. In the second project, which is part of *marTech*, a research project funded by the Federal Ministry for Economic Affairs and Energy (BWMi), the influence of extreme hydrodynamic conditions, as they are expected to come with climate change, will be investigated. Also, tests with various stone sizes and gradings are planned to optimise the material composition of scour protection for practical applications.

BIBLIOGRAPHY

Aberle, J. and V. Nikora (2006). "Statistical properties of armored gravel bed surfaces:" in: *Water Resources Research* 42.11. DOI: 10.1029/2005WR004674 (cit. on p. 81).

Aberle, J. and G. M. Smart (2003). "The influence of roughness structure on flow resistance on steep slopes." In: *Journal of Hydraulic Research* 41.3, pp. 259–269. DOI: 10.1080/00221680309499971 (cit. on pp. 11, 81).

Achmus, M., Y.-S. Kuo, and K. Abdel-Rahman (2010). "Numerical investigation of scour effect on lateral resistance of windfarm monopiles." In: *Proc. 20th International Offshore and Polar Engineering Conference (ISOPE)*. Beijing, China (cit. on p. 1).

Andrews, E. D. (1983). "Entrainment of gravel from naturally sorted riverbed material." In: *Geological Society of America Bulletin* 94.10, pp. 1225–1231. DOI: http://dx.doi.org/10.1130/0016-7606(1983)94<1225:EOGFNS>2.0.CO;2 (cit. on p. 23).

Ashida, K. and M. Michiue (1971). "An investigation of the river bed degradation of a dam." In: *Proc. of 14th Congress of the IAHR*. Vol. 3. Paris, France, pp. 247–255 (cit. on p. 23).

Baker, R. E. (1986). *Local scour at bridge piers in non-uniform sediment*. Tech. rep. Report No. 402. Auckland, New Zealand: University of Auckland (cit. on pp. 29, 30).

Bakker, K. J., H. J. Verheij, and M. B. de Groot (1994). "Design Relationship for filters in bed protection." In: *Journal of Hydraulic Engineering* 120.9. DOI: https://doi.org/10.1061/(ASCE)0733-9429(1994)120:9(1082) (cit. on p. 41).

Baykal, C., B. M. Sumer, D. R. Fuhrman, N. G. Jacobsen, and J. Fredsøe (2017). "Numerical simulation of scour and backfilling around a circular pile in waves." In: *Coastal Engineering*, pp. 87–107. DOI: 10.1016/j.coastaleng.2017.01.004 (cit. on p. 5).

Bertin, S., J. Groom, and H. Friedrich (2017). "Isolating roughness scales of gravel-bed patches." In: *Water Resources Research* 53.8, pp. 6841–6856. DOI: 10.1002/2016WR020205 (cit. on p. 81).

Bihs, M. (2011). "Three-dimensional numerical modeling of local scouring in open channel flow." PhD thesis. Norwegian University of Science and Technology, NTNU (cit. on p. 5).

Bonnefille, R. (1963). "Essais de synthese des lois de debut d'entrainment des sediments sous l'action d'un courant en regime uniforme." In: *Bull. du CREC* Nr. 5 (cit. on p. 18).

Brahms, A. (1754). *Die Anfangsgründe der Deich- und Wasserbaukunst*. (In German). Aurich: Verlag H. Tapper (cit. on p. 19).

Breusers, H. N. C., G. Nicollet, and H.W. Shen (1977). "Local Scour Around Cylindrical Piers." In: *Journal of Hydraulic Research* 15.3,

pp. 211–252. DOI: 10.1080/00221687709499645 (cit. on pp. 26, 30, 35, 37).

Breusers, H. N. C. and A. J. Raudkivi (1991). *Scouring*. A. A. Balkema, Rotterdam (cit. on pp. 27, 28, 42, 85).

BSH (2015). *Standard Konstruktion: Mindestanforderung an die konstruktive Ausführung von Offshore-Bauwerken in der ausschließlichen Wirtschaftszone (AWZ).* Tech. rep. (In German). Bundesamt für Seeschifffahrt und Hydrographie. (cit. on p. 35).

Buffington, J. M. and D. R. Montgomery (1997). "A systematic analysis of eight decades of incipient motion studies, with special reference to gravel-bedded rivers." In: *Water Resources Research* 33, pp. 1993–2029. DOI: 10.1029/96WR03190 (cit. on pp. 14, 18, 23, 25, 86, 87).

Bunte, K. and S. R. Abt (2001). *Sampling surface and subsurface particle-size distributions in wadable gravel- and cobble-bed streams for analyses in sediment transport, hydraulics, and streambed monitoring.* Ed. by K. Bunte and S. R. Abt. U.S. Department of Agriculture, Forest Service, Rocky Mountain Research Station (cit. on pp. 8, 20).

Buscombe, D. and D. C. Conley (2012). "Effective shear stress of graded sediments." In: *Water Resources Research* 48. DOI: 10.1029/2010WR010341 (cit. on pp. 86, 88).

Caliskan, U. and D. R. Fuhrman (2017). "RANS-based simulation of wave-induced sheet-flow transport of graded sediments." In: *Coastal Engineering*, pp. 90–102. DOI: 10.1016/j.coastaleng.2016.11.007 (cit. on p. 5).

Carreiras, J., P. Larroudé, F. Seabra-Santos, and M. Mory (2000). "Wave scour around piles." In: *Proc. 27th International Conference on Coastal Engineering (ICCE), Sydney, Australia* (cit. on p. 26).

Charlton, F. G., P. M. Brown, and R. W. Benson (1978). *The hydraulic geometry of some gravel rivers in Britain.* Tech. rep. Report No. IT180. HR Wallingford (cit. on p. 80).

Cheng, N.-S. (2015). "Representative grain size and equivalent roughness height of a sediment bed." In: *Journal of Hydraulic Engineering* 142.1. DOI: 10.1061/(ASCE)HY.1943-7900.0001069 (cit. on p. 81).

Chien, N. and Z. Wan (1999). *Mechanics of sediment transport.* ASCE Press (cit. on p. 15).

Chiew, Y.-M. (1984). "Local scour at bridge piers." PhD thesis. Auckland University, New Zealand (cit. on pp. 26, 29, 31).

– (1995). "Mechanics of riprap failure at bridge piers." In: *Journal of Hydraulic Engineering* 121.9, pp. 635–643. DOI: 10.1061/(ASCE)0733-9429(1995)121:9(635) (cit. on pp. 37, 42, 44).

Chiew, Y.-M. and F.-H. Lim (2000). "Failure behaviour of riprap layer at bridge piers under live-bed conditions." In: *Journal of Hydraulic Engineering* 126.1, pp. 43–55. DOI: 10.1061/(ASCE)0733-9429(2000)126:1(43) (cit. on p. 37).

Chin, C. O. (1985). *Stream bed armoring*. Tech. rep. Report No. 403. School of Engineering, University of Auckland, New Zealand (cit. on p. 24).

Chin, C. O., B. W. Melville, and A. J. Raudkivi (1994). "Streambed armoring." In: *Journal of Hydraulic Engineering* 120, pp. 899–918. DOI: 10.1061/(ASCE)0733-9429(1994)120:8(899) (cit. on pp. 20, 21, 84).

CIRIA (2007). *The rock manual. The use of rock in hydraulic engineering*. CIRIA C683, London (cit. on pp. 20, 39–41, 77, 83, 84, 86, 87, 91).

Dargahi, B. (1989). "The turbulent flow field around a circular cylinder." In: *Experiments in Fluids* 8, pp. 1–12 (cit. on p. 27).

Davis, R. E. and L. A. Regier (1977). "Methods for estimating directional wave spectra from multi-element arrays." In: *Journal of Marine Research* (cit. on p. 53).

Day, T. J (1980). *A study of the transport of graded sediments*. Tech. rep. IT 190. HR Wallingford (cit. on pp. 87, 88).

de Graauw, A. F., T. van der Meulen, and M. R. van der Does de Bye (1984). "Granular filters: Design criteria." In: *Journal of Waterway Port, Coastal, and Ocean Engineering* 110.1, pp. 84–96. DOI: 10.1061/(ASCE)0733-950X(1984)110:1(80) (cit. on p. 41).

de Sonneville, B., R. Joustra, and H. J. Verheij (2014). "Winnowing at circular piers under currents." In: *Proc. 7th International Conference on Scour and Erosion, Perth, Australia* (cit. on pp. 37, 41).

De Vos, L. (2008). "Optimisation of scour protection design for monopiles and quantification of wave run-up: Engineering the influence of an offshore wind turbine on local flow conditions." PhD thesis. Ghent University (cit. on pp. 1, 13, 43, 45, 80).

De Vos, L., J. De Rouck, P. Troch, and P. Frigaard (2011). "Empirical design of scour protections around monopile foundations. Part 1: Static Approach." In: *Coastal Engineering* 58, pp. 540–553. DOI: 10.1016/j.coastaleng.2011.02.001 (cit. on pp. 43, 44, 83, 85, 86).

– (2012). "Empirical design of scour protections around monopile foundations. Part 2: Dynamic Approach." In: *Coastal Engineering* 60, pp. 286–298 (cit. on pp. 44, 45, 71, 72, 76, 83).

Delft Hydraulics (1972). *Systematic investigation of two-dimensional and three-dimensional scour*. Tech. rep. Report M648/M863. The Netherlands: Delft (cit. on p. 17).

den Boon, J. H., J. Sutherland, R. J. S. Whitehouse, R. Soulsby, C. J. M. Stam, K. Verhoeven, M. Høgedal, and T. Hald (2004). "Scour behaviour and scour protection for monopile foundations of offshore wind turbines." In: *European Wind Energy Conference and Exhibition (EWEC), London* (cit. on pp. 43, 45, 83, 86).

Dessens, M. (2004). "The influence of flow acceleration on stone stability." MA thesis. Delft University of Technology, Delft, Netherlands (cit. on p. 99).

Dey, S. and R. V. Raikar (2007). "Characteristics of Horseshoe Vortex in Developing Scour Holes at Piers." In: *Journal of Hydraulic Engi-*

neering 133.4, pp. 399–413. DOI: `10.1061/(ASCE)0733-9429(2007)133:4(399)` (cit. on p. 27).

Dey, S., B. M. Sumer, and J. Fredsøe (2006). "Control of scour at circular piles under waves and currents." In: *Journal of Hydraulic Engineering* 132, pp. 270–279. DOI: `10.1061/(ASCE)0733-9429(2006)132:3(270)` (cit. on p. 36).

DHI (2007). *Borkum West - Hydrographische Standortbedingungen. Modellierung und statistische Analyse.* Tech. rep. (In German). Danish Hydraulic Institute (cit. on p. 89).

DIN (2016). *DIN EN 61400-3. Wind turbines - Part 3-1: Design requirements for offshore wind turbines.* Tech. rep. Deutsches Institut füÃŒr Normung e. V. (cit. on p. 35).

Dittrich, A. (1998). *Wechselwirkung Morphologie/Strömung naturnaher Fliessgewässer.* Vol. Heft 198. (In German). Mitteilungen des Institutes für Wasserwirtschaft und Kulturtechnik, Universität Karlsruhe (cit. on pp. 17, 21, 80).

Dixen, M., F. Hatipoglu, B. M. Sumer, and J. Fredsøe (2008). "Wave boundary layer over a stone-covered bed." In: *Coastal Engineering* 55, pp. 1–20. DOI: `10.1016/j.coastaleng.2007.06.005` (cit. on pp. 13, 44).

DNV-GL (2016). *Support structures for wind turbines.* Tech. rep. DNVGL-ST-0126, Edition 2016. DNV GL AS (cit. on p. 35).

DVWK (1997). *Maßnahmen zur naturnahen Gewässerstabilisierung.* 118. Bonn: Deutscher Verband für Wasserwirtschaft und Kulturbau e. V., DVWK Schriften (cit. on pp. 41, 82).

Dyer, K. R. (1986). *Coastal and Estuarine Sediment Dynamics.* Chichester: John Wiley and Sons (cit. on p. 20).

Eadie, R. W. and J. B. Herbich (1986). "Scour about a single, cylindrical pile due to combined random waves and current." In: *Proc. of 20th International Conference on Coastal Engineering (ICCE), Taipei, Taiwan* (cit. on pp. 26, 34).

Efthymiou, N. P. (2012). "Transient bedload transport of sediment mixtures und disequilibrium conditions." PhD thesis. Lehrstuhl für Wasserbau und Wasserwirtschaft, TU München (cit. on pp. 22, 24, 25).

Egiazaroff, I. V. (1965). "Calculation of nonuniform sediment concentration." In: *Journal of the Hydraulics Division* 91.4, pp. 225–247 (cit. on p. 23).

Einstein, H. A. (1950). "The bedload function for sediment transport in open channel flows." In: *U.S. Dep. Agric. Soil Conserv. Serv. Tech. Bull.* 1026 (cit. on p. 23).

Engelund, F. and E. Hansen (1967). *A monograph on sediment transport in alluvial streams.* Tech. rep. TU Denmark, Copenhagen (cit. on p. 80).

Escarameia, M. (1998). *River and channel revetments: A design manual.* Thomas Telford Publications, London (cit. on p. 36).

Escarameia, M. and R. W. P. May (1992). *Channel protection: turbulence downstream of structures*. Tech. rep. Report SR 313. HR Wallingford (cit. on p. 41).

– (1999). *Scour around structures in tidal flows.* Tech. rep. SR 521. UK: HR Wallingford (cit. on p. 49).

Ettema, R. (1976). *Influence of bed material gradation on local scour*. Tech. rep. University of Auckland, New Zealnd (cit. on p. 30).

– (1980). *Scour at bridge Piers.* University of Auckland, New Zealand (cit. on pp. 27, 31).

Ettema, R., G. Kirkil, and M. Muste (2006). "Similitude of large-scale turbulence in experiments on local scour cylinders." In: *Journal of Hydraulic Engineering* 132, pp. 33–40. DOI: `10.1061/(ASCE)0733-9429(2006)132:1(33)` (cit. on p. 30).

Ettema, R., B. W. Melville, and B. Barkdoll (1998). "Scale effect in pier-scour experiments." In: *Journal of Hydraulic Engineering* 124, pp. 639–642. DOI: `10.1061/(ASCE)0733-9429(1998)124:6(639)` (cit. on pp. 29, 30).

Fenton, J. D. and W. D. McKee (1990). "On calculating the lengths of water waves." In: *Coastal Engineering* 14, pp. 499–513. DOI: `10.1016/0378-3839(90)90032-R` (cit. on p. 12).

Ferguson, R. (2007). "Flow resistance equations for gravel- and boulder-bed streams." In: *Water Resources Research* 43.5. DOI: `10.1029/2006WR005422` (cit. on p. 11).

Forristall, G. Z. (2000). "Wave crest distributions: observations and second-order theory." In: *Journal of Physical Oceanography* 30, pp. 1931–1843 (cit. on p. 33).

Fredsøe, J. (1984). "Turbulent boundary layer in wave-current motion." In: *Journal of Hydraulic Engineering* 110, pp. 1103–1120 (cit. on p. 14).

Fredsøe, J., B. M. Sumer, and M. M. Arnskov (1992). "Time scale for wave/current scour below pipelines." In: *International Journal of Offshore and Polar Engineering* 2.2, pp. 13–17 (cit. on p. 31).

Fuhrman, D. R., C. Baykal, B. M. Sumer, N. G. Jacobsen, and J. Fredsøe (2014). "Numerical simulation of wave-induced scour and backfilling processes beneath submarine pipelines." In: *Coastal Engineering* 94, pp. 10–22. DOI: `10.1016/j.coastaleng.2014.08.009` (cit. on pp. 5, 31).

Gessler, J. (1965). "Der Geschiebebeginn bei Mischungen untersucht an natürlichen Abpflästerungserscheinungen in Kanälen." (In German). PhD thesis. ETH-Zürich (cit. on pp. 20, 21, 82).

– (1971). "River Mechanics." In: ed. by H. W. Shen. Colorado: Water Resources Publications. Chap. Beginning and ceasing of sediment motion, Chapter 7, pp. 1–22 (cit. on pp. 18, 22).

– (1990). "Friction factor of armored river beds." In: *Journal of Hydraulic Engineering* 116.4. DOI: `10.1061/(ASCE)0733-9429(1990)116:4(531)` (cit. on p. 82).

Gomez, B. (1984). "Typology of segregated (armoured/paved) surfaces: some comments." In: *Earth Surface Processes and Landforms* 9, pp. 19–24. DOI: 10.1002/esp.3290090103 (cit. on pp. 21, 22).

– (1993). "Roughness of stable, armored gravel beds." In: *Water Resources Research* 29.11, pp. 3631–3642. DOI: 10.1029/93WR01490 (cit. on p. 82).

Grabemann, I., N. Groll, J. Möller, and R. Weisse (2015). "Climate change impact on North Sea wave conditions: a consistent analysis of ten projections." In: *Ocean Dynamics* 65, pp. 255–267. DOI: 10.1007/s10236-014-0800-z (cit. on p. 2).

Graf, W. H. (1971). *Hydraulics of sediment transport.* McGraw-Hill Book Company (cit. on p. 17).

Graf, W. H. and G. C. Pazis (1977). "Deposition and erosion in an alluvial channel." In: *Journal of Hydraulic Research* 15.2, pp. 151–166 (cit. on p. 17).

Grant, W. D. and O. S. Madsen (1979). "Combined wave and current interaction with a rough bottom." In: *Journal of Geophysical Research* 84, pp. 1797–1808 (cit. on p. 14).

Grass, A. J. (1970). "Initial instability of fine bed sand." In: *Journal of the Hydraulics Division ASCE* 96.3, pp. 619–632 (cit. on p. 18).

Günter, A. (1971). "Die kritische mittlere Sohlenschubspannung bei Geschiebemischungen unter Berücksichtigung der Deckschichtausbildung und der turbulenzbedingten Sohlenschubspannungsschwankungen." (In German). PhD thesis. Institut für Hydromechanik Wasserwirtschaft, ETH-Zürich (cit. on pp. 24, 82, 84).

Harris, J. M. and R. J. S. Whitehouse (2012). "Scour management: a risk based approach." In: *Proc. 6th International Conference on Scour and Erosion, Paris, France* (cit. on p. 36).

Harris, J. M., R. J. S. Whitehouse, and T. Benson (2010). "The time evolution of scour around offshore structures." In: *Proc. ICE, Maritime Engineering* 163.1, pp. 3–17. DOI: 10.1680/maen.2010.163.1.3 (cit. on p. 35).

Hassan, W. N., D. F. Kroekenstoel, and J. S. Ribberink (2001). "Size-gradation effect on sand transport rates under oscillatory sheetflows." In: *Proc. of 4th Conference on Coastal Dynamics* (cit. on p. 88).

Hayashi, T. S., S. Ozaki, and T. Ichibashi (1980). "Study on bed load transport of sediment mixture." In: *Proc. of 24th Japanese Conference on Hydraulics, Japan Society of Civil Engineers.* (In Japanese) (cit. on p. 23).

Hjorth, P. (1975). "Studies on the nature of local scour." In: *Bull. Series A, No. 46, Department of Water Resources Engineering, Lund Institute of Technology, Schweden.* (Cit. on p. 27).

Hjulström, F. (1935). "Studies on the morphological activity of rivers as illustrated by the river fyris." In: *Bulletin of the Geological Institute of the University of Uppsala* (cit. on p. 19).

Hoffmans, G. J. C. M. (2010). "Stability of stones under uniform flow." In: *Journal of Hydraulic Engineering* 136.2. DOI: 10.1061/(ASCE)0733-94292010136:2(129) (cit. on p. 99).

– (2012). *The Influence of Turbulence on Scour and Erosion.* Deltares Select Series, TU Delft, The Netherlands (cit. on p. 41).

Hoffmans, G. J. C. M. and H. J. Verheij (1997). *Scour manual.* A. A. Balkema, Rotterdam (cit. on p. 27).

Hofland, B. (2005). "Rock & Roll: Turbulence-induced damage to granular bed protection." PhD thesis. Delft University of Technology, Delft, Netherlands (cit. on p. 99).

Isbash, S. V. (1936). "Construction of dams by depositing rock in running water." In: *Second congress on large dams.* Washington, DC, pp. 123–136 (cit. on pp. 19, 20).

Jain, S. C. (1990). "Armor or pavement." In: *Journal of Hydraulic Engineering* 116.3, pp. 436–440. DOI: 10.1061/(ASCE)0733-9429(1990)116:3(436) (cit. on p. 21).

Ji, X., S. Liu, and W. Jia (2015). "Experimental investigation of the interaction of multidirectional irregular waves with a large cylinder." In: *Ocean Engineering* 93, pp. 64–73. DOI: 10.1016/j.oceaneng.2014.10.004 (cit. on p. 51).

Keulegan, G. H. (1938). "Laws of turbulent flow in open channels." In: *Journal of Research of the National Bureau of Standards* 21, pp. 707–741 (cit. on p. 10).

Kirkegaard, J., G. Wolters, J. Sutherland, R. Soulsby, L. E. Frostick, S. J. McLelland, T. G. Mercer, and H. Gerritsen (2011). *Users guide to physical modelling and experimentation: Experience of the HYDRALAB network.* Ed. by L. E. Frostick, S. J. McLelland, and T. G. Mercer. IAHR Design Manual. CRC Press (cit. on p. 51).

Kobayashi, T. and K. Oda (1994). "Experimental study on developing process of local scour around a vertical cylinder." In: *Proc. 24th International Conference on Coastal Engineering, Kobe, Japan* (cit. on p. 32).

Komar, P. D. (1987). "Selective grain entrainment by a current from a bed of mixed sizes: A reanalysis." In: *Journal of Sedimentary Petrology* 57.2, pp. 203–211. DOI: 10.1306/212F8AE4-2B24-11D7-8648000102C1865D (cit. on pp. 23, 24).

Kothyari, U. C., R. J. Garde, and K. G. Ranga Raju (1992). "Temporal variation of scour around circular bridge piers." In: *Journal of Hydraulic Engineering* 118.8, pp. 1091–1106. DOI: 10.1061/(ASCE)0733-9429(1992)118:8(1091) (cit. on p. 26).

Krumbein, W. C. (1936). "Application of logarithmic moments to size-frequency distributions of sediments." In: *Journal of Sedimentary Research* 6 (cit. on p. 8).

Kuhnle, R. A. (1993). "Incipient motion of sand-gravel sediment mixtures." In: *Journal of Hydraulic Engineering* 119.12, pp. 1400–1415. DOI: https://doi.org/10.1061/(ASCE)0733-9429(1993)119:12(1400) (cit. on p. 23).

Lauchlan, C. S. (1999). "Countermeasures to pier scour." PhD thesis. Unversity of Auckland, New Zealand (cit. on p. 42).

Lauchlan, C. S. and B. W. Melville (2001). "Riprap protection at bridge piers." In: *Journal of Hydraulic Engineering* 127.5, pp. 412–418. DOI: `10.1061/(ASCE)0733-9429(2001)127:5(412)` (cit. on p. 38).

Lee, S. O. and T. W. Sturm (2009). "Effect of sediment size scaling on physical modelling of bridge piers." In: *Journal of Hydraulic Engineering* 135, pp. 793–802. DOI: `10.1061/(ASCE)HY.1943-7900.0000091` (cit. on p. 31).

Li, J. X., Z. H. Wang, and S. X. Liu (2012). "Experimental study of interactions between multi-directional focused wave and vertical circular cylinder. Part I: Wave run-up." In: *Coastal Engineering* 64, pp. 151–160. DOI: `10.1016/j.coastaleng.2012.02.003` (cit. on p. 51).

– (2014). "Experimental study of interactions between multi-directional focused wave and vertical circular cylinder. Part II: Wave force." In: *Coastal Engineering* 83, pp. 233–242. DOI: `10.1016/j.coastaleng.2013.06.004` (cit. on p. 51).

Little, W. C. and P. G. Mayer (1976). "Stability of channel beds by armoring." In: *Journal of the Hydraulics Division ASCE* HY11, pp. 1647–1661 (cit. on pp. 21, 22, 25, 82, 85).

Liu, Z. (2001). *Sediment transport*. Tech. rep. University Aalborg, Denmark (cit. on p. 44).

López, R. and J. Barragán (2008). "Equivalent roughness of gravel-bed rivers." In: *Journal of Hydraulic Engineering* 134.6, pp. 847–851. DOI: `10.1061/(ASCE)0733-9429(2008)134:6(847)` (cit. on p. 80).

MacKenzie, L. G. and B. C. Eaton (2017). "Large grains matter: contrasting bed stability and morphodynamics during two identical experiments." In: *Earth Surface Processes and Landforms* 42.8, pp. 1287–1295. DOI: `10.1002/esp.4122` (cit. on p. 85).

Mansard, E. and E. Funke (1980). "The measurement of incident and reflected wave spectra using a least square method." In: *Proc. 17th Coastal Engineering Conference*, pp. 154–172 (cit. on p. 53).

Mao, L., J. R. Cooper, and L. E. Frostick (2011). "Grain size and topographical differences between static and mobile armour layers." In: *Earth Surface Processes and Landforms* 36.10, pp. 1321–1334. DOI: `10.1002/esp.2156` (cit. on pp. 22, 81, 82).

Marion, A., S. J. Tait, and I. K. McEwan (2003). "Analysis of small-scale gravel bed topography during armoring." In: *Water Resources Research* 39.12. DOI: `10.1029/2003WR002367` (cit. on p. 81).

May, R. W. P., J. C. Ackers, and A. M. Kirby (2002). *Manual on scour at bridges and other hydraulic structures*. CIRIA C551, London (cit. on p. 36).

Maynord, S. T. (1987). "Stable riprap size for open channel flows." PhD thesis. Colorado, USA: Department of Civil Engineering, Colorado State University (cit. on pp. 20, 41).

– (1991). "Flow resistance of riprap." In: *Journal of Hydraulic Engineering* 117.6. DOI: 10.1061/(ASCE)0733-9429(1991)117:6(687) (cit. on p. 81).

– (1993). "Corps riprap design guidance for channel protection." In: *Preprints of the International Riprap Workshop, Fort Collins, USA* (cit. on p. 41).

McGovern, D. J., S. Ilic, A. M. Folkard, S. J. McLelland, and B. Murphy (2012). "Evolution of local scour around a collared monopile through tidal cycles." In: *Proc. 33rd International Conference on Coastal Engineering (ICCE), Santander, Spain.* (Cit. on p. 36).

– (2014). "Time development of scour around a cylinder in simulated tidal currents." In: *Journal of Hydraulic Engineering*. DOI: 10.1061/(ASCE)HY.1943-7900.0000857 (cit. on pp. 35, 49).

Melville, B. W. (1997). "Pier and abutment scour: Integrated approach." In: *Journal of Hydraulic Engineering* 123, pp. 125–136. DOI: 10.1061/(ASCE)0733-9429(1997)123:2(125) (cit. on p. 35).

Melville, B. W. and Y.-M. Chiew (1999). "Time scale for local scour at bridge piers." In: *Journal of Hydraulic Engineering* 125, pp. 59–65. DOI: 10.1061/(ASCE)0733-9429(1999)125:1(59) (cit. on pp. 26, 32, 35).

Melville, B. W. and S. E. Coleman (2000). *Bridge Scour*. University of Auckland: Water Resources Publications (cit. on pp. 20, 27, 29, 31, 42).

Melville, B. W. and A. J. Sutherland (1988). "Design method for local scour at bridge piers." In: *Journal of Hydraulic Engineering* 114.10, pp. 1210–1226. DOI: 10.1061/(ASCE)0733-9429(1988)114:10(1210) (cit. on p. 31).

Meyer-Peter, M. and R. Müller (1948). "Formulas for bed-load transport." In: *Porc. of IAHSR 2nd Meeting*. Stockholm (cit. on pp. 8, 18).

Myrhaug, D. and M. C. Ong (2013). "Scour around vertical pile foundations for offshore wind turbines due to long-crested and short-crested nonlinear random waves." In: *Journal of Offshore Mechanics and Arctic Engineering* 135. DOI: 10.1115/1.4007048 (cit. on pp. 33, 51, 67).

Neill, C. R. (1967). "Mean velocity criterion for scour of coarse uniform bed material." In: *Proc. 12th IAHR Congress*. Fort Collins (cit. on pp. 20, 41).

Nielsen, A. W., B. M. Sumer, J. Fredsøe, and E. D. Christensen (2011). "Sinking of armour layer around a cylinder exposed to a current." In: *Proc. ICE, Maritime Engineering* 164, pp. 159–172. DOI: 10.1680/maen.2011.164.4.159 (cit. on p. 37).

Nielsen, A. W., F. Schlütter, J. V. Tornfeldt Sørensen, and H. Bredmose (2012). "Wave loads on a monopile in 3d waves." In: *Proc. 31st International Conference on Ocean, Offshore and Artic Engineering.* Rio de Janeirao, Brazil (cit. on p. 51).

Nielsen, P. (1992). *Coastal bottom boundary layers and sediment transport.*
World World Scientific - New Jersey - Singapore - London - Hong
Kong. (cit. on pp. 13, 80).

Nikuradse, J. (1933). "Strömungsgesetze in rauhen Rohren." In: *VDI
Forschungsheft* 361. (In German) (cit. on pp. 10, 80).

Ockenden, M. C. and R. Soulsby (1994). *Sediment transport by currents
plus irregular waves.* Tech. rep. Report SR 376. HR Wallingford (cit.
on p. 12).

Ong, M. C., D. Myrhaug, and P. Hesten (2013). "Scour around vertical
piles due to long-crested and short-crested nonlinear random waves
plus a current." In: *Coastal Engineering* 73, pp. 106–114. DOI: 10 .
1016/j.coastaleng.2012.10.005 (cit. on pp. 33, 51, 67).

Paintal, A. S. (1971). "Concept of critical shear stress in loose bound-
ary open channels." In: *Journal of Hydraulic Research* 9, pp. 91–113
(cit. on p. 18).

Parker, G., S. Dhamotharan, and H. Stefan (1982). "Model experi-
ments on mobile, paved gravel bed streams." In: *Water Resources
Research* 18.5, pp. 1395–1408. DOI: 10.1029/WR018i005p01395 (cit.
on pp. 22, 23).

Parker, G. and P. C. Klingeman (1982). "On why gravel bed streams
are paved." In: *Water Resources Research* 18.5, pp. 1409–1423. DOI:
10.1029/WR018i005p01409 (cit. on pp. 21–24, 87).

Patel, P. and K. G. Ranga Raju (1999). "Critical tractive stress of
nonuniform sediments." In: *Journal of Hydraulic Research* 37.1, pp. 39–
58. DOI: 10.1080/00221689909498531 (cit. on pp. 23, 85).

Patel, S. B., P. L. Patel, and P. D. Porey (2014). "Estimation of frac-
tional critical tractive stress from fractional bed load transport mea-
surements of unimodal and bimodal sediments." In: *Measurement*
47, pp. 393–400. DOI: 10.1016/j.measurement.2013.08.025 (cit. on
pp. 23, 87).

Peters, K. and K. Werth (2012). "Offshore wind energy foundations:
geotextile sand-filled containers as effective scour protection sys-
tems." In: *Proc. 6th International Conference on Scour and Erosion
(ICSE), Paris, France* (cit. on p. 36).

Petersen, T. U., B. M. Sumer, and J. Fredsøe (2012). "Time scale of
scour around a pile in combined waves and currents." In: *Proc. 6th
International Conference on Scour and Erosion (ICSE), Paris, France* (cit.
on pp. 34, 66).

Petersen, T. U., B. M. Sumer, J. Bøgelund, A. Yazici, J. Fredsøe, and K.
E. Meyer (2014). "Flow and edge scour in current adjacent to stone
covers." In: *Journal of Waterway Port, Coastal, and Ocean Engineering*
141. DOI: 10.1061/(ASCE)WW.1943-5460.0000287 (cit. on p. 38).

Petersen, T. U., B. M. Sumer, J. Fredsøe, T. Raaijmakers, and J.-J.
Schouten (2015). "Edge scour at scour protections around piles in
the marine environment: Laboratory and field investigation." In:

Coastal Engineering 106, pp. 42–72. DOI: `10.1016/j.coastaleng.2015.08.007` (cit. on p. 38).

Pilarczyk, K. W. (1995). *Simplified unification of stability formulae for revetments under current and wave attack*. Ed. by C. R. Thorne, S. R. Abt, F. B. J. Barends, S. T. Maynord, and K. W. Pilarczyk. John Wiley and Sons (cit. on p. 41).

Porter, K. E., R. P. Simons, and J. M. Harris (2014). "Laboratory investigation of scour development through a spring-neap tidal cycle." In: *Proc. of the 7th International Conference on Scour and Erosion*. Perth, Australia, pp. 667–677 (cit. on p. 49).

Powell, D. M. (2014). "Flow resistance in gavel-bed rivers: Progress in research." In: *Earth-Science Reviews* 136, pp. 301–338. DOI: `10.1016/j.earscirev.2014.06.001` (cit. on pp. 11, 80, 81).

Proffitt, G. T. (1980). "Selective transport and armouring of nonuniform alluvial sediments." PhD thesis. University of Canterbury, New Zealand (cit. on p. 82).

Proffitt, G. T. and A. J. Sutherland (1983). "Transport of non-uniform sediments." In: *Journal of Hydraulic Research* 21.1, pp. 33–43. DOI: `10.1080/00221688309499448` (cit. on p. 22).

Qi, W.-G. and F.-P. Gao (2014). "Physical modelling of local scour development around a large-diameter monopile in combined waves and current." In: *Coastal Engineering* 83, pp. 72–81. DOI: `10.1016/j.coastaleng.2013.10.007` (cit. on pp. 26, 34).

Raaijmakers, T. and D. Rudolph (2008). "Time-dependent scour development under combined current and waves conditions: laboratory experiments with online monitoring technique." In: *Proc. 4th International Conference on Scour and Erosion (ISCE), Tokyo, Japan.* (Cit. on p. 35).

Raudkivi, A. J. (1976). *Loose boundary hydraulics*. Pergamon Press (cit. on p. 41).

Raudkivi, A. J. and R. Ettema (1983). "Clear-water scour at cylindrical piers." In: *Journal of Hydraulic Engineering* 109.3, pp. 338–350. DOI: `10.1061/(ASCE)0733-9429(1983)109:3(338)` (cit. on pp. 26, 29).

Recking, A. and J. Pitlick (2012). "Shields versus Isbash." In: *Journal of Hydraulic Engineering* 139, pp. 51–54. DOI: `10.1061/(ASCE)HY.1943-7900.0000647` (cit. on pp. 15, 20).

Richardson, E. V. and S. R. Davis (2001). *Evaluation scour at bridges*. Tech. rep. Publication No. FHwA NHI 01-001. Washington, D.C.: Federal Highway Administration, U.S. Dept. of Transportation (cit. on p. 35).

Rickenmann, D. and A. Recking (2011). "Evaluation of flow resistance in gravel-bed rivers through a large field data set." In: *Water Resources Research* 47. DOI: `10.1029/2010WR009793` (cit. on p. 11).

Roulund, A., B. M. Sumer, J. Fredsøe, and J. Michelsen (2005). "Numerical and experimental investigation of flow and scour around

a circular pile." In: *Journal of Fluid Mechanics* 534, pp. 351–401. DOI: 10.1017/S0022112005004507 (cit. on p. 27).

Rudolph, D. and J. K. Bos (2006). "Scour around a monopile under combined wave-current conditions and low KC-numbers." In: *Proc. 3rd International Conference on Scour and Erosion (ISCE)*. Amsterdam, The Netherlands (cit. on pp. 26, 34, 35, 59, 61).

Schendel, A., N. Goseberg, and T. Schlurmann (2015). "Experimental study on the erosion stability of coarse grain materials under waves." In: *Journal of Marine Science and Technology* 23.6, pp. 937–942 (cit. on pp. 4, 69–71, 75, 82, 88, 94).

– (2016). "Erosion stability of wide-graded quarry-stone material under unidirectional current." In: *Journal of Waterway, Port, Coastal, Ocean Engineering* 142.3. DOI: 10.1061/(ASCE)WW.1943-5460.0000321 (cit. on pp. 4, 15, 69, 75, 77, 82, 83, 85, 87–89).

– (2017). "Influence of reversing currents on the erosion stability and bed degradation of widely graded grain material." In: *International Journal of Sediment Research* 33.1, pp. 68–83. DOI: 10.1016/j.ijsrc.2017.07.002 (cit. on pp. 4, 7, 69, 77, 82, 87, 88, 94).

Schendel, A., A. Hildebrandt, and T. Schlurmann (2016). "Experimental study on the progression of scour around a monopile in unidirectional and tidal currents." In: *Proceedings of the 6th International Conference on the Application of Physical Modelling in Coastal and Port Engineering and Science (Coastlab16)*. Ottawa, Canada (cit. on p. 59).

Schendel, A., A. Hildebrandt, N. Goseberg, and T. Schlurmann (2018). "Processes and evolution of scour around a monopile induced by tidal currents." In: *Coastal Engineering* 139, pp. 65–84. DOI: 10.1016/j.coastaleng.2018.05.004 (cit. on p. 4).

Schiereck, G. J. (2012). *Introduction to bed, bank and shore protection*. 2nd Edition. VSSD, TU Delft (cit. on pp. 36, 38–40).

Schlichting, H. and K. Gersten (2006). *Grenzschichttheorie*. Ed. by H. Schlichting and K. Gersten. (In German). Springer-Verlag - Berlin - Heidelberg - New York (cit. on p. 9).

Schöberl, F. (1979). "Zur Frage der Gefälllsausbildung beim Selbststabilisierungsprozess von erodierenden Flußstrecken." (In German). PhD thesis. Institut für Konstruktiven Wasser- und Tunnelbau, Universität Innsbruck (cit. on pp. 24, 84).

Schoklitsch, A. (1914). *Über Schleppkraft und Geschiebebewegung.* (in German). Englemann, Leipzig (cit. on p. 17).

Schürenkamp, D., M. Bleck, and H. Oumeraci (2012). "Granular filter design for scour protection at offshore structures." In: *Proc. 6th International Conference on Scour and Erosion (ICSE), Paris, France* (cit. on p. 41).

Sheppard, D. M. and W. Miller (2006). "Live-bed local pier scour experiments." In: *Journal of Hydraulic Engineering* 132.7, pp. 635–642. DOI: 10.1061/(ASCE)0733-9429(2006)132:7(635) (cit. on pp. 29, 35).

Sheppard, D. M., M. Odeh, and T. Glasser (2004). "Large scale clear-water local pier scour experiments." In: *Journal of Hydraulic Engineering* 130, pp. 957–963. DOI: 10.1061/(ASCE)0733-9429(2004)130:10(957) (cit. on pp. 26, 31).

Shields, A. (1936). "Anwendung der Ähnlichkeitsmechanik und der Turbulenzforschung auf die Geschiebebewegung." In: *Mitteilungen der Preußischen Versuchsanstalt fü Wasserbau und Schiffbau, Berlin.* (In German) (cit. on pp. 17, 18, 20, 22, 24, 77, 84).

Shvidchenko, A. B., G. Pender, and T. B. Hoey (2001). "Critical shear stress for incipient motion of sand/gravel streambeds." In: *Water Resources Research* 37.8, pp. 2273–2283. DOI: http://dx.doi.org/10.1029/2000WR000036 (cit. on pp. 23, 26, 74).

Smart, G. M. (1999). "Turbulent velocity profiles and boundary shear in gravel bed rivers." In: *Journal of Hydraulic Engineering* 125, pp. 106–116. DOI: 10.1061/(ASCE)0733-9429(1999)125:2(106) (cit. on p. 10).

Smart, G. M., M. J. Duncan, and J. M. Walsh (2002). "Relativelx rough flow resistance equations." In: *Journal of Hydraulic Engineering* 128.6. DOI: 10.1061/(ASCE)0733-9429(2002)128:6(568) (cit. on p. 81).

Soulsby, R. (1995). *Bed shear-stresses due to combined waves and currents. Advances in Coastal Morphodynamics: An Overview of the G8-Coastal Morphodynamics project.* Tech. rep. Delft Hydraulics (cit. on pp. 14, 43, 91).

– (1997). *Dynamics of marine sands: A manual for practical applications.* London: Thomas Telford Publications (cit. on pp. 12–14, 43, 83, 86, 90).

– (2006). *Simplified calculation of wave orbital velocities.* Tech. rep. Report TR 155. HR Wallingford (cit. on p. 12).

Soulsby, R. and S. Clarke (2005). *Bed shear-stresses under combined waves and currents on smooth and rough beds.* Tech. rep. Report 137. HR Wallingford (cit. on pp. 14, 56).

Soulsby, R. and R. J. S. W. Whitehouse (1997). "Threshold of sediment motion in coastal environments." In: *Proc. Pacific Coasts and Ports Conference 97.* Christchurch, University of Canterbury, New Zealand (cit. on p. 19).

Soulsby, R., L. Hamm, G. Klopman, D. Myrhaug, R. R. Simons, and G. P. Thomas (1993). "Wave-current interaction within and outside the bottom boundary layer." In: *Coastal Engineering* 21, pp. 41–69. DOI: 10.1016/0378-3839(93)90045-A (cit. on pp. 13, 14).

Stahlmann, A. (2013). "Numerical and experimental modelling of scour at foundation structures for offshore wind turbines." In: *Journal of Ocean and Wind Energy.* 1.2, pp. 82–89 (cit. on pp. 6, 26).

Steenstra, R., B. Hofland, A. Smale, A. Paarlberg, F. Huthoff, and W. Uijttewaal (2016). "Stone stability under stationary nonuniform flows." In: *Journal of Hydraulic Engineering.* DOI: 10.1061/(ASCE)HY.1943-7900.0001202 (cit. on pp. 74, 99).

Sumer, B. M. (2014). *Liquefaction around marine structures*. World Scientific (cit. on p. 38).

Sumer, B. M., N. Christiansen, and J. Fredsøe (1992). "Time scale of scour around a vertical pile." In: *Proc. 2nd International Offshore and Polar Engineering Conference (ISOPE), San Francisco, USA* (cit. on pp. 31, 35).

– (1997). "Horseshoe vortex and vortex shedding around a vertical wall-mounted cylinder exposed to waves." In: *Journal of Fluid Mechanics* 332, pp. 41–70. DOI: 10.1017/S0022112096003898 (cit. on p. 28).

Sumer, B. M. and J. Fredsøe (1997). *Hydrodynamics Around Cylindrical Structures.* World Scientific Publications (cit. on p. 28).

– (2001a). "Scour around a pile in combined waves and current." In: *Journal of Hydraulic Engineering* 127, pp. 403–411. DOI: 10.1061/(ASCE)0733-9429(2001)127:5(403) (cit. on pp. 12, 26, 32–34, 54, 56, 59, 61, 62).

– (2001b). "Wave scour around a large vertical circular cylinder." In: *Journal of Waterway Port, Coastal, and Ocean Engineering* 127.3, pp. 125–134. DOI: 10.1061/(ASCE)0733-950X(2001)127:3(125) (cit. on p. 26).

– (2002). *The mechanics of scour in the marine environment*. Ed. by B. M. Sumer and J. Fredsøe. World Scientific - New Jersey - Singapore - London - Hong Kong. (cit. on pp. 27, 28, 30, 33, 35, 62).

Sumer, B. M., J. Fredsøe, and N. Christiansen (1992). "Scour around vertical pile in waves." In: *Journal of Waterway Port, Coastal, and Ocean Engineering* 118.1, pp. 15–31. DOI: 10.1061/(ASCE)0733-950X(1992)118:1(15) (cit. on pp. 26, 32, 35, 91).

Sumer, B. M. and A. W. Nielsen (2013). "Sinking failure of scour protection at wind turbine foundation." In: *Proc. ICE, Energy* 166. DOI: 10.1680/ener.12.00006 (cit. on p. 41).

Sumer, B. M., T. U. Petersen, L. Locatelli, J. Fredsøe, R. E. Musumeci, and E. Foti (2013). "Backfilling of a scour hole around a pile in waves and current." In: *Journal of Waterway Port, Coastal, and Ocean Engineering* 139.1, pp. 9–23. DOI: 10.1061/(ASCE)WW.1943-5460.0000161 (cit. on pp. 26, 34).

Swart, D. H. (1974). *Offshore sediment transport and equilibrium beach profiles.* Tech. rep. Delft Hydraulics Lab. (cit. on p. 90).

van der Meer, J. W. (1988). *Rock Slopes and Gravel Beaches under Wave Attack.* Delft Hydraulics, The Netherlands (cit. on pp. 44, 45).

Van der Tempel, A. (2006). "Design of support structures for offshore wind turbines." PhD thesis. TU Delft (cit. on p. 1).

Van Rijn, L. C. (1982). "Equivalent roughness of alluvial Bed." In: *Journal of the Hydraulics Division* 108.10, pp. 1215–1218 (cit. on pp. 80, 83).

– (1993). *Principles of sediment transport in rivers, estuaries and coastal seas.* Ed. by L. C. Van Rijn. Amsterdam: Aqua Publications (cit. on pp. 9, 17, 18).

– (2007). "Unified view of sediment transport by currents and waves. III: Graded beds." In: *Journal of Hydraulic Engineering* 133, pp. 761–775. DOI: 10.1061/(ASCE)0733-9429(2007)133:7(761) (cit. on p. 88).

Whitehouse, R. J. S. W. (1998). *Scour at marine structures: A manual for practical applications.* Thomas Telford Publications, London (cit. on pp. 2, 26–28, 35, 42).

Whitehouse, R. J. S., J. M. Harris, and J. Sutherland (2011). "Evaluating scour at marine gravity foundations." In: *Proc. ICE, Maritime Engineering* 164, pp. 143–157. DOI: 10.1680/maen.2011.164.4.143 (cit. on pp. 36, 37).

Wilcock, P. R. (1988). "Methods for estimating the critical shear stress of individual fractions in mixed-size sediment." In: *Water Resources Research* 27, pp. 1127–1135. DOI: 10.1029/WR024i007p01127 (cit. on p. 15).

– (1993). "Critical shear stress of natural sediments." In: *Journal of Hydraulic Engineering* 119.4, pp. 491–505. DOI: 10.1061/(ASCE)0733-9429(1993)119:4(491) (cit. on p. 23).

Wilcock, P. R., S. T. Kenworthy, and J. C. Crowe (2001). "Experimental study on the transport of mixed sand and gravel." In: *Water Resources Research* 37.12, pp. 3349–3358. DOI: 10.1029/2001WR000683 (cit. on p. 87).

Wilcock, P. R. and J. B. Southard (1988). "Experimental study of incipient motion in mixed-size sediment." In: *Water Resources Research* 24.7, pp. 1137–1151. DOI: 10.1029/WR024i007p01137 (cit. on pp. 25, 26).

WindEurope (2017). *The European offshore wind industry: Key trends and statistics 2016.* Tech. rep. WindEurope (cit. on pp. 1, 5).

Wörman, A. (1989). "Riprap Protection without Filter Layers." In: *Journal of Hydraulic Engineering* 115. DOI: 10.1061/(ASCE)0733-9429(1989)115:12(1615) (cit. on p. 41).

Yu, Y. X., N. C. Zhang, and Q. Zhao (1996). "Wave actions on a vertical cylinder in multidirectional random waves." In: *Proc. 25th Conference of Coastal Engineering.* Orlando (cit. on p. 51).

Zanke, U. (1977). "Neuer Ansatz zur Berechnung des Transportbeginns von Sedimenten unter Strömungseinfluss." In: *Mitteilungen des Franzius-Instituts der Unversität Hannover* 46. (In German) (cit. on p. 19).

– (1982). *Grundlagen der Sedimentbewegung.* Ed. by U. Zanke. (In German). Springer-Verlag - Berlin - Heidelberg - New York (cit. on pp. 8–10, 15, 17, 19, 41).

Zanke, U. (1990). "Der Beginn der Sedimentbewegung als Wahrschein-
    lichkeitsproblem." In: *Wasser und Boden* 1. (In German), pp. 40–43
    (cit. on p. 18).

Zanke, U., T.-W. Hsu, A. Roland, O. Link, and R. Diab (2011). "Equi-
    librium scour depth around piles in noncohesive sediments under
    currents and waves." In: *Coastal Engineering* 58, pp. 986–991. DOI:
    10.1016/j.coastaleng.2011.05.011 (cit. on p. 35).

A

A.1 CURRICULUM VITAE

Personal Data

Name	Alexander Schendel
Date of Birth	February 6th, 1984
Place of Birth	Hildesheim, Germany
Nationality	German
Marital status	Single
Email	schendel@lufi.uni-hannover.de
Phone	+49 (0)511 762.2592

Education

10/2006 - 03/2012	University education in Civil Engineering at Leibniz Universität Hannover
	Degree: Diplomingenieur, Dipl.-Ing. Specialization: Water and Environmental Engineering
	Thesis: "Numerische Strömungsanalyse zur Leistungsfähigkeit eines Entwässerungstunnels mit Tideeinfluss"
08/2004 - 06/2006	Vocational training as technical draftsman
08/1996 - 06/2003	School education at the Goethegymnasium Hildesheim, Germany Graduated with German Abitur

Work Experience

04/2012 - current	Research Associate at Ludwig-Franzius-Institute for Hydraulic, Estuarine and Coastal Engineering, Leibniz University Hannover
	Projects involved: "BRAKE - Hydraulische Leistungsfähigkeit des Braker Sieltunnels"
	"MIBAU - Phase 2: Durchführung von wissenschaftlichen Modelluntersuchungen mit weitgestuftem Steinmaterial zum Einsatz als Kolkschutz"
	"MIBAU - Phase 3: Durchführung von wissenschaftlichen Modelluntersuchungen mit weitgestuftem Steinmaterial zum Einsatz als Kolkschutz"
	"GIGAWIND life: Lebensdauer-Forschung on den OWEA Tragstrukturen im Offshore-Testfeld alpha ventus"
	"NAUE - Dichtungsbahnen: Lagestabilität von geosynthetischen Dichtungsbahnen unter Strömungsbelastung"
	"SUMITOMO - Hydraulic model tests on sinking of granular scour protection systems"
	"PROTEUS - Large scale experiments to improve monopile scour protection design adapted to climate change"
	"MARTECH - Erprobung und Entwicklung maritimer Technologien zur zuverlässigen Energieversorgung"
05/2009 - 12/2011	Student assistant at Ludwig-Franzius-Institute for Hydraulic, Estuarine and Coastal Engineering, Leibniz University Hannover
07/2006 - 08/2006	Technical draftsman at Pabsch & Partner, Hildesheim